THE ROLE OF P73 IN MURINE OVARIAN FOLLICLE DEVELOPMENT AND FUNCTION

By

Gabriela Lynette Santos Guasch

Dissertation

Submitted to the Faculty of the

Graduate School of Vanderbilt University

in partial fulfillment of the requirements

for the degree of

DOCTOR OF PHILOSOPHY

in

Biochemistry

December 15, 2018

Nashville, Tennessee

Approved:

Jennifer A. Pietenpol, Ph.D.

Bruce D. Carter, Ph.D.

Rebecca S. Cook, Ph.D.

Scott W. Hiebert, Ph.D.

Ian G. Macara, Ph.D.

To my parents,

Pedro and Giovanna

and

to my brother, Pedro

ACKNOWLEDGEMENTS

There have been so many wonderful people that have played a crucial role in my professional success and personal growth during graduate school. I plan to devote a few pages of this dissertation to put into words the overwhelming amount of gratitude I feel toward the many people that made this dissertation possible.

First and foremost, I like would to acknowledge my mentor Dr. Jennifer Pietenpol. Since before I started at Vanderbilt, I knew I wanted someone like Jennifer as a mentor. She was one of the faculty I emailed to ask if she was going to be accepting new rotation students when I needed to decide whether to join the Interdisciplinary Graduate Program at Vanderbilt. From our first meeting, even thou she was very intimidating, I knew I wanted to join her lab and that she would push me further than I ever thought possible. Jennifer's excitement, drive and energy even with just a couple of hours of sleep is contagious. Despite her hectic schedule and array of administrative responsibilities, Jennifer has always prioritized time for her students and reminds us constantly that the sky is the limit. I am so thankful that I had the privilege and opportunity to be mentored by Jennifer, not just in science but also as a professional. Sometimes Jennifer jokes that I am one of her children, she has definitely become not only an amazing mentor but also my lab mom.

I would like to thank the members of my thesis committee Drs. Bruce Carter, Scott Hiebert, Ian Macara and Rebecca Cook. My thesis project was significantly improved because of the unmeasurable guidance, constructive support and feedback that each committee member provided. I am extremely grateful to Dr. Cook, who was a constant collaborator and advisor in the development of mouse experiments. Her positivity and enthusiasm for my project always made committee meetings less intimidating.

I have to thank the members of the Pietenpol lab, Hailing Jin, Brian Lehmann, Hanbing An, Qing Zhang, Lynnette Stanton-Williams and “The Honorable” Kim Johnson. Each provided amazing feedback and support for my project, and helped make the lab a family. I am grateful to Lynnette for helping me navigate Jennifer’s busy schedule and coordinating all the committee meetings. I am forever in the debt of “The Honorable” Kim Johnson. As she said to me many times: “Gaby you would not be able to defend your thesis without my blood, sweat and tears”. Kim provided an endless supply of greatly appreciated doughnuts and cake that helped me stay awake and finish experiments. Although not Kim’s favorite thing to do, I will miss doing laser capture microdissection (LCM) with her.

My fellow trainees, Clayton Marshall, Scott Beeler, Tim Shaver, Johanna Schafer, Lindsay Redman and Spencer Lea, have been key collaborators and provided so much insight and helpful discussions on how to move my project forward. I owe an immense amount of debt and gratitude

to Clayton and Scott (Team p73). Clayton, and appreciate all the time they spent training me and showing me everything in lab as a rotation student. I am sad that Clayton will not be able to attend my defense, and am jealous he is going on vacation. I am very grateful to Scott for all the bioinformatics analyses that he did for my studies and his willingness to always help even when he had too much work himself.

I am grateful for all my collaborators at Vanderbilt, specially Drs. Bryan Venters and Kelli Boyd. Dr. Venters provided significant expertise and guidance on my ChIP experiments and was always willing to troubleshoot experimental issues. I also owe immense gratitude to Dr. Boyd who provided support and suggestions from the beginning of my thesis project. I really appreciate all the time she spent examining murine ovarian tissue sections under the microscope and providing her expertise.

I would like to acknowledge others at Vanderbilt for their guidance and support: Dr. John York, Chuck Sanders, David Cortez and Patty Mueller in Biochemistry; Sandra Zinkel, Dave Cortez and Christine Lovly for their support and feedback during lab meeting as well as everyone in their laboratories. I am also grateful to the Initiative for Maximizing Student Diversity (IMSD), especially for the support from Drs. Linda Sealy and Christina Keeton during my time at Vanderbilt. My dissertation research was supported by NIH grants CA105436, CA098131, and CA068485 to J.A.P and training grant support GM062459 to G.L.S.G.

During my time in graduate school, I have relied on the support of my family and friends in Nashville. To my parents, my brother and my dog Vinny, thank you for never losing hope that I was going to graduate one day and for helping me always focus on the positive side of things. Their constant support is one of the main reasons I was able to complete my studies. All my Nashville friends, thank you for keeping me sane and making me laugh after a bad science day.

TABLE OF CONTENTS

LIST OF TABLES

LIST OF FIGURES

LIST OF ABBREVIATIONS

AR	Androgen Receptor
ATP	Adenosine Triphosphate
BPE	Bovine Pituitary Extract
cDNA	Complimentary DNA
ChIP	Chromatin Immunoprecipitation
CMV	Cytomegalovirus
COX4I1	Cytochrome C Oxidase Subunit 4I1
CY3	Cyanine 3
CYP17A1	Cytochrome P450 17A1
DAPI	4',6-Diamidino-2-Phenylindole
DMEM	Dulbecco's Modified Eagle's Medium
DNA	Deoxyribonucleic Acid
EDTA	Ethylenediaminetetraacetic Acid
EGFR	Epidermal Growth Factor Receptor
ELISA	Enzyme-linked Immunosorbet Assay
ER	Estrogen Receptor
FBS	Fetal Bovine Serum
FDR	False Discovery Rate
FITC	Fluorescein Isothiocyanate
FOXJ1	Forkhead Box Protein J1

FOXL2	Forkhead Box Protein L2
FSH	Follicle Stimulating Hormone
GAPDH	Glyceraldehyde-3-Phosphate Dehydrogenase
GnRH	Gonadotropin Releasing Hormone
GTPases	Guanosine Triphosphatase
h	Hours
HMECs	Human Mammary Epithelial Cells
HNSCC	Head and Neck Squamous Cell Carcinoma
HRP	Horseradish Peroxidase
IGV	Integrative Genomics Viewer
INHA	Inhibin Subunit Alpha
INHB	Inhibin Subunit Beta
LCM	Laser Capture Microdissection
LH	Luteinizing Hormone
MAtS	Magnetically Attachable Stencils
MDM2	Mouse Double Minute 2
MEFs	Mouse Embryonic Fibroblasts
MGCs	Murine Granulosa Cells
M.O.M	Mouse on Mouse Block
mRNA	Messenger RNA
NBF	Neutral Buffered Formalin
NOXA	Phorbol-12-myristate-13-acetate-induced protein 1

OCT	Optimal Cutting Temperature
p21	Cyclin-dependent Kinase inhibitor 1A (CDKN1A)
p53	Tumor protein p53
p63	Tumor protein p73-like
p73	Tumor protein p73
PBS	Phosphate Buffered Saline
PCR	Polymerase Chain Reaction
PR	Progesterone Receptor
PUMA	p53 Up-regulated Modulator of Apoptosis
QC	Quality Control
qRT-PCR	quantitative Real-Time Polymerase Chain Reaction
Rho	Ras Homolog Gene Family
RIPA	Radio Immunoprecipitation Assay
RNA	Ribonucleic Acid
RNA-seq	RNA Sequencing
ROS	Reactive Oxygen Species
RPMI	Roswell Park Memorial Institute
shRNA	Short Hairpin RNA
SNPs	Single Nucleotide Polymorphisms
SV40	Simian Virus 40
TA	Transactivation Domain
TGF-β	Transforming Growth Factor Beta

TSA	Tyramide Signal Amplification
TSS	Transcriptional Start Site
UV	Ultraviolet

CHAPTER I

INTRODUCTION

Sexual reproduction is evolutionarily conserved across the majority of eukaryotic organisms, which maintains a diverse genetic pool within each species. Despite extensive research, critical biological pathways required for proper reproduction and fertility remain poorly understood. Transcription factors are key proteins that dictate the expression of genes during development and regulate complex biological processes essential for sexual reproduction and fertility. This dissertation focuses on the role of the transcription factor p73 in proper ovarian follicle development, ovulation, hormone signaling and mammary gland branching. In this chapter, the p53 family of transcription factors will be presented with particular emphasis on p73 and its function, as it relates to female reproduction, ovarian function and hormone signaling.

The p53 Family of Transcription Factors

The mammalian p53 family of transcription factors are required for appropriate cell cycle, DNA repair, apoptosis, tissue development and cell differentiation. p53 was discovered in the late 1970s as part of a protein complex with the Simian virus 40 (SV40) large T antigen in transformed cells

(DeLeo et al. 1979; Lane and Crawford 1979; Linzer and Levine 1979). Initially, p53 was acknowledged to be an oncogene given that it was highly expressed in transformed cell lines but not in non-transformed cell lines or normal tissues (DeLeo et al. 1979; Rotter et al. 1980). This misconception was disproved by the late 1980s, when advances in technology allowed for the identification of the murine Trp53 coding sequence from normal tissue (Eliyahu et al. 1988; Finlay et al. 1988). When compared to p53 wild-type murine sequence, tumor-derived p53 cDNAs harbored mutations with cell transforming ability (Eliyahu et al. 1988; Finlay et al. 1988; Halevy et al. 1991). Later, several studies demonstrated that wild-type p53 was frequently mutated in human colorectal tumors (Baker et al. 1989) and the overexpression of wild-type p53 repressed cellular transformation through ras oncoprotein in cultured cells further supporting its roles as a tumor suppressor (Eliyahu et al. 1989; Finlay et al. 1989).

p53 homologous proteins, p73 (Jost et al. 1997; Kaghad et al. 1997) and p63 (Yang et al. 1998), were discovered in 1997 and 1998, respectively. Due to high sequence homology between family members, p73 and p63 were initially thought to be redundant to p53 as tumor suppressors (Harms and Chen 2006). However, the generation of p73- and p63-deficient mouse models revealed unique phenotypes and biological functions necessary for proper developmental processes (Yang et al. 1999; Yang et al. 2000) that

differed from phenotypes observed in p53-deficient mice (Donehower et al. 1992; Barbieri and Pietenpol 2005).

Structure and Function of the p53 Family

The p53 family of genes, p53, p63 and p73 are highly conserved, sequence-specific transcription factors (Schmale and Bamberger 1997; Blandino and Dobbelstein 2004). All three family members share significant structural and amino acid sequence identity within the transactivation (TA) domains, DNA binding domains and oligomerization domains (Harms and Chen 2006; Dotsch et al. 2010). In terms of whole amino acid sequence, p53 and p73 share 30% sequence identity, p63 shares 25% sequence identity with p53, and p73 shares 52% sequence identity with p63 (Yang and McKeon 2000; Yang et al. 2002). The DNA binding domain of all three p53 family members exhibit 60% sequence homology with 100% identity of the essential amino acid residues that contact DNA (Harms et al. 2004; Vilgelm et al. 2008), conferring binding to the canonical p53 consensus response element (el-Deiry et al. 1992). Each family member can drive apoptosis through the p53 response element providing functional similarities among p53, p63 and p73 (Jordan et al. 2008). However, p63 (Osada et al. 1998; Sasaki et al. 2005; Perez et al. 2007) and p73 (Zhu et al. 1998; Liu et al. 2004; Rosenbluth et al. 2008) are able to bind different response elements that allows specific regulation of unique target genes.

Alternate splicing and promoter use provide biological complexity and regulation among the p53 family members. There are 9 known isoforms for p53 (Bourdon et al. 2005), 6 for p63 and 35 for p73 (Murray-Zmijewski et al. 2006). p63 and p73 each are transcribed from two separate upstream promoters (P1 and P2) generating functionally distinct isoforms. P1 gives rise to transcriptionally active (TA) isoforms (TAp63 and TAp73), while isoforms transcribed from P2 lack the TA domain (ΔNp63 and ΔNp73) (Kaghad et al. 1997; Yang et al. 1998). The ΔN isoforms have been shown to act as dominant-negative regulators of the transcriptional activity of the p53 family of transcription factors (Liu et al. 2004; Harms and Chen 2006).

The p53 family bind to DNA as dimers of dimers (tetramers) (Chene 2001) mediated through the oligomerization domain (Harms et al. 2004). Physical interactions amongst p63 and p73 are necessary for co-regulation of many of the shared target genes. p63 and p73 regulate each other's transcriptional activity through the binding of ΔN isoforms to TA isoforms forming heterotetramers (Chene 2001). The functional and biological complexity of each p53 family member are further described below.

p53

p53 functions as a master regulator of cell cycle control, DNA repair and programmed cell death (Diller et al. 1990; Kastan et al. 1992; Hall et al. 1993). In response to stress, p53 induces the expression of target genes such as cyclin-dependent kinase inhibitor p21 (CDKN1A) (el-Deiry et al. 1993) and mouse double-minute 2 homolog (MDM2) (Barak et al. 1993) to regulate cell cycle arrest, DNA damage repair and apoptosis. The early hypotheses of the tumor suppressive role of p53 were proven when germline p53 mutations were identified in families harboring a predisposition to Li-Fraumeni syndrome (Malkin et al. 1990; Srivastava et al. 1990), and p53 inactivating mutations were discovered in over half of all human cancers (Kandoth et al. 2013). These findings were further validated by the observed high frequency of tumor formation in p53-deficient mouse models (Donehower et al. 1992; Purdie et al. 1994). Aside from tumor suppression, p53 plays an important role during normal tissue development, specifically in reproductive organs. Male mice that lack p53 are fertile, however, the seminiferous tubule exhibit germ-cell degeneration with multinucleated giant cells due to the inability of the spermatocytes to successfully complete meiotic cell division (Rotter et al. 1993). After ionizing radiation, p53-/- testis show decreased DNA damage-induced apoptosis in spermatogonia cells (Beumer et al. 1998; Hasegawa et al. 1998). During female reproduction, p53 regulates oocyte implantation to the uterine walls through

Table 1.1. Reproductive Phenotypes in Mouse Models Deficient for p53 Family Members			
Knockout Models	**Fertility Status**	**Reproduction-Associated Defects**	**Other Mouse Phenotype**
p53-/-	Fertile	Multinucleated spermatocytes within seminiferous tubules, decreased radiation-induced spermatogonial apoptosis	Increased susceptibility to develop spontaneous tumors including lymphomas and soft tissue sarcomas
	Subfertile	Oocyte implantation defects through regulation of LIF	
p63-/-	N/A	p63-deficient embryos exhibit increased germ cell survival after radiation	Perinatal lethality, craniofacial malformations, lack of stratified epithelial and absence of limbs
ΔNp63-/-	N/A	N/A	Perinatal lethality, craniofacial malformations, lack of stratified epithelial and absence of limbs
TAp63-/-	Fertile	Decreased ionizing radiation-induced apoptosis in oocytes	Premature aging, skin blisters and ulcerations, and impaired wound healing response
p73-/-	Infertile	Sperm cells exhibit defective flagella in the testis	Hydrocephalus, hippocampal dysgenesis, chronic inflammation and infection of repiratory tract due to absence of multiciliated cells
		Aberrant ovarian follicle development, lack of corpus luteum and decreased circulating progesterone	
ΔNp73-/-	Fertile	N/A	Hydrocephalus and hippocampal dysgenesis
TAp73-/-	Infertile	Increased DNA damage and apoptosis in spermatogonial cells within seminiferous tubule resulting in the absence of mature sperm	Hydrocephalus, hippocampal dysgenesis, chronic inflammation and infection of repiratory tract due to absence of multiciliated cells
		Abnormal spindle formation during meiosis resulting in poor oocyte quality, aberrant ovarian follicle development and ovulation	

*

* Table lists all previously published reproductive phenotypes in male and female mouse models deficient for p53 (Donehower et al. 1992; Purdie et al. 1994; Rotter et al. 1993; Beumer et al. 1998; Hasegawa et al. 1998; Hu et al. 2007), p63 (Mills et al. 1999; Yang et al. 1999; Suh et al. 2006), ΔNp63 (Candi et al. 2006; Romano et al. 2009; Romano et al. 2012), TAp63 (Kurita et al. 2005; Su et al. 2009; Gonfloni et al. 2009; Deutsch et al. 2011), p73 (Yang et al. 2000; Marshall et al. 2016; Santos Guasch et al. 2018), ΔNp73 (Wilhelm et al. 2010) and TAp73 (Tomasini et al. 2008; Nemajerova et al. 2016).

transcriptional regulation of leukemia inhibitory faction (LIF), and loss of p53 in female mice results in subfertility (Table 1.1) (Hu et al. 2007).

p63

p63 is a transcription factor required for skin and limb development, epithelial stem cell proliferation, differentiation and self-renewal, and plays a role in the maintenance of genome integrity and reproduction. p63-deficient mice fail to develop stratified epithelia, and die shortly after birth due to dehydration (Mills et al. 1999; Yang et al. 1999). Loss of p63 results in craniofacial malformations and lack of epithelial appendages including hair follicles, teeth, mammary, salivary and lachrymal glands (Mills et al. 1999; Yang et al. 1999). Given the functional complexity of p63, genetic complementation experiments were achieved by re-introducing isoform-specific ΔNp63 or TAp63 in p63-deficient mice. Such experiments provided biological insight to the distinct roles of p63 isoforms and demonstrated that ΔNp63, but not TAp63, was necessary for the formation of the epidermal basal layer (Candi et al. 2006; Romano et al. 2009). An isoform-specific knockout mouse model validated the indispensable role of ΔNp63 during epithelial development and differentiation (Romano et al. 2012). In contrast, TAp63α is the predominant isoform expressed in mouse oocytes (Kurita et al. 2005) and plays a crucial role in maintaining genome integrity during meiotic arrest of female germ cells (Suh et al. 2006; Su et al. 2009). TAp63-

deficient mice fail to induce apoptosis of DNA-damaged oocytes compared to wild type or p53-deficient mice suggesting a p53-independent apoptotic response (Suh et al. 2006). In response to DNA damaging agents like cisplatin (Gonfloni et al. 2009) or ionizing radiation (Livera et al. 2008), TAp63α is activated by c-Abl-mediated phosphorylation and induces apoptosis through regulation of proapoptotic genes Puma and Noxa, therefore ensuring oocyte quality (Table 1.1) (Deutsch et al. 2011).

p73

Given the high structural and sequence homology with p53, p73 was initially thought to act as a tumor suppressor due to the ability of p73 to bind p53-responsive genes, induce cell cycle arrest and apoptosis *in vitro* (Jost et al. 1997; Dotsch et al. 2010). The complex p73 C-terminus splicing gives rise to multiple isoforms (α, β, γ, δ, ε, ζ and η) that have different function, transcriptional activity (De Laurenzi et al. 1998; Melino et al. 2002) and tissue expression patterns (Grespi et al. 2012). For example, TAp73α and TAp73β are the predominant isoforms expressed in the ovaries (Santos Guasch et al. 2018) and play an important in normal myeloid cell differentiation (Tschan et al. 2000). Further, TAp73γ and TAp73δ transactivate the promoters of genes involved in terminal differentiation of human keratinocytes (De Laurenzi et al. 2000).

Unlike p53, p73 is frequently expressed rather than mutated in human cancers suggesting a possible therapeutic target (Moll and Slade 2004). The role of p73 in tumorigenesis is not well understood due to the antagonistic functions of ΔNp73 versus TAp73 isoforms. ΔNp73 is anti-apoptotic and acts as a dominant negative regulator of p53, p63 and p73 (Murray-Zmijewski et al. 2006). ΔNp73 has been shown to inhibit the tumor-suppressive activities of TAp73 in head and neck squamous cell carcinoma (HNSCC) (Deyoung et al. 2006; Rocco et al. 2006) and basal-like breast cancer (Leong et al. 2007). Patients with lung tumors that overexpress ΔNp73 have less favorable clinical outcomes than patients lacking expression (Uramoto et al. 2004). In contrast to ΔNp73, TAp73 is proapoptotic and exhibits tumor suppressive functions similar to p53. In response to DNA damaging agents like cisplatin (Irwin et al. 2003), TAp73 is phosphorylated by tyrosine kinase c-Abl, resulting in protein stabilization and increased transcriptional regulation of proapoptotic target genes including p21, PUMA, NOXA, PIG3, PARP and BAX (Vilgelm et al. 2008). However, the role of p73 as tumor suppressor was challenged by the observation that p73-deficient mouse models do not develop cancer but instead exhibit severe developmental abnormalities (Yang et al. 2000) further elucidated in the next section.

p73 Knockout Mouse Models

The first mouse model functionally deficient for all p73 isoforms was developed by targeting exons 5 and 6 within the DNA binding domain; resulting in hippocampal dysgenesis, hydrocephalus, sterility, runting, abnormal pheromone signaling, chronic infections and inflammation as well as increase rate of postnatal lethality (Yang et al. 2000). The hippocampal dysgenesis observed in p73-deficient mice was due to the loss of Reelin expression in the neural cortex (Yang et al. 2000). Subsequent studies demonstrated that p73 is essential during neurological development by promoting self-renewal and proliferation in progenitor and neural stem cells (Pozniak et al. 2002; Talos et al. 2010). In addition, p73 has been implicated in the development and maintenance of ependymal cells (Gonzalez-Cano et al. 2015) and loss of p73 was associated with dysfunctional ciliogenesis (Medina-Bolivar et al. 2014).

Our laboratory generated a p73-deficient mouse model that lacks the DNA binding and oligomerization domain (exons 7, 8 and 9) (Marshall et al. 2016); which recapitulated all previously reported phenotypes (Yang et al. 2000). The major insights gained from the new model was that p73-deficient mice lack cilia in the oviduct, middle ear, sinus mucosa, flagella of the sperm in the testis and respiratory tract (Marshall et al. 2016). These observations led us to discover that p73 is required for multiciliated cell differentiation in the mouse and acts as transcriptional regulator of Foxj1-associated gene

network required for ciliogenesis (Marshall et al. 2016). This discovery provided a unifying mechanism for the many diverse phenotypes observed in p73-deficient mouse models including hydrocephalus; hippocampal dysgenesis; sterility; and chronic inflammation and infection. Validating our discoveries, the Moll laboratory provided evidence that loss of isoform-specific TAp73 in mice caused impaired pulmonary function and ciliogenesis defects in murine airways (Nemajerova et al. 2016). Similarly, Nemajerova and colleagues identified TAp73 as a transcriptional regulator of Foxj1 (Nemajerova et al. 2016).

The development of p73 isoform-specific knockout mouse models have further elucidated the independent roles of p73 isoforms in murine development and tumorigenesis. Much like the global knockout, the TAp73-deficient mouse model exhibits infertility, hippocampal dysgenesis, hydrocephalus, premature aging, genomic instability and increased frequency of tumors (Tomasini et al. 2008). Other studies indicated that TAp73 regulates mitochondrial function by directly transactivating Cox4i1, a mitochondrial subunit required for reactive oxygen species (ROS) homeostasis (Rufini et al. 2012).

In contrast to TAp73-deficient animal models, mice that lack ΔNp73 are fertile and display signs of neurodegeneration, including hippocampal dysgenesis and hydrocephalus (Wilhelm et al. 2010). Mouse embryonic fibroblast (MEFs) isolated from ΔNp73 knockouts exhibit increased

expression of p53 target genes p21, Mdm2 and Puma, as well as enhanced apoptosis. Transformed ΔNp73-/- MEFs subcutaneously injected into athymic nude mice generated smaller and slower-growing tumors compared to wild-type transformed MEFs, demonstrating the anti-apoptotic or growth-inhibitory role of ΔNp73. In summary, the use of isoform-specific mouse models provided significant insight to the individual functions of the select p73 isoforms and provided evidence of the complex signaling mechanisms of this transcription factor.

p73 and Reproduction

p73 is required for reproduction as male and female mice deficient for all p73 isoforms are sterile (Table 1.1) (Yang et al. 2000; Marshall et al. 2016). Loss of the transcriptionally active TAp73 isoform (Tomasini et al. 2008), not ΔNp73 (Wilhelm et al. 2010), leads to the infertility phenotypes observed in p73-deficient animal models. Male mice that lack TAp73 exhibit increased DNA damage and apoptosis in spermatogonial cells within the testes, which results in defective germ cell maturation and differentiation required for proper spermatogenesis (Inoue et al. 2014). TAp73 regulates the expression of crucial genes involved in spermatid maturation including matrix metalloproteinase 13 (MMP13) and ADAM metallopeptidase 17 (ADAM17) as well as steroidogenesis cytochrome P450 CYP21A2 enzyme (Inoue et al. 2014). In addition, TAp73 regulates a network of genes

necessary for cell-to-cell adhesion between germ and Sertoli nurse cells in the testis (Holembowski et al. 2014).

TAp73 plays multiple roles in female reproduction including ovarian follicle development, ovulation and oocyte transport through the oviduct (Tomasini et al. 2008; Marshall et al. 2016; Nemajerova et al. 2016). Oocytes derived from TAp73-/- ovaries exhibit spindle abnormalities including multipolar spindles, spindle relaxation and misalignment during meiosis (Tomasini et al. 2008). TAp73 directly interacts with essential proteins (e.g. Bub1, Bib3 and BubR1) required for the spindle assembly checkpoint (SAC) complex necessary for proper meiosis arrest in oocytes (Tomasini et al. 2009). Further, as a result of my dissertation research and described in Chapter 3 of this thesis, we recently discovered that p73 is expressed in granulosa cells within the ovarian follicle, and regulates a gene network involved granulosa-to-granulosa cell adhesion critical for oocyte development, ovulation and fertility (Santos Guasch et al. 2018).

Female Reproduction

In the US, 12.1% of women between the ages of 15 to 44 suffer from impaired fertility (Chandra et al. 2013). The complexity of female reproduction spans cyclic regulation of signaling pathways involved in cellular processes across multiple organs including the hypothalamus, the pituitary gland, the ovaries and the mammary gland. The hormone signaling

dictated by the hypothalamic-pituitary-gonadal (HPG) axis plays a critical role in the development and maturation of reproductive organs, specially the mammary gland and the ovaries throughout the lifespan of the organism. The mammary gland is a complex secretory organ formed by epithelial cells that line the ductal network embedded in the fat pad. The mammary duct consists of an outer myoepithelial layer and an inner luminal layer that differentiates into milk-producing alveolar cells during pregnancy and lactation (Forsyth and Neville 2009). The main function of the mammary gland is to produce, secrete and deliver nutrient-rich milk to the newborn. The ovaries are formed by multi-cellular structures, known as follicles, where granulosa and theca cells provide all the nutrients necessary for proper oocyte maturation and ovulation.

Hormonal Regulation

Hormonally-modulated tissues like the mammary gland and ovaries are regulated not only by cell-to-cell interactions within each tissue, but also by circulating hormones from the hypothalamus and the pituitary gland. Gonadotropin-releasing hormone (GnRH) is produced and secreted by the hypothalamus to regulate the production and release of FSH and LH from the pituitary gland (Figure 1.1) (Amoss et al. 1971). The pituitary gland is divided into two major regions: anterior and posterior lobes. The posterior

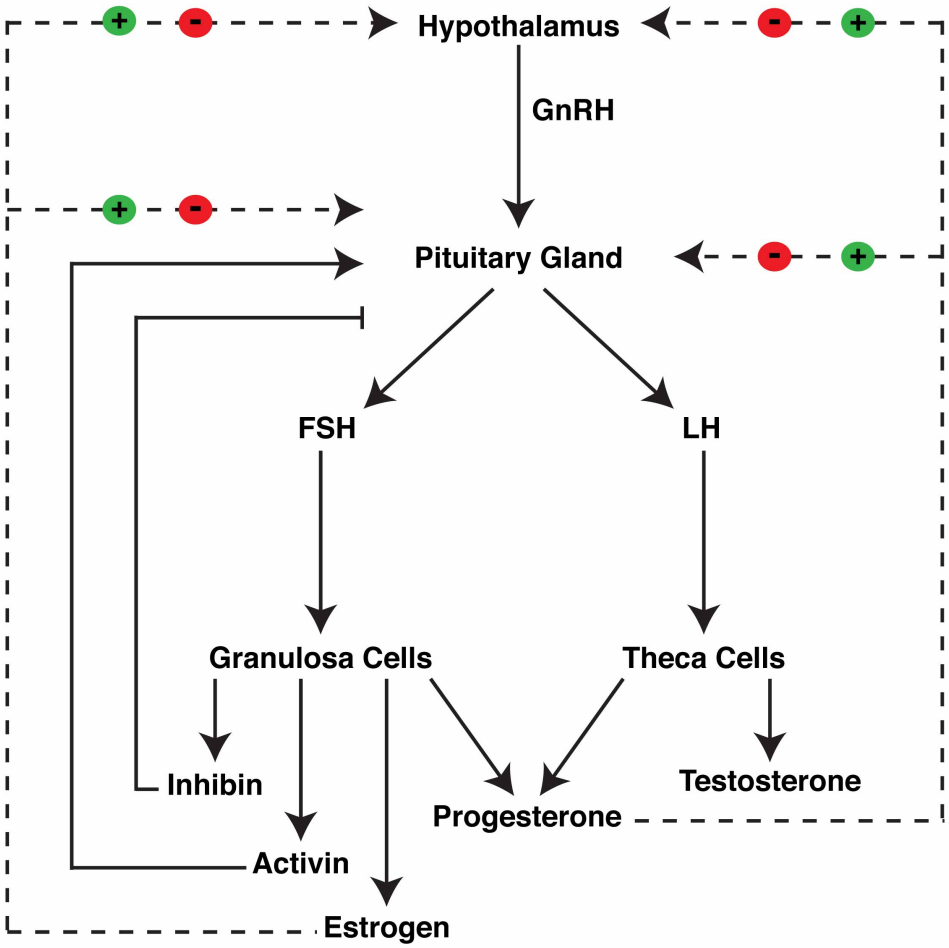

Figure 1.1. Hypothalamus-Pituitary-Ovaries Signaling Axis.
Diagram represents the female hypothalamus-pituitary-ovarian signaling axis and the positive and negative feedback loop between each tissue. Gonadotropin releasing hormone (GnRH), follicle stimulating hormone (FSH) and luteinizing hormone (LH).

lobe secretes antidiuretic hormone (ADH) and oxytocin, while the anterior lobe secretes FSH, LH, thyroid-stimulating hormone (TSH), adenocorticotrophic hormone (ACTH), growth hormone (GH) and prolactin (PRL). FSH and LH are key players necessary for female fertility and regulation of puberty and the estrous cycle in mammals.

Puberty and Estrous Cycle

Puberty is triggered by the increased frequency of GnRH secretion from the hypothalamus into the pituitary gland, which then stimulates the secretion of FSH and LH (Steele and Weisz 1974). Circulating FSH and LH activate ovarian follicle development and estrogen secretion, which initiates mammary gland branching and the estrous cycle (Foster and Ryan 1979). The murine estrous cycle repeats every 4-5 days and is divided into two phases: the follicular phase (proestrus and estrus stage) and the luteal phase (metestrus and diestrus stage) (Nelson et al. 1982). During proestrus, GnRH is secreted by the hypothalamus into the pituitary gland to increase FSH levels. FSH binds the FSH receptor in granulosa cells of developing follicles to induce cell growth (Richards and Midgley 1976), activin A production (Katayama et al. 1990; Rabinovici et al. 1992) and aromatase activity for the conversion of androgen into estradiol (McNatty et al. 1979). As granulosa cells proliferate, estradiol and inhibin B levels increase, suppressing FSH levels secreted by the pituitary (Groome et al. 1996; Welt

et al. 1997). High estradiol levels stimulate a sudden increase in LH production triggering ovulation (estrus stage) followed by the beginning of the luteal phase of the estrous cycle (Goldman et al. 2007). The luteal phase, divided into two stages: metestrus and diestrus, is characterized by the formation of the corpus luteum and progesterone production to promote oocyte fertilization and implantation (Khan-Dawood et al. 1989). In addition to progesterone, the corpus luteum secretes inhibin A, which inhibits FSH secretion from the pituitary and the start of the estrous cycle and follicle development (Welt et al. 1997). In the absence of oocyte fertilization and implantation, the corpus luteum degenerates promoting FSH levels and the beginning of proestrus (Parkening et al. 1982).

Steroid Hormone Receptor Knockout Mouse Models

Ovarian follicle development and mammary gland branching are regulated by the interactions between circulating hormones and their steroidal (estrogen, progesterone and androgen) and non-steroidal (FSH and LH) hormone receptors. Estrogen signaling begins at puberty and stimulates mammary gland ductal branching, maturation of the uterus and ovaries, and the estrous cycle. There are two known types of estrogen receptor ERα and ERβ in the ovaries, however ERβ (Byers et al. 1997) is predominantly expressed in granulosa cells while ERα is found in interstitial and theca cells (Lubahn et al. 1993). Mouse models that specifically target

each ER (α or β) or both ERα and ERβ have been developed to parse apart the individual phenotypes of each receptor type. Female mice that lack ERα exhibit rudimentary mammary gland branching (Bocchinfuso and Korach 1997), follicle development defects, impaired ovulation, hemorrhagic cysts, elevated levels of LH and abnormal steroidogenesis resulting in infertility (Lubahn et al. 1993; Schomberg et al. 1999; Dupont et al. 2000; Couse et al. 2003). In contrast, mice deficient of ERβ (Krege et al. 1998) exhibit normal ovarian morphology and follicle development, however, they show decreased ovulation rate with significantly smaller litter size leading to subfertility (Krege et al. 1998; Dupont et al. 2000).

Progesterone is a crucial regulator of female reproduction. Circulating progesterone stimulates extensive side-branching and alveologenesis in the mammary gland required for milk production. In the ovaries, the progesterone receptor is induced in mural granulosa cells of pre-ovulatory follicles in response to the LH surge (Park and Mayo 1991; Conneely et al. 2003; Teilmann et al. 2006). Like ER, there are two isoforms of progesterone receptor (PR): PRA and PRB (Kastner et al. 1990). PRA is the predominant isoform expressed in granulosa cells of pre-ovulatory follicle (Natraj and Richards 1993). Female mice deficient of PRA are infertile because the ovaries fail to ovulate (Lydon et al. 1995) due to lack of expression of metalloproteinases ADAMTS-1 and cathepsin-L in granulosa cells necessary for follicle rupture (Robker et al. 2000). PRB is expressed in pre-

ovulatory follicles in response to LH (Natraj and Richards 1993), however, mice that lack PRB (Mulac-Jericevic et al. 2000) are fertile suggesting that only PRA expression is necessary for proper ovulation.

The androgen receptor (AR) is expressed in the oocyte as well as in theca and granulosa cells through most stages of follicle development (Hirai et al. 1994; Tetsuka and Hillier 1996; Szoltys and Slomczynska 2000). Previous studies have shown that androgens enhance follicular growth beginning at the secondary follicle stage, promote FSH response and differentiation of granulosa cells, and decrease follicular atresia (Mori et al. 1977; Ware 1982; Sen et al. 2014). Oocyte- and granulosa cell-specific AR-deficient mouse models were developed to determine individual contributions of AR expression necessary for female fertility. Mice with oocyte-specific targeted ablation of AR (ARKO) have no reproductive phenotypes, however, granulosa cell-specific ARKO female mice exhibit abnormal estrous cycle, fewer ovulated oocytes and corpora lutea, increased follicular atresia and smaller litter size resulting in subfertility (Sen and Hammes 2010).

Ovaries

The development of the ovaries can be separated into two main stages: embryonic and pubertal/adult, each of which is regulated through different pathways. Embryonic development is characterized by the

formation of the primordial follicle from the primordial germ cells in the ovaries (Pepling and Spradling 2001; Grive and Freiman 2015). In mice, primordial germ cells differentiate from the epiblast and migrate to the genital ridge between embryonic days 8.5-11, where they undergo several rounds of mitosis forming germ cell cysts known as nests (Monk and McLaren 1981; Pepling et al. 1999; Pepling and Spradling 2001). At embryonic day 13.5, primordial germ cells enter meiosis (Borum 1961) until they arrest at the diplotene stage of prophase I at embryonic day 17.5, becoming oocytes (Motta et al. 1997). Around the time of birth, the germ cell cysts break down undergoing germ cell selection (Tingen et al. 2009), and high quality oocytes differentiate into primordial follicles until the onset of puberty (Bergeron et al. 1998; Pepling and Spradling 2001; Mork et al. 2012). During puberty, FSH and LH are secreted from the pituitary gland stimulating follicle development and maturation, hormone production and ovulation (Hennighausen and Robinson 2005; Sarraj and Drummond 2012).

Follicle Development

Follicle development also known as folliculogenesis, is regulated by hormones secreted from the pituitary gland and ovaries during the estrous cycle. A primordial follicle matures into a pre-ovulatory/antral follicle giving rise to a competent oocyte for ovulation and fertilization (McGee and Hsueh 2000). The ovarian follicle consists of the oocyte and two supporting

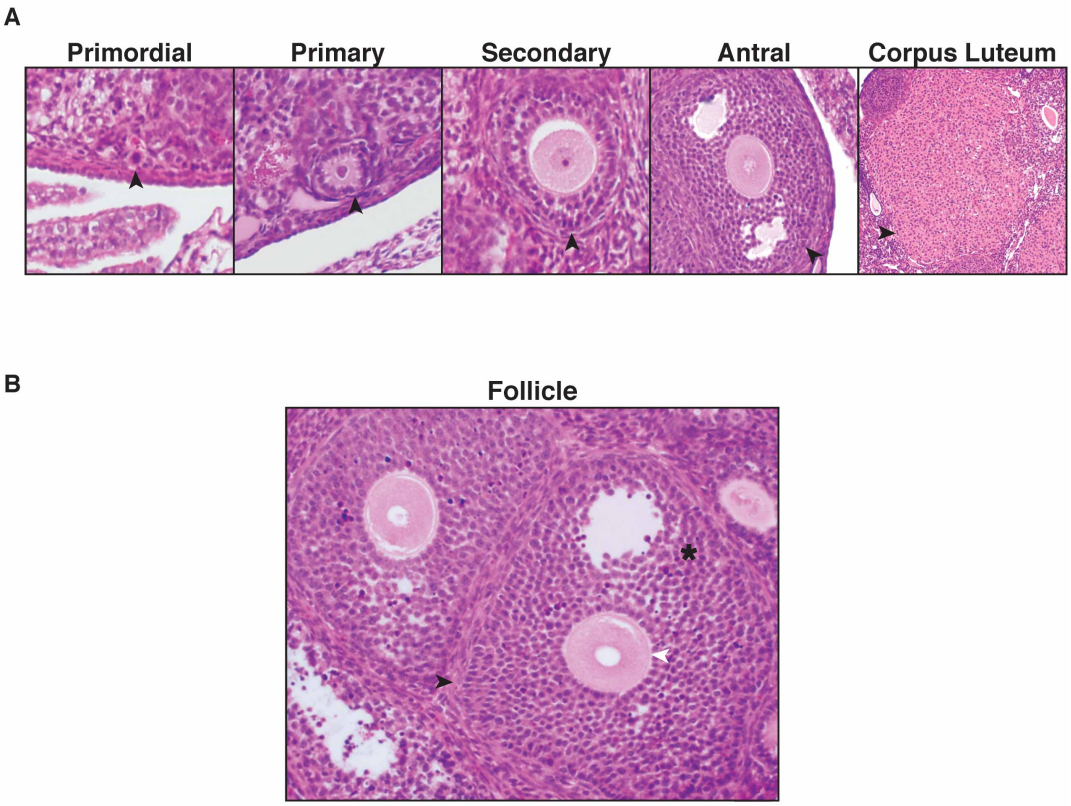

Figure 1.2. Ovarian Follicle Development.
Representative H&E images show (A) diffferent stages of ovarian follicle development (primordial, primary, secondary and antral follicle) and corpus luteum (arrowhead). (B) The follicle is composed of theca cells (black arrowhead), granulosa cells (asterisk) and oocyte (white arrowhead).

cell types, granulosa cells and theca cells Figure 1.2). Granulosa cells directly support the oocyte through all the stages of follicle development. As the granulosa cells proliferate and differentiate, the follicle gets encapsulated by a basement membrane and a theca cell layer.

The oocyte advances through multiple follicular stages as it matures, including primordial follicle, primary follicle, secondary follicle and antral/preovulatory follicle (Figure 1.2). Primordial follicles, characterized by the lack of granulosa cells or a single layer of squamous pre-granulosa cells, are derived from primordial germ cells during embryonic development and represents the first step of folliculogenesis (Hirshfield 1991). The oocyte of primordial follicles remains arrested in prophase I of meiosis until puberty (Borum 1961). Primordial follicles are activated in response to FSH and the squamous pre-granulosa cells differentiate into a single layer of cuboidal granulosa cells forming a primary follicle (Foster and Ryan 1979).

Proteins required for the differentiation and development of follicles are FOXL2, GDF9, FSH and LH. FOXL2 (transcription factor forkhead box L2) is required for granulosa cell differentiation and it is expressed throughout all the stages of follicle development (Schmidt et al. 2004). However, GDF9 (growth differentiation factor-9) promotes granulosa cell proliferation and is required for primary to secondary follicle transition (Carabatsos et al. 1998). Secondary follicles are classified by the presence of two or more granulosa cell layers surrounded by theca cells. The

secondary to antral follicle transition is dependent on the follicle's ability to respond to gonadotropins follicle stimulating hormone (FSH) and luteinizing hormone (LH) produced in the pituitary gland. Theca cells produce androgens in response to LH, while granulosa cells convert androgens to estrogen and proliferate in response to FSH (Hillier 1994; Orisaka et al. 2009). The increase in androgen production by the theca cells promotes FSH receptor (FSHR) expression and estradiol production in granulosa cells (Palermo 2007). As the antral follicle grows, the granulosa cells within the follicle differentiate into mural and cumulus cells forming a fluid filled cavity known as antrum (Gosden et al. 1988). The cumulus cells surround the oocyte providing nutrients through gap junctions (Kidder and Mhawi 2002), while the mural cells are responsible for steroid production located along the basement membrane of the follicle (Carletti and Christenson 2009). The increase levels of estradiol induces LH receptor (LHCGR) expression in mural granulosa cells priming the follicle for ovulation (Peng et al. 1991).

Ovarian Steroidogenesis

The ovaries are responsible for the synthesis of multiple steroid hormones from cholesterol, including estrogen, progesterone and testosterone, to maintain female reproduction. Within the ovarian follicle, granulosa and theca cells are differentially regulated by FSH and LH, respectively, signaling known as the two-cell two-gonadotropin theory

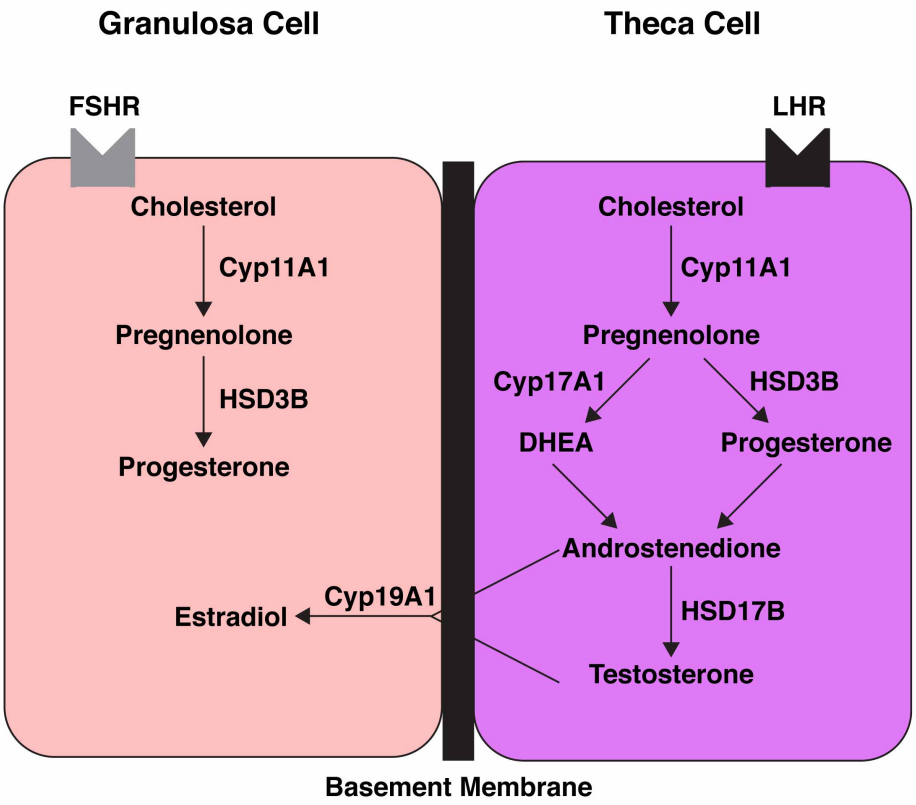

Figure 1.3. Two-Cell Two-Gonadotropin Model.
The diagram shows the steroidogenesis pathways in granulosa and theca cells activated by FSH and LH, respectively.

(Figure 1.3) (Fowler et al. 1978; Moon et al. 1978). LH binds to the LH receptor in theca cells to stimulate cyclic adenosine monophosphate (cAMP) and cholesterol intake (Brannian et al. 1992). Steroidogenic acute regulatory protein (StAR) transports the intracellular cholesterol to the inner mitochondrial membrane, where cholesterol is cleaved into pregnenolone by CYP11A1, the rate-limiting step for biosynthesis (Boyd et al. 1975; Chung et al. 1986; Hanukoglu 1992; Clark et al. 1994). Pregnenolone is then converted to progesterone by 3-hydroxysteroid dehydrogenase (HSD3B) or to dehydroepiandrosterone (DHEA) by CYP17A1 (Auchus et al. 1998). Both progesterone and DHEA can be converted into androstenedione by CYP17A1 and HSD3B, respectively (Hanukoglu 1992). In theca cells, 17β-hydroxysteroid dehydrogenase (HSD17B) catalyzes the conversion of androstenedione to testosterone (Dufort et al. 1999). Androstenedione and testosterone diffuse into granulosa cells and are then converted to estradiol by CYP19A1 (aromatase) (McNatty et al. 1979) in response to FSH (Hsueh et al. 1984).

ECM in Follicular Development

The extracellular matrix (ECM) and cell-to-cell adhesions play an essential role during follicle development, ovulation, corpus luteum formation and hormone secretion (Aten et al. 1995; Oktay et al. 2000; Rodgers et al. 2003; Woodruff and Shea 2007). Within the ovarian follicle, cell-to-cell

adhesion and ECM interactions between the granulosa cell layers are necessary for proper proliferation and differentiation into later stages of follicle development (Huet et al. 2001). The extracellular matrix between the granulosa cells of mature follicles is known as focimatrix (focal intra-epithelial matrix) (Irving-Rodgers et al. 2004). The focimatrix is a specific basal lamina mainly composed of collagen type IV, laminin, nidogen 1 and 2, and perlecan, which aggregates between granulosa cells (Irving-Rodgers et al. 2004; Irving-Rodgers et al. 2010). The focimatrix increases as the follicle progresses to the pre-ovulatory stage (Irving-Rodgers et al. 2004; Irving-Rodgers et al. 2006). Observed increases in focimatrix between granulosa cells are accompanied by increases in Cyp11a1 and steroid production in granulosa cells (Tian et al. 1995; Irving-Rodgers et al. 2009; Matti et al. 2010). As the follicle enters the pre-ovulatory or antral stage, proper steroidogenesis is essential for final maturation and ovulation.

Ovulation and Corpus Luteum Formation

In response to high estradiol, LH levels rapidly increase (LH surge) binding to the LH receptor in mural granulosa cells, which triggers ovulation (Richards 1980). There are several contributing processes necessary for proper ovulation and fertilization including cumulus expansion, follicle rupture, granulosa and theca cell luteinization and corpus luteum formation. Following the LH surge, cumulus granulosa cells produce hyaluronic acid

(HA)-rich ECM (Salustri et al. 1992) as well as laminin, collagen IV, fibronectin (Familiari et al. 1996) and proteoglycans around the oocyte called cumulus expansion (Russell et al. 2003b). Mouse models have identified several genes critical for cumulus expansion including hyaluronan synthase 2 (Has2) (Chen et al. 1993), prostaglandin endoperoxide synthase 2 (Ptgs2) (Lim et al. 1997), pentraxin 3 (Ptx3) and tumor necrosis factor alpha-induced protein 6 (Tnfaip6) (Fulop et al. 2003).

Ovulation requires the breakdown of the ECM around mural granulosa cells through proteinase activity, allowing the release of the cumulus-oocyte complex (COC) from the follicle (Curry et al. 1992; Iwamasa et al. 1992). Some of these proteases include matrix metalloproteinases (MMPs), tissue inhibitors of metalloproteinases (TIMPs) and ADAM metallopeptidase with thrombospondin type 1 motif (ADAMTS1). Upon ovulation, MMP9 and MMP19 levels increase in antral follicles to facilitate the breakdown of the follicular wall (Hagglund et al. 1999; Robker et al. 2000; Curry and Osteen 2003). Further, ADAMTS1 is induced by LH in granulosa cells of antral follicles for the breakdown of key ECM components (Russell et al. 2003a; Brown et al. 2010). Female mice that lack ADAMTS1 exhibit decreased ovulation rate due to abnormal extracellular matrix formation in cumulus granulosa cells followed by entrapped oocytes within antral follicle and subfertility (Mittaz et al. 2004; Brown et al. 2010).

After ovulation, the remaining granulosa and theca cells in the follicle terminally differentiate into luteal cells forming a corpus luteum, this process is known as luteinization (Richards et al. 1986). The corpus luteum is the primary site of progesterone production in females (Allen 1941), which is required for the establishment and maintenance of pregnancy (Rothchild 1981). For proper corpus luteum formation and function, extensive remodeling and vascularization, driven by the vascular endothelial growth factor (VEGF) (Reynolds et al. 1992), is necessary to facilitate cholesterol as a substrate for progesterone synthesis (Fraser et al. 2000; Reynolds et al. 2000). VEGF is upregulated during granulosa and theca cell differentiation into luteal cells as well as other angiogenic factors including angiopoietins (ANGPT) (Hazzard et al. 1999; Hazzard et al. 2000), vascular endothelial-cadherin (VE-cadherin) (Nakhuda et al. 2005) and thrombospondins (TSP-1 and TSP-2) (Petrik et al. 2002).

Oviduct

The oviduct is divided in three functionally distinct regions: the fimbria, which captures and transports the newly ovulated oocyte into the oviducts; the ampulla, where fertilization occurs; and the isthmus, which regulates transport of the sperm to the ampulla and the fertilized oocyte to the uterus for implantation (Croxatto and Ortiz 1975; Croxatto et al. 1978). The main cell types found in the oviductal epithelium are ciliated and non-ciliated

secretory (peg) cells, however, the proportion of ciliated cells to secretory cells decreases from over 50% in the fimbriated infundibulum to less than 35% in the isthmus (Patek et al. 1972; Patek 1974; Amso et al. 1994; Crow et al. 1994). Peg cells have been described as stem-like cells that secrete mucous into the oviduct (Paik et al. 2012). The role of the ciliated cells is to capture and transport the ovulated oocyte through the ampulla as well as fluid movement necessary for fertilization (Patton et al. 1989). The rate at which motile cilia beat is known as ciliary beat frequency (CBF). CBF is an ATP-dependent process that stimulates intracellular calcium concentrations (Verdugo 1980; Salathe and Bookman 1999). The changes in circulating hormones throughout the ovarian cycle have been shown to regulate the cilia beat frequency. Previous studies have shown that estrogen increases ciliary beat frequency in the oviduct, while progesterone decreases cilia beating (Mahmood et al. 1998; Nakahari et al. 2011).

The Role of p73 in Murine Ovarian Follicle Development: Scope of Dissertation

The p53 family of transcription factors regulates a wide array of cellular processes from cell cycle control to organ development and cell differentiation. Recently, our laboratory (Marshall et al. 2016) and others (Nemajerova et al. 2016) discovered that p73 is required for multiciliated cell differentiation and ciliogenesis providing mechanistic insight to some of the

diverse phenotypes observed in p73-deficient mouse models. Further analysis of our p73-deficient mouse model led to the discovery of novel phenotypes that involves mammary gland branching, hormone signaling and ovarian follicle development, likely to originate from processes unrelated to ciliogenesis. I designed experiments to dissect the role of p73 in these cell autonomous and non-autonomous interactions. Herein, I provide mechanistic evidence that supports the non-autonomous role of p73 in mammary gland branching and development through circulating progesterone. In addition, I show that p73 regulates cell adhesion- and migration-associated gene network, and loss of p73 leads to defective ovarian follicle development, ovulation and corpus luteum formation. Through analyses of *in vitro* migration assay, I show that p73 is necessary for cell migration and there are p73 binding near the transcriptional start site of crucial regulators of cell adhesion- and migration-associated genes. This dissertation focuses on the role of p73 in granulosa function and proper ovarian follicle development.

CHAPTER II

MATERIALS AND METHODS

Cell Culture and *in vitro* Experiments

Cell Culture

The majority of the cell lines used in this dissertation were purchased from American Type Culture Collection (ATCC). HCC1806, RH30 and NCI-H2122 cells were cultured in RPMI + GlutaMAX (Gibco 61870). MDA-MB-231, 293FT and NCI-H2009 cells were cultured in DMEM (Gibco 11965). Immortalized human granulosa-lutein cells (SVOG cells)(Lie et al. 1996) were a generous gift from P. Leung (University of British Columbia, BC, Canada), cultured in DMEM/F12 (Gibco 11330). All cell lines were maintained in 10% (v/v) fetal bovine serum (FBS) (Gemini), 100U/ml penicillin and 100µg/ml streptomycin (Gemini), and trypsinized using 0.25% Trypsin-EDTA (Gibco 2500056) at 37°C.

Human Mammary Epithelial Cells (HMECs) were isolated from normal breast tissue obtained from the Vanderbilt-Ingram Cancer Center Human Tissue Acquisition and Pathology Shared Resource by Kimberly Johnson. Cells were cultured in DMEM/F12 1:1 supplemented with 1.0µg/ml insulin (Novo Nordisk), 1.0µg/ml hydrocortisone (Sigma-Aldrich), 0.1mM

phosphoethanolamine (Sigma-Aldrich), 2.0 beta-estradiol (Sigma-Aldrich), 10nM 3,3',5-triiodo-L-thyronine sodium salt (Sigma-Aldrich), 15nM sodium selenite, 2.0mM L-glutamine (Gibco), 1% penicillin-streptomycin (Gemini), 1ng/ml cholera toxin (Sigma-Aldrich), 1% FBS and 35µg/ml BPE (Gibco).

Murine Granulosa Cells (MGCs) were grown in DMEM/F12 supplemented with 10% Charcoal/Dextran FBS, 2µg/ml insulin, 5nM sodium selenite, 5µg/ml apo-transferrin, 0.04µg/ml hydrocortisone and 50µg/ml sodium pyruvate (Life Technologies).

Lentiviral shRNA and Overexpression Vector Generation

Lentiviral vectors were transfected with viral packaging vectors (15 µg PAX2 and 10 µg pMD2.G) and Lipofectamine 2000 (Invitrogen) into 293FT cells. Media containing viral particles was collected 48 hours after transfection and filtered through 0.45 µM filter. Viral media with 10 µg/ml of polybrene (Sigma-Aldrich) was added to target cells for infection (Rubinson et al. 2003).

For stable p73 shRNA knockdown, the pSicoR lentiviral system was used (Ventura et al. 2004; Rosenbluth et al. 2008; Rosenbluth et al. 2011). The combination of TAp73-1 and TAp73-2 shRNAs yielded the best knockdown of p73 in human epithelial cell lines. Viral production and transduction were performed as described above.

For exogenous p73 expression, TAp73β and Fg12-CMV control expression vectors (De Laurenzi et al. 1998; Niemantsverdriet et al. 2005) were transfected into 293FT cells as described above. Media containing viral particles was used to infect murine isolated granulosa cells (MGCs).

Cell Protein Harvest and Immunoblotting

Cells were lysed in RIPA or EBC buffer supplemented with phosphatase inhibitors (50 mM sodium fluoride, 0.2 mM sodium vanadate, 10 mM p-nitrophenyl phosphate) and protease inhibitors (10 mg/ml antipain, 10 mg/ml leupeptin, 10 mg/ml pepstatin, 10 mg/ml chymostatin [Sigma-Aldrich], 200mg/ml 4-(2-aminoethyl)-benzenesulfonylfluoride [Millipore]). Cells were lysed in ice for 30 min and vortex every 10 min. Protein concentration was quantified using DC Protein Assay or Bradford Protein Assay (both from Bio-Rad). Protein lysates were separated on polyacrylamide gels and transferred to Immobilon-P membranes (Millipore) using the Transblot Turbo (Bio-Rad). All antibodies used for immunoblotting analysis described in Table 1 were incubated overnight at 4°C. HRP-conjugated secondary antibodies were incubated for 1 hour at room temperature. Membranes were incubated with Pierce ECL Western Blotting Substrate (Fisher) and film was exposed for protein expression visualization.

Magnetically Attachable Stencil (MAtS) Migration Assay

Magnetically attachable stencils (MAtS) (Ashby et al. 2012) were rinsed in ethanol and sterilized under UV light for 30 minutes. 12-well Plates were coated with collagen at a concentration of 100μg/ml in PBS for one hour at 37°C. Collagen solution was aspirated, plates were rinsed with sterile PBS twice and 500 μl of culture media was added per well, followed by MAtS. Cells were plated in triplicate at 50-70% confluency per well around the MAtS in serum-containing media. After cells adhered to the plates (approximately 1 hour depending on the cell line), serum-containing media was removed and cells were serum-starved overnight. Stencils were removed the following morning and fresh growth media containing serum was added. Images were taken at the time of MAtS removal and at indicated times (8, 9 or 11 hours) depending on the cell line. Gap closure was quantified using TScratch software (Geback et al. 2009). Migration rate was calculated with the following equation: rate per hour= (average gap closure x image width in μm)/total hours and then divided by 2 to account for the migration of each cell boundaries towards each other.

HCC1806 Cell Crosslinking and ChIP-seq

HCC1806 cells were grown to 70% confluency, rinsed with PBS to remove media, cross-linked with (1%) formaldehyde for 10 minutes and quenched with glycine. The plates were scraped in PBS with protease

inhibitors (cOmplete, Mini, Roche) and 50 million cells were collected per ChIP replicate. Samples were sonicated for 20 minutes on the high setting (30 second ON, 30 second OFF cycles) using a Bioruptor to yield ~300bp DNA fragments in length. After sonication, samples were centrifuged at 14,000 rpm at 4°C to remove cellular debris and immunoprecipitated with antibodies specific for p73 (EP436Y, Abcam) and Pol II (sc-899, Santa Cruz Biotechnology). ChIP libraries were prepared as previously described (Marshall et al. 2016). Input DNA control was harvested from cross-linked and sonicated HCC1806 cells prior to immunoprecipitation. DNA fragments were sequenced at Vanderbilt Technologies for Advanced Genomics core.

ChIP-seq Analysis

Libraries were prepared for each input and ChIP sample (duplicate replicates for p73 and single replicate for Pol II). Sequencing was conducted on the Illumina HiSeq and 15-40 million reads were generated for each library. QC analysis was performed on FASTQ files using FastQC v0.11.5 (Andrews 2018). Reads were trimmed to remove adapter sequences using cutadapt v1.16 (Martin 2011; Dodt et al. 2012) and aligned to the mm10 genome using bwa (Li and Durbin 2009). Duplicate reads were marked using Picard Tools v2.17.11 (Institute 2018) and removed along with reads with low quality alignments ($q < 30$) using samtools v1.5 (Li et al. 2009). MACS2 was used to identify transcription factor binding sites (Zhang et al. 2008).

The distance to the nearest GENCODE vM10 protein coding TSS was calculated using bedtools v2.25.0 (Quinlan and Hall 2010). Motif analysis was performed using MEME-ChIP (Machanick and Bailey 2011). deepTools v3.0.1 (Ramirez et al. 2016) was used to compute the correlation of read coverage between p73 ChIP-seq replicates at p73 peaks, assess the strength of p73 and Pol II ChIPs (via fingerprint plots), and generate 1x depth normalized coverage tracks for each sample.

Mouse Model

p73 Knockout Mice

The conditional p73 knockout mouse with a deletion of exons 7, 8 and 9 was previously described (Marshall et al. 2016), and data included herein was generated using CMV-Cre congenic BALB/c and interbreeding with $p73^{floxE7\text{-}9}$ to obtain p73+/+, p73+/- and p73-/- mice. All procedures involving mice were in compliance with NIH guidelines and following Institutional Animal Care and Use Committee (IACUC) approved protocols.

Estrous Cycle Staging

Estrous cycle stages were determined by cytological evaluation of vaginal smears (Caligioni 2009; Byers et al. 2012). Proestrus stage is characterized by the predominance of nucleated epithelial cells. Estrus

exhibits clusters of cornified squamous epithelial cells (no visible cell nucleus). Metestrus is characterized by a mix of cornified epithelial cells and leukocytes and diestrus consists predominantly of leukocytes. Nulliparous p73+/+ and p73-/- female BALB/c mice at various ages were given vaginal smears daily for up to 10 days. Samples were collected by introducing 10 µl of saline solution into the vaginal canal of each mouse. The canal was flushed 2-3 times until the saline solution appears cloudy and transferred to a glass slide for analysis. Mice were sacrificed during diestrus for hormone analysis.

Hormone Analysis

Mice were anesthetized and blood was collected through cardiac puncture. For plasma isolation, 50 µl of 3.8% Sodium Citrate (Ricca Chemical) was added to each sample and centrifuged at 2,000 x g for 15 minutes. Progesterone, estradiol, testosterone and growth hormone levels were measured by ELISA at the Vanderbilt Hormone and Analytical Services Core.

For serum isolation, samples were collected in capped tubes and allowed to clot for 90 minutes at room temp. A wooden applicator stick was used to disrupt the coagulated blood from the tube wall and then sampes were centrifuged at 2,000 x g for 15 minutes. LH, FSH, inhibin A and inhibin B were measured by ELISA at University of Virginia Ligand Core Facility.

Progesterone Pellet Implantation

Progesterone pellets (15 mg/pellet, 60 d extended release) and placebo control were purchased from Innovative Research of America. Animals were anesthetized with isoflurane and iodine was applied at the incision site. Using a trocar, progesterone or placebo control pellets were implanted subcutaneously between shoulder blades in 5-week old nulliparous female p73+/+ and p73-/- BALB/c mice (Morrison et al. 2013). Animals were monitored for the following 7 days and identified no signs of distress. Tissue was harvested 3 weeks after pellet implantation.

For mating trials experiments and corpus luteum analysis, 5 mg/pellet, 21 days extended release was implanted in 12-week old nulliparous female p73+/+ and p73-/- BALB/c mice. After 7 days from pellet implantation, female mice were housed with wild-type males for a period of 14 days, at that point tissue was collected for analysis.

Murine Tissue Processing and Histological Staining

Mouse tissues were fixed in 10% neutral buffered formalin (NBF) overnight and paraffin embedded at Vanderbilt University Translational Pathology Shared Resource (TPSR). For hematoxylin and eosin (H&E), paraffin sections were rehydrated and stained for 5 minutes using Mayer's hematoxylin (Richard-Allen Scientific). Tissue sections were washed in water to remove excess staining and then stained in Eosin Y (Richard-Allen

Scientific) for 20 seconds. Sections were washed in 100% ethanol, dehydrated and coverslipped using Permount (Fisher). For TUNEL staining, apoptotic cells were detected using ApopTag Peroxidase In Situ Apoptosis Detection Kit (Millipore).

For whole mount analysis, murine mammary glands were fixed in Carnoy's fixative for 4 hours and then stained with carmine alum overnight. Lobular alveolar budding was determined by counting the average number of side branches per primary branch per animal (Morrison et al. 2015). Differences between p73+/+ and p73-/- groups were analyzed by unpaired two-tailed t-test.

Immunofluorescence

Tissue sections were de-paraffinized and rehydrated in ethanol (100%, 90%, 50% and H_2O) followed by (10X) Antigen Retrieval Citra Plus Solution (BioGenex) diluted in H_2O for a final concentration of (1X). Slides were heated in the microwave for 13 minutes at high power. Tissue was permeabilized in 0.1% Tween 20 in PBS for 10 minutes and blocked with 5% goat serum and 0.3% Triton X in PBS for 1 hour at room temperature. Endogenous HRP in tissue sections was quenched with a 3% hydrogen peroxide solution for 5 minutes. Tissues were blocked with Image-it Enhancer (Life Technologies) for 30 minutes at room temperature and then incubated in M.O.M block (Vector) as needed. All primary antibodies were

incubated overnight at 4°C at concentrations shown in Table 2.1. For secondary antibodies, we used either fluorescently labeled AlexaFlour (Life Technologies) or HRP-conjugated with CY3/FITC TSA amplification kit (Perkin Elmer). For TSA amplification was used for the detection of Cyp17a1, Foxl2 and p73, tissue was incubated for 8 minutes using CY3 or FITC diluted at 1:50 in dilution buffer. Sections were coverslipped using SlowFade Gold with DAPI (Life Technologies).

Ovarian Follicle Quantification

Ovaries from adult p73+/+ and p73-/- nulliparous mice were collected. The entire murine ovaries were sectioned through at 5 μm thickness and follicles were counted in every 10^{th} section. Follicles without a layer of granulosa cells or a single layer of squamous granulosa cells were classified as primordial follicles. Follicles with a single layer of cuboidal granulosa cells were classified as primary follicles. Secondary follicles were classified as two or more layers of granulosa cells and antral follicles by the presence of an atrium. Secondary and antral follicles were counted only when the nucleolus was present in the oocyte. To determine the overall follicle number per ovary, the total number of sections was multiplied by the average number of follicles per section as previously described (Kim et al. 2015).

Table 2.1 List of Antibodies Used in this Dissertation					
Epitope	**Catalog no.**	**Company**	**Species**	**Western Blot**	**Immunofluorescence / IHC**
Cyp17a1	sc-46081	Santa Cruz	Goat		1 to 1000
Cytokeratin 14	20R-CP002	Fitzgerald	Guinea Pig		1 to 200
Foxl2	ab5096	Abcam	Goat		1 to 1000
GAPDH	MAB374	Millipore	Mouse	1 to 25000	
Ki67	CRM325B	Biocare	Rabbit		1 to 100
Laminin	ab11575	Abcam	Rabbit		1 to 4000
PARP	9542L	Cell Signaling	Rabbit	1 to 1000	
p63 (H-129)	sc-8344	Santa Cruz	Rabbit		1 to 40
p73 (EP436Y)	ab40658	Abcam	Rabbit	1 to 500	1 to 1000

‡

‡ Table shows antibody epitope target with catalog number and company. Antibodies were used at the indicated concentrations for Western blot analysis and/or immunofluorescence or immunohistochemistry.

Murine Protein Harvest and Immunoblotting

Whole mouse ovaries were collected at 6, 9, 12 and 16 weeks from p73+/+ and p73-/- mice, homogenized on ice and lysed in RIPA buffer. Immunoblot analysis was conducted using 100 μg of tissue lysate.

Mouse Embryonic Fibroblasts (MEFs) Isolation and Culture

Mouse embryos were harvested from p73+/- female mice 13-14 days after the appearance of vaginal plug (Durkin et al. 2013). Mice were sacrificed and uterus with embryos were collected in sterile PBS supplemented with penicillin/ streptomycin, fungizone and gentamicin. Embryos were dissected from the yolk sac and separated individually into petri dishes. The head and red tissues (heart and liver) were removed from the embryo using forceps and surgical scissors, and the embryo placed in a clean petri dish with 5 ml of 0.25% trypsin-EDTA. The embryo was then finely minced with a scalpel blade and mixed by pipetting the solution up and down several times. The dish was incubated at 37°C for 10 min, mixed by pipetting several times and then incubated for an additional 10 min. The cell suspension was transferred to a 50 ml conical tube with 10 ml of MEF culture media (DMEM, 20% FBS and 1% penicillin-streptomycin) to inactivate trypsin and mixed. After the cell suspension settled for 5 min, the supernatant was transferred to T75 cell culture flask. Genotypes were confirmed by PCR.

mRNA Isolation and qRT-PCR Analysis

Cell pellets from p73+/+ and p73-/- MEFs were harvested for RNA using the Aurum Total RNA Mini kit (Bio-Rad). Samples were needle passage in lysis buffer and DNAse treated for 30 min at room temperature on the RNA purification column. cDNA was generated using oligo(dT)-mediated single strand synthesis with the TaqMan Reverse Transcription kit (Applied Biosystems) and IQ SYBR Green Supermix (Bio-Rad) for quantification. p73 mRNA primers were designed to target exon 6/7 junction (GTGGATGACCCTGTCACCGG /GAAGTTGTACAGGATGGTGG).

Laser Capture Microdissection (LCM) of Murine Follicles and RNA Harvest

Samples were collected from three p73+/+ and p73-/- nulliparous female mice; ovaries were embedded in optimal cutting temperature (OCT) compound (Tissue-Tek) and 8 µm sections were mounted on non-charged glass slides (Fisher). Slides were dehydrated and loaded onto the laser capture microdissection stage (ArcturusXT Laser Capture Microdissection System) at Vanderbilt Translational Pathology Shared Resource. A Capsure Macro LCM cap (Life Technologies) was placed over tissue and antral follicles were captured using an infrared capture laser. RNA was harvested using PicoPure RNA Isolation Kit (Applied Biosystems). Samples were

submitted to the Vanderbilt Technologies for Advanced Genomics Core for library preparation and sequencing.

Murine Granulosa Cell (MGC) Isolation and Culture

Ovaries from p73+/+ and p73-/- adult mice were collected in DPBS and 1mg/ml BSA, then rinsed in PBS supplemented with penicillin/streptomycin, fungizone and gentamicin. Granulosa cells were isolated through mechanical dissociation followed by enzymatic digestion (1.5 ml of 0.05% Trypsin and 20 µl of DNAse per animal) at 37°C for 45 min (Eppig and Wigglesworth 2000; Eppig et al. 2000). Enzymatic digestion was later inactivated with FBS; granulosa cells were then filtered using a 30µm cell strainer (Wolflabs) and centrifuged at 1000rpm for 5 min. Collected cells were cultured on 60mm fibronectin-coated culture dish in DMEM/F12 (Life Technologies; supplemented with insulin, transferrin and sodium selenite) with 10% FBS for 48 hours before further experiments.

MGCs Ectopic Overexpression of p73 and RNA Harvest

Isolated granulosa cells from four p73+/+ and p73-/- mice were infected 48 hours after isolation with TAp73β and Fg12-CMV control expression vector as previously described (Rosenbluth et al. 2008; Rosenbluth et al. 2011). Cells were grown for 48 hours after infection and RNA was harvested using RNAqueous-Micro Total RNA isolation kit

(Fisher). Samples were submitted in duplicate to the Vanderbilt Technologies for Advance Genomics core for library preparation and sequencing.

RNA-seq Analysis

Stranded RNA-seq libraries were prepared for each sample by poly-A selection. RNA-seq was conducted on the Illumina HiSeq 3000 (PE75) and 20-30 million reads were generated for each library. Reads were trimmed to remove adapter sequences using Flexbar v3.0 (Dodt et al. 2012) and aligned to the mm10 genome using STAR v2.5.2 (Dobin et al. 2013). GENCODE vM10 gene annotations were provided to STAR to improve the accuracy of mapping. featureCounts v1.5.3 (Liao et al. 2014) was used to count the number of mapped reads to each GENCODE vM10 gene. Differential gene expression analysis and PCA was performed with DESeq2 v1.14.0 (Love et al. 2014). Genes were classified as differentially expressed if they had a FDR-adjusted p-value <0.1 Heatmaps of gene expression were generated using the pheatmap package (Kolde 2015). Genome Ontology pathway over-representation analysis was performed on protein-coding genes that were differentially expressed using the WebGestaltR package (Wang et al. 2017).

CHAPTER III

P73 IS REQUIRED FOR OVARIAN FOLLICLE DEVELOPMENT AND REGULATES A GENE NETWORK INVOLVED IN GRANULOSA-TO-GRANULOSA CELL ADHESION

Introduction

The p53 family of proteins, p53, p63 and p73, are sequence-specific transcription factors required for cell cycle control, DNA repair, apoptosis, adhesion, organ development and cell differentiation (Kaghad et al. 1997; Schmale and Bamberger 1997; Osada et al. 1998; Trink et al. 1998; Yang et al. 1998; Holembowski et al. 2014). All three p53 family members share a high degree of structural and amino acid sequence similarities within their transactivation domains, DNA binding domains and oligomerization domains (Harms and Chen 2006; Dotsch et al. 2010), which accounts for similar genomic binding sites and regulation of overlapping target genes. Unlike p53, p63 and p73 are transcribed from two separate promoters that encode functionally divergent variants. While the transcriptionally active (TA) isoform encodes the full-length protein, the alternative transcript (ΔN), encodes an isoform lacking the amino terminal transactivation domain (Kaghad et al. 1997; Yang et al. 1998). Thus, ΔNp63 and ΔNp73 isoforms act as dominant

negative regulators of TAp63 and TAp73 (Yang et al. 1998; Grob et al. 2001; Stiewe et al. 2002).

p63 and p73 play important roles in cell differentiation and tissue development. p63 is a key regulator of ectodermal differentiation and stratification of the epidermis. Mice lacking p63 fail to develop stratified epithelia, exhibit defective limb and glandular epithelial development, and die shortly after birth due to dehydration (Mills et al. 1999; Yang et al. 1999). Mice deficient for all isoforms of p73 exhibit runting, sterility, hippocampal dysgenesis and hydrocephalus, as well as chronic infection and inflammation in the lungs, sinus and ears (Yang et al. 2000). The development of p73 isoform-specific knockout mouse models provided significant insight to the roles of select p73 isoforms. TAp73-deficient mice exhibit sterility, hippocampal dysgenesis, hydrocephalus, premature aging, genomic instability and increased frequency of tumors (Tomasini et al. 2008). In contrast, mice that lack ΔNp73 are fertile and display signs of neurodegeneration, including hippocampal dysgenesis and hydrocephalus (Wilhelm et al. 2010). Thus, the sterility defects observed in the global p73-deficient animals are due to a deficiency in the TAp73 isoform. Recently, our lab (Marshall et al. 2016) and others (Nemajerova et al. 2016) discovered that TAp73 is required for multiciliated cell differentiation and acts as a transcriptional regulator of a gene network required for ciliogenesis. The discovery provided mechanistic insight to the diverse phenotypes observed

in p73-deficient mouse models. Impaired cilia formation in p73-deficient mice leads to insufficient clearance of pathogens from the lungs and sinuses causing chronic inflammation. Further, loss of cilia in reproductive tissues decreases transport of the sperm and ova through epididymis and fallopian tubes, respectively, leading to infertility.

Other phenotypes of p73-deficient mice have been reported that are likely to originate from processes unrelated to ciliogenesis. Male mice that lack TAp73 exhibit increased DNA damage and apoptosis in spermatogonial cells within the testes, which results in defective germ cell maturation and differentiation required for proper spermatogenesis (Holembowski et al. 2014; Inoue et al. 2014). TAp73-deficient female mice exhibit meiotic spindle formation abnormalities during oocyte maturation and impaired ovulation (Tomasini et al. 2008). We report herein that p73 expression in the ovarian follicle, the structure in which the oocyte develops, is critical for oocyte development, ovulation, and fertility. Specifically, p73 is required in granulosa cells for expression of a p73-dependent gene set that regulates cell-to-cell adhesion, including genes that encode key components of granulosa cell-associated focimatrix.

Results

p73 is Required for Murine Ovarian Follicle Maturation

We analyzed ovaries from age-matched nulliparous female mice genetically engineered to lack functional p73 in all tissues [referred to a p73-/- hereafter and described in (Marshall et al. 2016)]. Histological analysis of ovaries in 12 week-old p73+/+ female mice confirmed the presence of corpus luteum, the final stage of the mature ovarian follicle, suggesting that follicle maturation and ovulation were ongoing in mice at this age. While p73+/+ ovaries harbored an average of 12 luteal structures per ovary, age-matched p73-/- ovaries had an average of 1 luteal structure per ovary (p-value <0.01) (Figure 3.1 A and B). We quantified the total number of follicles per ovary at various stages of development (primordial, primary, secondary and antral stage) using methodology as previously described (Kim et al. 2015) (Figure 3.2 A and B). We observed a 35% decrease in the number of primary follicles (p-value <0.001), a 59% decrease in the number of secondary follicles (p-value <0.001) and a 49% decrease in the number of antral follicles (p-value <0.001); but no significant difference in the number of primordial follicles in p73-/- mice compared to p73+/+ littermates (Figure 3.2 C).

Analysis of p73 protein levels in murine ovaries, at 6, 9, 12 and 16 weeks of age, confirmed that full-length p73 protein was expressed in

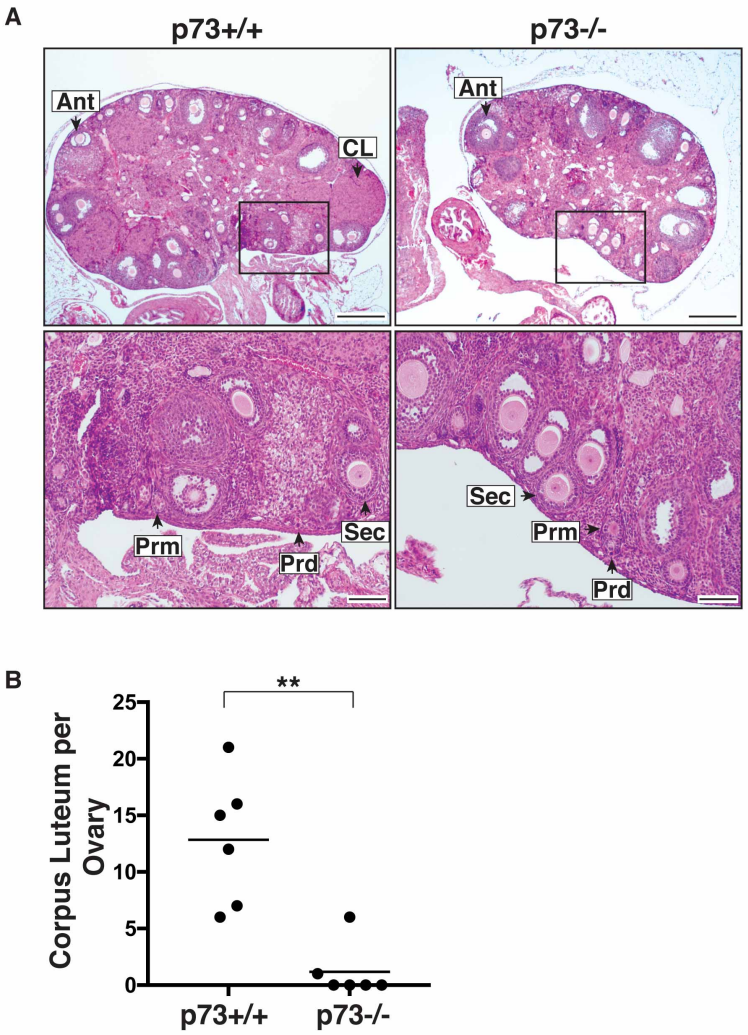

Figure 3.1. p73 is Required for Ovarian Follicle Development and Corpora Lutea Formation.

(A) Representative H&E images of p73+/+ and p73-/- ovaries (scale bars = 400 μm and 100 μm). Arrowheads and labels represent corpora lutea (CL) and different stages of follicle development: primordial (Prd), primary (Prm), secondary (Sec) and antral (Ant) follicles. (B) Total number of corpus luteum per ovary . Bars represent the mean. p-values represent <0.01 (**).

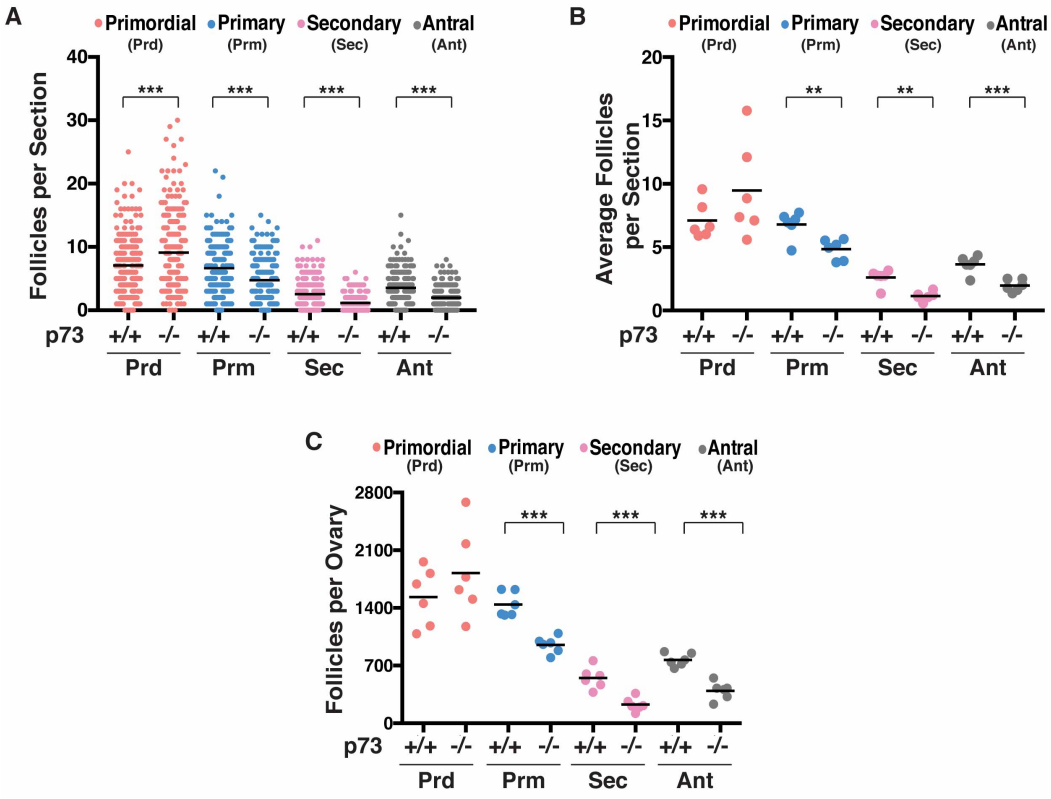

Figure 3.2. Attenuated Follicle Development Observed in p73-/- Ovaries.
(A) Total follicles counted per section in p73+/+ and p73-/- primordial (Prd), primary (Prm), secondary (Sec) and antral (Ant) and (B) Average number of follicles per section. (C) Total number of follicles per ovary. Each data point represents the average of two independent manual quantifications of six ovaries per genotype. Bars represent the mean. Asterisks represent p-values <0.01(**) and <0.001 (***).

ovaries collected at all time points in p73+/+ animals and was not expressed in p73-/- animals (Figure 3.3 A). To determine the localization of p73 protein within the ovary, we used well-established cell markers to stain follicular granulosa cells (Foxl2) (Schmidt et al. 2004) and follicular theca cells (Cyp17a1) (Park et al. 2010). Through immunofluorescence (IF) staining, p73 was expressed in Foxl2-positive granulosa cells (Figure 3.3 B, top panel) but not in Cyp17a1-positive theca cells (Figure 3.3 C, top panel). Although the number of follicles were reduced in the absence of p73, we found that, in cases in which follicles were able to form in p73-/- ovaries, the lack of p73 did not block formation of the granulosa or theca cell layer in the follicle (Figure 3.3 B and C, lower panels). p73 expression was observed in Foxl2-positive granulosa cells at different stages of follicle development including primary, secondary and antral follicles (Figure 3.4). We further analyzed p73 expression in human ovaries using data obtained from the Genotype-Tissue Expression (GTEx) Project (analysis date: January 19, 2018), and found that p73 is expressed at 0.6 transcript per million (TPM). Specifically, TAp73α and TAp73β are the predominant N-terminal isoforms expressed in human ovaries (Table 3.1).

Given the potential for hetero-oligomerization between p73 and its family member p63 (Chan et al. 2004; Harms and Chen 2006; Rocco et al. 2006), we determined if p63 and p73 were co-expressed during follicular development using dual IF detection of the proteins. p63 expression was

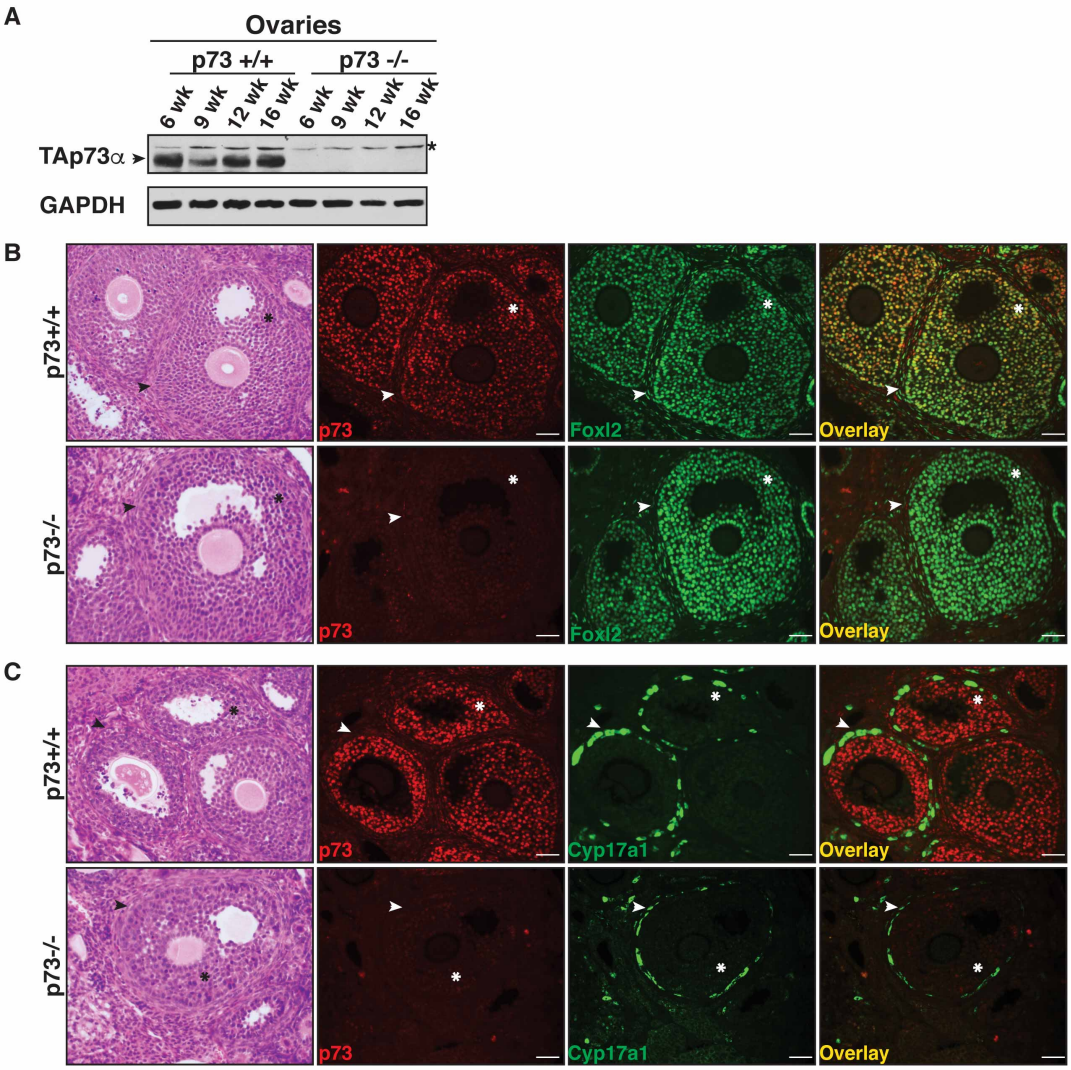

Figure 3.3. p73 Expression in Murine Ovaries.
(A) Western analysis of the indicated proteins harvested from ovaries of the indicated genotypes at various ages show an absence of p73 protein expression (arrowhead) in p73-/- mice (Top panel, * represents non-specific bands). (B-C) Representative H&E (asterisks represent granulosa cells and arrowheads represent theca cells) and IF images of p73+/+ and p73-/- ovaries show (B) p73 (red) co-localizes with granulosa cell marker Foxl2 (green) in the follicles. (C) p73 (red) is not expressed in theca cells, which are stained by Cyp17a1 (green) (scale bar = 50 μm).

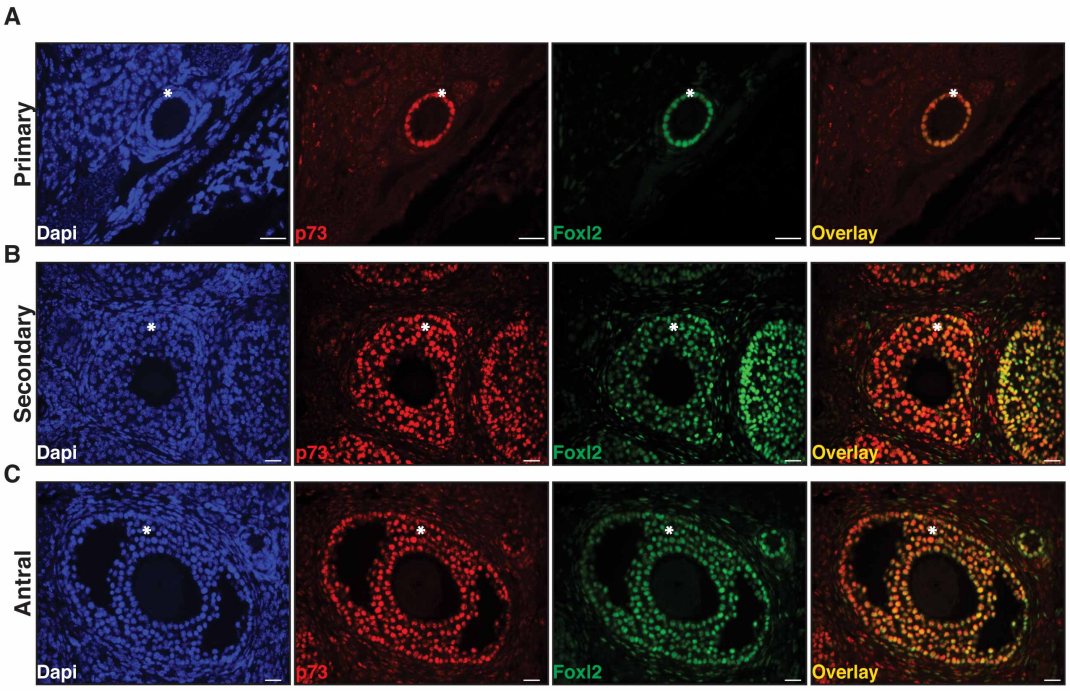

Figure 3.4. p73 is Necessary in Granulosa Cells at Different Stages of Follicle Development.
(A-C) IF images of p73+/+ ovaries show p73 (red) co-localizes with granulosa cell marker Foxl2 (green) at different stages of follicle development (asterisks represent granulosa cells). (A) Primary, (B) Secondary and (C) Antral follicles (scale bar=25 μm).

Table 3.1 p73 Expression in Human Ovaries	
p73 Isoform	**Percentage (%)**
TAp73	100.0
ΔNp73	0.0
C-Terminal Isoform	**Percentage (%)**
TAp73α	59.8
TAp73β	40.2
TAp73γ	4.1
TAp73δ	0.0
TAp73ε	4.1
TAp73ζ	0.0

§

§ Table shows p73 isoform-specific expression in human ovaries obtained from the GTEx Project on January 19, 2018.

restricted to oocytes (arrowhead) of primordial follicles in p73+/+ (Figure 3.5, top panel), consistent with previously published data showing p63 expression in primordial follicles promotes genome integrity during meiotic arrest (Suh et al. 2006). The oocyte-restricted expression pattern of p63 was unaltered in p73-/- ovaries (Figure 3.5, lower panel).

Due to the previously published role of p73 in cell cycle control and DNA damage, we hypothesized the loss of p73 in granulosa cells leads to apoptosis and cell cycle arrest consistent with the decreased ovarian follicle development observed in our p73-/- female mice. We determined if the attenuated follicle development observed in p73-/- female mice is due to increased atretic follicles. TUNEL staining, a marker for apoptosis, show no difference in apoptotic figures between p73+/+ and p73-/- ovaries from adult female mice (Figure 3.6). In addition, murine ovaries were stained with Ki67 to determine granulosa cell proliferation. We observed no difference in Ki67 positive granulosa cells between p73+/+ and p73-/- ovaries (Figure 3.7).

The ovarian phenotypes observed in our p73-/- female mice are consistent with the fertility defects reported in TAp73-deficient animals, but not ΔNp73-deficient mice, given that both females and males are fertile in the latter (Tomasini et al. 2008; Wilhelm et al. 2010). TAp73-deficient females showed defective follicle development and significantly decreased ovulation rate relative to wild-type animals in response to exogenous hormone stimulus, and the few ovulated oocytes observed were trapped

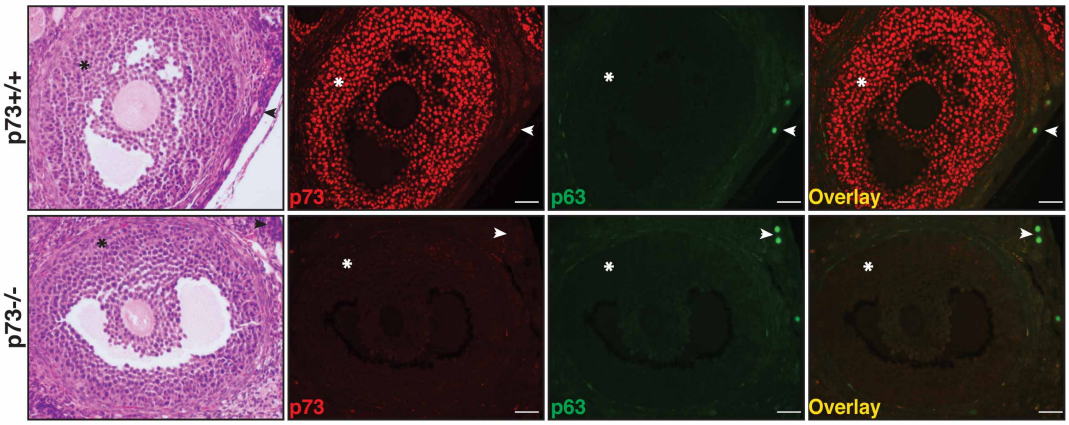

Figure 3.5. p73 and p63 Expression in Murine Ovaries.
Representative H&E (asterisks represent granulosa cells and arrowheads represent primordial follicle) and IF images of p73+/+ and p73-/- ovaries show p63 (green) is expressed in the oocyte of primordial follicles, while p73 (red) is expressed in granulosa cells (scale bar = 50 μm).

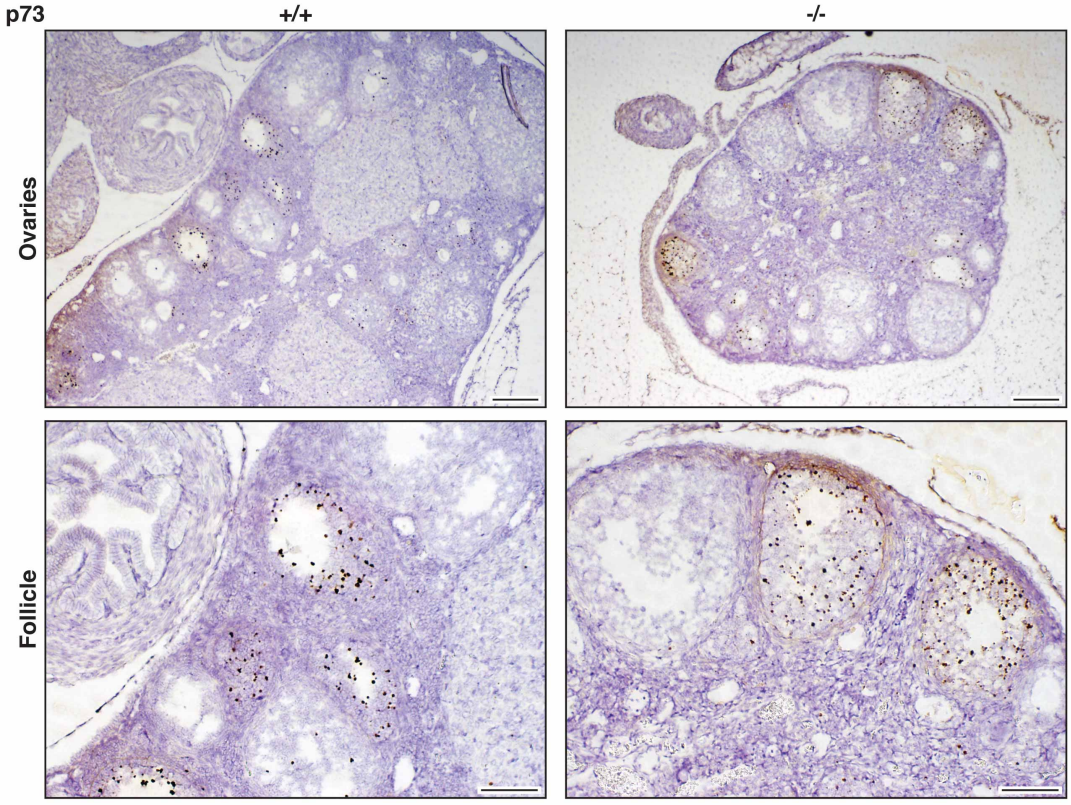

Figure 3.6. p73+/+ and p73-/- Mice Exhibit Similar Levels of Apoptosis in the Ovaries. Representative images of TUNEL staining show no difference in apoptotic figures between p73+/+ and p73-/- follicles from adult female mice (scale bars=200 and 100μm).

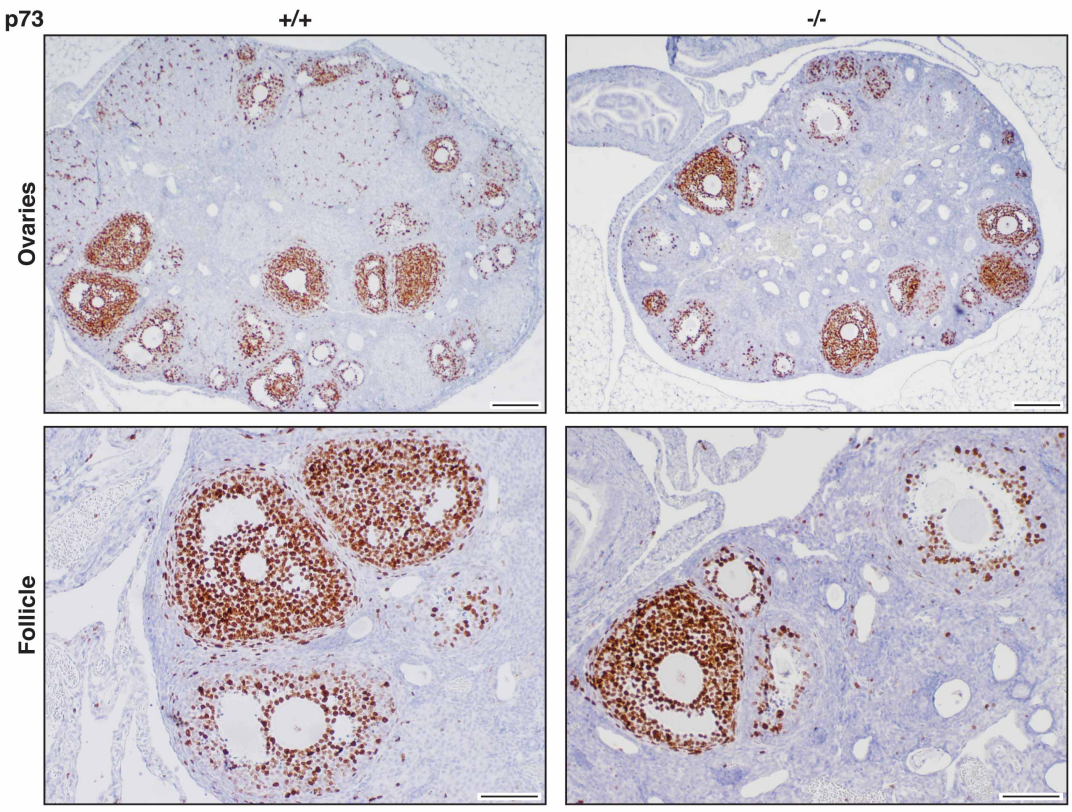

Figure 3.7. Similar Proliferation Pattern in the Ovaries of p73+/+ and p73-/- Mice. Representative images of Ki67 staining show similar Ki67 expression between p73+/+ and p73-/- follicles from adult female mice (scale bars=200 and 100μm).

under the bursa and unable to reach the fallopian tube for implantation (Tomasini et al. 2008), possibly due to the lack of ciliated cells lining the oviduct (Marshall et al. 2016). The corpora lutea are the primary sites of progesterone production after ovulation in mice (Allen 1941; Rothchild 1981). Therefore, the lack of corpora lutea observed in our p73-/- female mice (Figure 3.1 B) led us to compare the levels of circulating hormones in the p73+/+ and p73-/- female mice.

Loss of p73 Leads to a Significant Decrease in Circulating Progesterone

Given the impact of p73 loss on folliculogenesis and the number of corpora lutea, we measured circulating progesterone in nulliparous p73+/+ and p73-/- mice at 6, 9 and 12 weeks of age. Progesterone levels fluctuate throughout the stages of the estrous cycle (Byers et al. 2012). We assessed the estrous cycle through vaginal cytology and observed that p73-/- mice exhibit aberrant estrous cycle with prolonged diestrus stage compared to p73+/+ (Figure 3.8). Given the acyclic nature of p73-/- female mice, all circulating hormones were analyzed from the only shared stage (diestrus) between both phenotypes. Progesterone levels decreased nearly 75% in p73-/- samples collected at 6 weeks of age (p-value <0.05), and 82% (p-value <0.01) at 12 weeks of age relative to p73+/+ mice (Figure 3.9 A). Circulating estradiol levels in p73-/- mice were similar to p73+/+ at each time

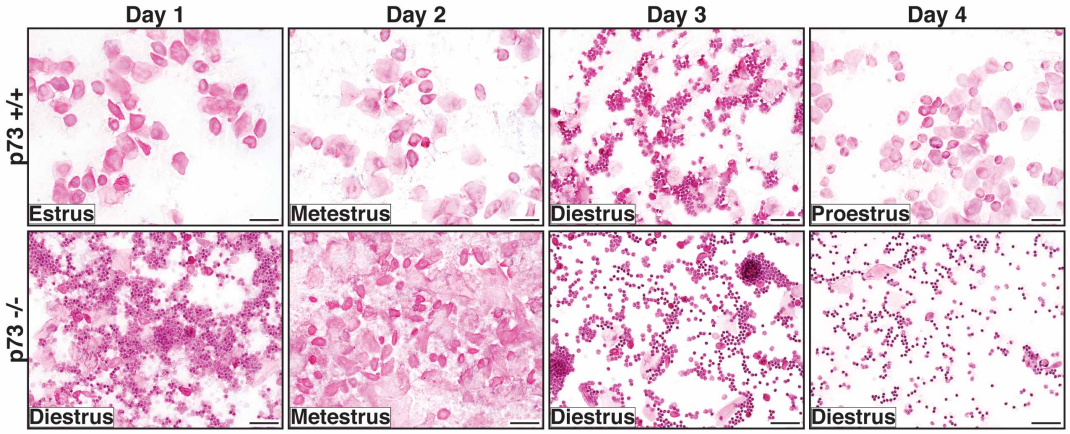

Figure 3.8. Estrous Cycle Analysis of p73+/+ and p73-/- Female Mice.
H&E of vaginal cytology identifies stages of the estrous cycle; proestrus, estrus, metestrus and diestrus (scale bar = 50 μm).

point analyzed (Figure 3.9 B), although testosterone was reduced 55% in p73-/- samples harvested at 12 weeks of age (p-value <0.01) (Figure 3.9 C).

Circulating hormones originating from the pituitary gland and ovaries, including follicle-stimulating hormone (FSH), luteinizing hormone (LH), inhibin A, inhibin B and growth hormone (GH), are key regulator of the estrous cycle, thus could exert a marked influence in progesterone production and follicle development. Therefore, we measured circulating FSH levels in 12-week old nulliparous mice, finding a 50% decrease in FSH levels in p73-/- compared to age-matched p73+/+ mice (p-value <0.01) (Figure 3.10 A). These findings are consistent with previous studies showing that FSH promotes granulosa-theca cell interactions that drive the production of ovarian testosterone (Smyth et al. 1993), thus constituting a possible mechanism to explain the decrease in testosterone observed in p73-/- female mice. LH and inhibin A levels were modestly decreased in p73-/- mice, albeit not to a statistically significant degree (Figure 3.10 B and C). No difference in circulating inhibin B and GH were observed between p73+/+ and p73-/- samples (Figure 3.10 D and E).

To determine if the hormonal differences in the p73-/- mice were linked to gross abnormalities in pituitary gland morphology due to hippocampal dysgenesis and hydrocephalus (Yang et al. 2000; Talos et al. 2010), we analyzed pituitary gland tissue sections from p73+/+ and p73-/-

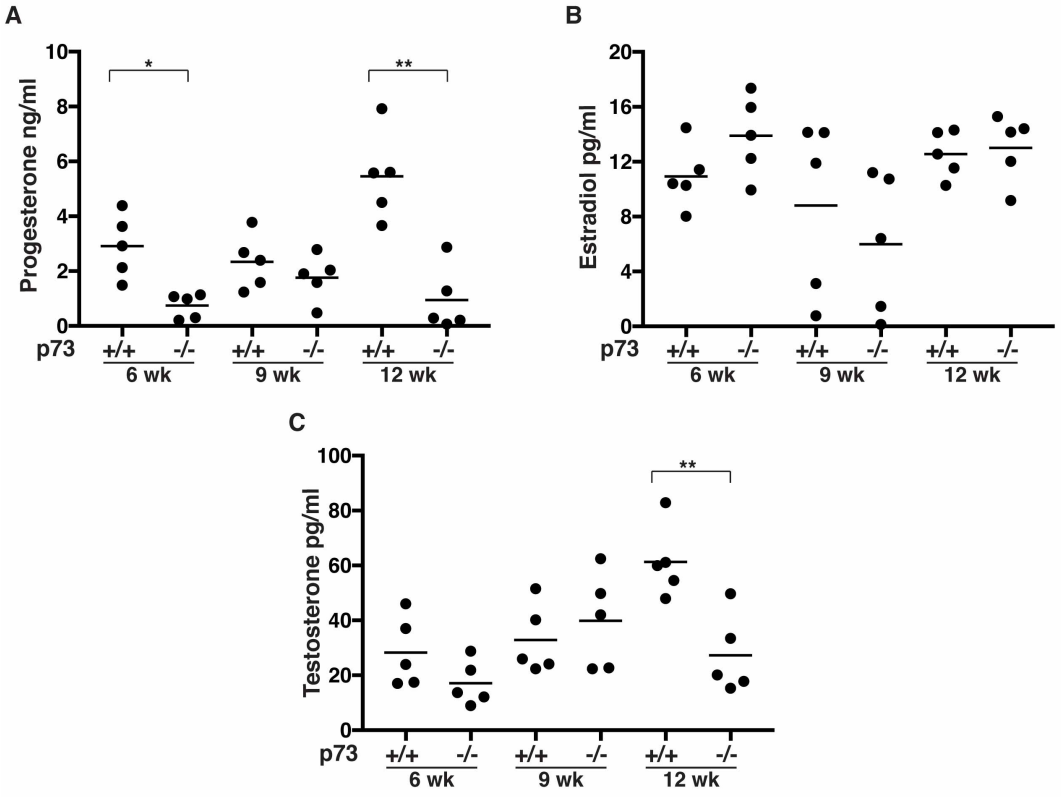

Figure 3.9. Analysis of Circulating Steroid Hormones throughout Development in p73+/+ and p73-/- Female Mice.

Plasma levels measure by ELISA of (A) progesterone, (B) estradiol and (C) testosterone from five female mice per genotype at 6, 9 and 12 weeks of age; assay sensitivity range 0.2-50 ng/ml, 1-100 pg/ml and 5-100 pg/ml, respectively. Bars represent the mean. Asterisks represent p-values <0.05 (*) and <0.01 (**).

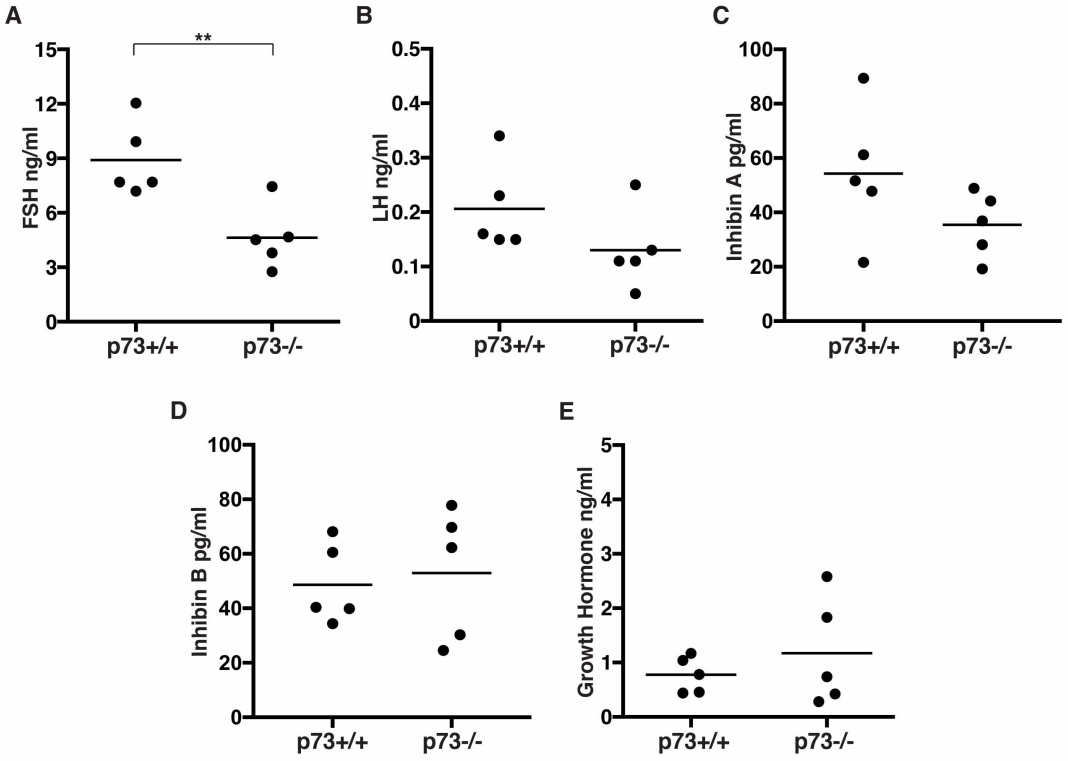

Figure 3.10. Circulating Hormone Analysis of p73+/+ and p73-/- Female Mice.
Serum levels of (A) FSH, (B) LH, (C) Inhibin A, (D) Inhibin B, (E) plasma levels of GH, measured by ELISA, from five mice per genotype at 12 weeks of age; assay sensitivity range 2.4-300 ng/ml, 0.016-4 ng/ml, 10-934 pg/ml, 10-950 pg/ml and 0.005-20 ng/ml, respectively. Asterisks represent p-values <0.01(**).

female mice. The murine pituitary gland is composed of anterior (pars distalis, D; and intermedia, I) and posterior (pars nervosa, N) lobes. Despite diminished FSH production in p73-/- mice, we did not observe any overt histological differences in the pars distalis (asterisk) (Figure 3.11 A), where gonadotropin hormones (FSH, LH and GH) are produced and secreted. In addition, we evaluated p73 expression in the pituitary gland of p73+/+ mice through IF. We observed p73-positive cells in pars intermedia (solid-line box), but not in pars distalis (dashed-line box) (Figure 3.11 B). Previous studies have shown that TAp73-deficient male mice have normal levels of FSH, LH and gonadotropin-releasing hormone (GnRH) supporting normal pituitary gland signaling (Holembowski et al. 2014). In addition, immature TAp73-deficient ovaries fail to respond to exogenous hormone stimulation and show a significant decreased ovulation rate compared to age-matched wild-type mice (Tomasini et al. 2008) suggesting a role of p73 in ovarian follicle development.

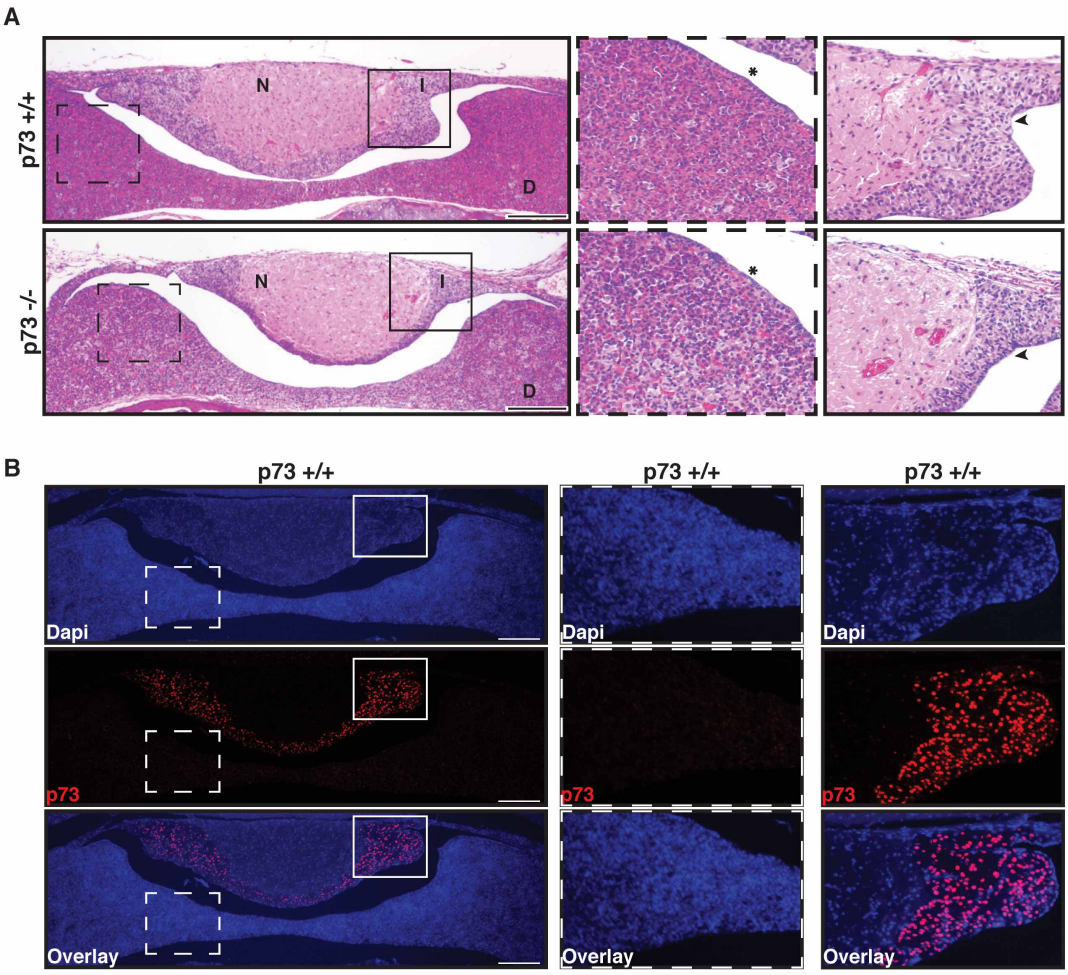

Figure 3.11. Pituitary Gland Analysis of p73+/+ and p73-/- Female Mice.
(A) Representative H&E images of pituitary gland sections showing all three layers (pars distalis [asterisk], D; pars intermedia [arrowhead], I; pars nervosa, N) between p73+/+ and p73-/- mice (scale bar = 200 μm). (B) Representative IF images of p73+/+ pituitary gland show p73 (red) expression in pars intermedia (solid-lined box) and not in pars distalis (dashed-line box) (scale bar = 200 μm).

Ectopic Progesterone Partially Rescues Ovarian Follicle Development in p73-deficient Mice

To determine if ectopic progesterone could rescue ovarian follicle maturation, 60 day-release progesterone pellets (15 mg) were implanted subcutaneously in 5-week old nulliparous p73+/+ and p73-/- female mice and ovaries were analyzed 21 days after implantation. The ovaries from p73-/- mice with the placebo pellet harbored fewer primary, secondary and antral follicles, and were substantially smaller than placebo-treated p73+/+ mice (Figure 3.12 A, left panel and B). However, ovaries from p73-/- mice treated with ectopic progesterone were similar in size to ovaries from placebo- or progesterone-treated p73+/+ mice (Figure 3.12 A, right panel), and contained a greater number of primary, secondary and antral follicles than placebo-treated p73-/- ovaries, similar to what was seen in progesterone- or placebo-treated p73+/+ mice (Figure 3.12 C). As a control, circulating progesterone was measured at the time of sacrifice to confirm that ectopic progesterone pellet increased circulating progesterone in p73-/- mice to levels comparable to both placebo- and progesterone-treated p73+/+ mice (Figure 3.12 D).

To assess the effect of ectopic progesterone on female sterility in our mouse model (Marshall et al. 2016), we determined the reproductive ability of placebo- or progesterone-treated p73+/+ and p73-/- female mice through mating trials. Twelve-week old p73+/+ and p73-/- female mice were

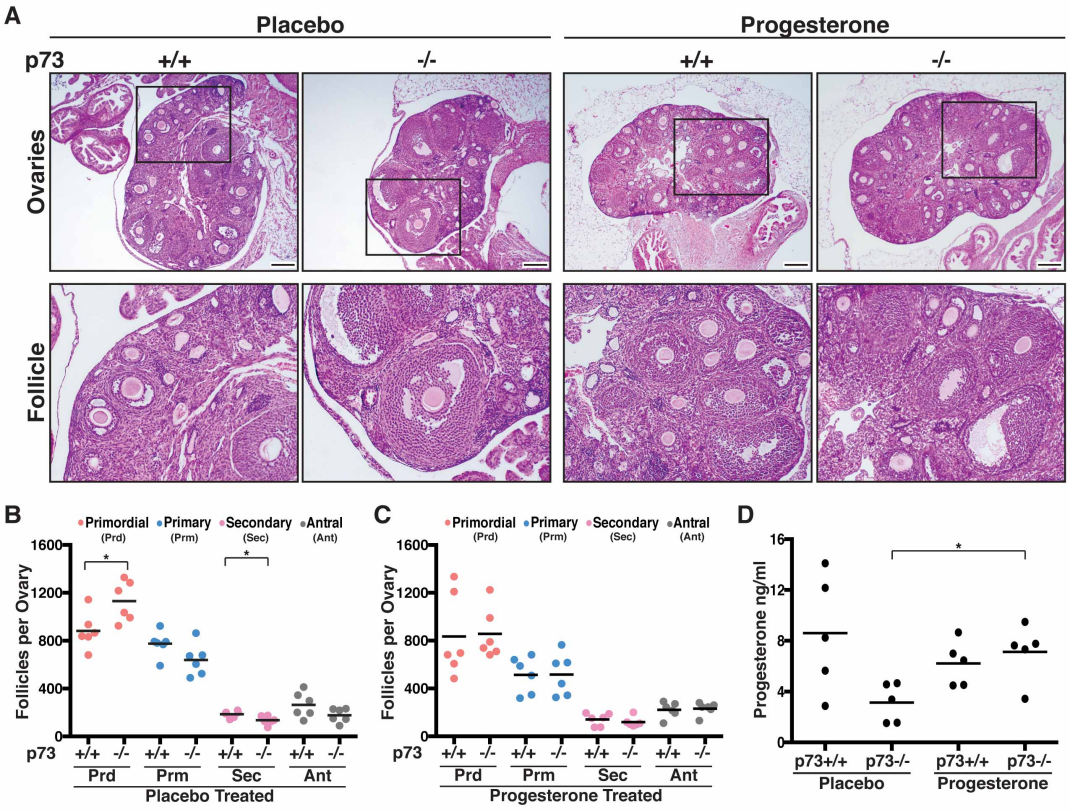

Figure 3.12. Ectopic Progesterone Rescues Follicle Development in p73-/- Ovaries. Progesterone slow-release pellet or placebo control (15 mg/pellet, 60 d extended release) were implanted in five female mice per genotype at 5 weeks of age. (A) Representative H&E images of placebo control and ectopic progesterone-treated ovaries of p73+/+ and p73-/- mice (scale bar = 200 μm). (B-C) Follicle quantification of placebo control and progesterone-treated p73+/+ and p73-/- ovaries, respectively. Data are shown as number of follicles per ovary, primordial (Prd), primary (Prm), secondary (Sec) and antral (Ant). (D) Plasma levels of progesterone were measured through ELISA from placebo control and progesterone-treated p73+/+ and p73-/- female mice. Asterisks represent p-values <0.05 (*).

implanted with placebo or progesterone pellets and housed with p73+/+ males for a period of 14 days. At day 15, pregnancy status was determined and tissue was harvested for histological analysis. In p73+/+, two of two placebo-treated and two of three progesterone-treated female mice became pregnant, indicating that the level of ectopic progesterone administered did not inhibit their reproductive ability. In contrast, zero of five p73-/- mice, either placebo- (two mice) or progesterone-treated (three mice) became pregnant. These results were not surprising given the lack of ovulation, corpus luteum formation and ciliated cells in the p73-deficient mice (Marshall et al. 2016). Ciliated cells are required for transport of the oocyte through the oviduct and to the uterus (Halbert et al. 1976; Critoph and Dennis 1977). Also, we analyzed the ability of ectopic progesterone to rescue corpus luteum formation by implanting placebo or progesterone pellets (5 mg) in twelve week-old nulliparous p73+/+ and p73-/- female mice. After 21 days, corpora lutea (arrowhead) were observed in p73+/+ with placebo or progesterone pellet. However, administration of ectopic progesterone in p73-/- mice was not able to rescue formation of corpora lutea (Figure 3.13, arrowhead).

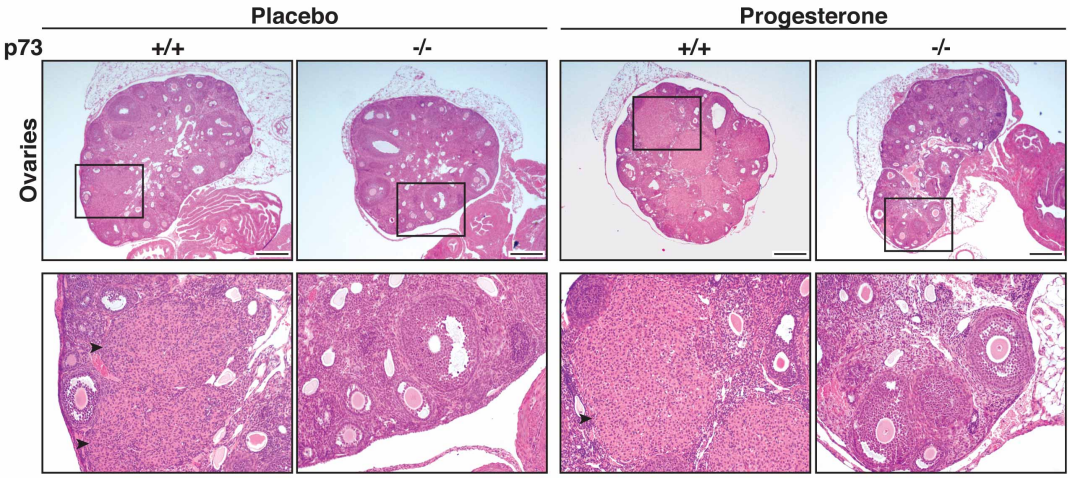

Figure 3.13. Ectopic Progesterone Fails to Rescue Corpus Luteum Formation in p73-/- Ovaries.

Progesterone slow-release pellet or placebo control (5 mg/pellet, 21 d extended release) was implanted in 12 week-old p73+/+ and p73-/- female mice. Representative H&E images of placebo control and ectopic progesterone-treated ovaries of p73+/+ and p73-/- mice at 15-weeks of age (scale bar = 400 μm). Corpus luteum (arrowhead) was observed in p73+/+ progesterone-treated or placebo control mice.

Ectopic Progesterone Rescues Lobulo-alveolar Budding in p73-deficient Mice

Mice that lack progesterone receptor exhibit defects in follicle rupture causing impaired ovulation, absence of corpora lutea and female infertility (Lydon et al. 1995; Lydon et al. 1996); similar to the phenotypes observed in our p73-/- female mice. Further, impaired progesterone signaling leads to defects in proper mammary gland development by impeding the formation of lobulo-alveolar buds, small grape-like epithelial protrusions that, in the event of pregnancy, will generate the milk-producing alveoli (Lydon et al. 1995; Bocchinfuso et al. 2000; Hennighausen and Robinson 2005). Given the similarities between the progesterone receptor-deficient mice and our p73-/- female mice, we assessed the hormonally-responsive function of the mammary glands from mice treated with slow-release progesterone pellets, as described above. Using whole mount Carmine staining to visualize the mammary epithelium, we noted a 50% reduction (p-value <0.01) in lobulo-alveolar budding in placebo-treated p73-/- mice compared to p73+/+ (Figure 3.14 A, left panel and B). Progesterone-treated p73-/- female mice exhibited a complete rescue of lobular alveolar budding and comparable mammary gland morphology to progesterone-treated p73+/+ control (Figure 3.14 A, right panel). Ectopic progesterone significantly increased the number of lobulo-alveolar buds in p73-/- mammary gland by 200% (p-value <0.001)

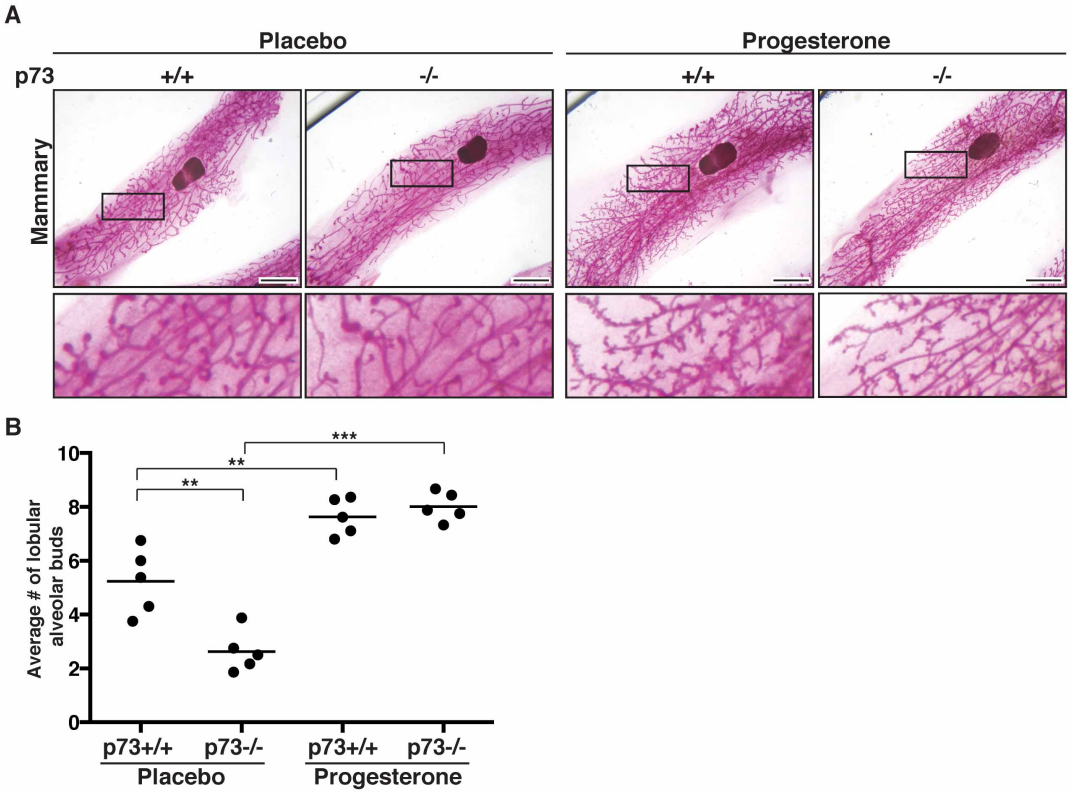

Figure 3.14. Ectopic Progesterone Rescues Lobulo-alveolar Budding Defect in p73-/- Mammary Gland.

(A) Whole mammary mount stained with Carmine Alum shows ectopic progesterone rescues lobular alveolar budding in p73-/- female mice (scale bar = 200 mm). (B) Lobular alveolar budding quantification of placebo control or progesterone from p73+/+ and p73-/-; values shown represent the average number of side branches per primary branch. Asterisks represent p-values <0.01 (**) and <0.001 (***).

compared to the mammary glands of placebo-treated p73-/- mice (Figure 3.14 B).

Of note, the average number of lobular alveolar buds was reduced in p73-/- mice by 45% at 6 weeks (p-value <0.05), 60% at 9 weeks (p-value <0.001) and 66% at 12 weeks (p-value <0.001) of age compared to p73+/+ littermates (Figure 3.15 A and B). Despite decreased lobulo-alveolar budding, the histological architecture of mammary glands were unaffected by loss of p73 (Figure 3.15 C), with a well-organized luminal cell layer displaying apico-basal polarization (asterisks) and basally-oriented myoepithelial cell layer (arrowheads), similar to what was seen in the mammary ductal epithelium of p73+/+ littermates. IF staining in p73+/+ mammary glands revealed nuclear p73 localization in basally located cells that stained positive for the myoepithelial/basal cell marker keratin 14 (Figure 3.15 C). As expected, we did not observe p73 expression in p73-/- mammary glands (Figure 3.15 C). Similar to our analyses in the ovaries, IF staining of p73+/+ mammary glands with antibodies against p63 confirmed myoepithelial/basal localization of p63 and p73 (Figure 3.15 D) (Yang et al. 1999; Barbareschi et al. 2001). Interestingly, p63 co-localized with a subset of p73-expressing cells in the myoepithelial layer suggesting that these two proteins interact in specific myoepithelial cells of the mammary gland. Further, we found that p63 expression was retained in the myoepithelial layer

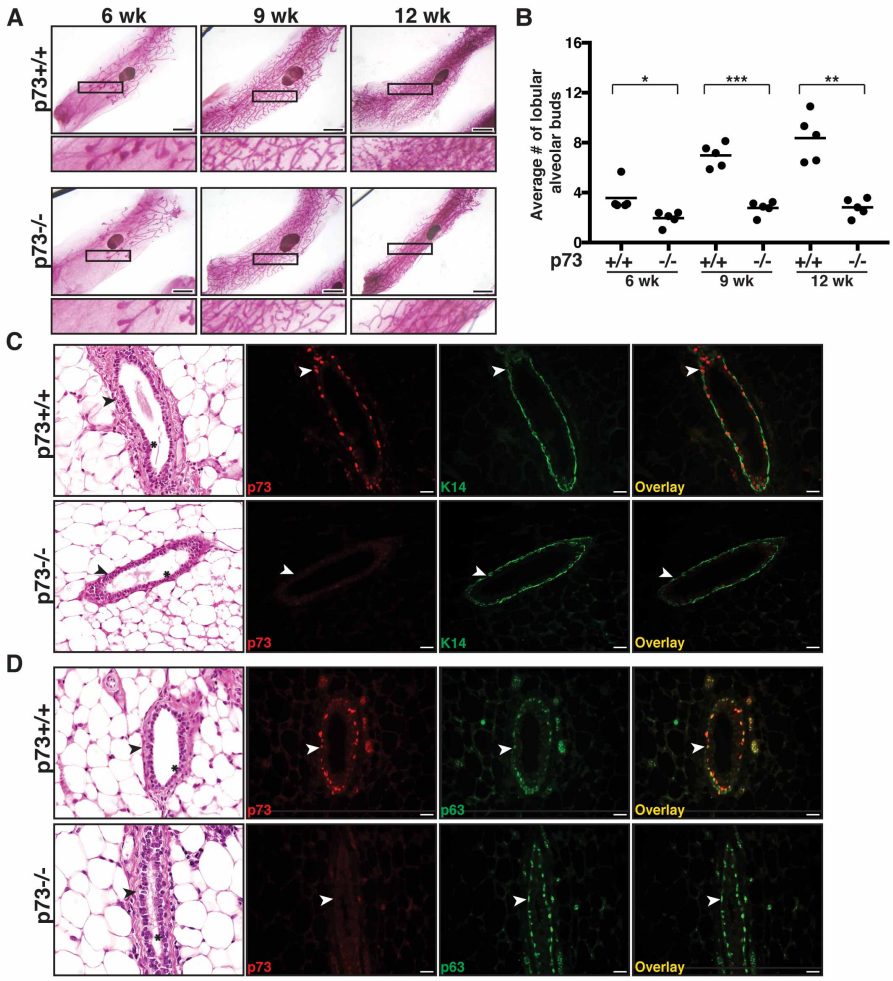

Figure 3.15. p73-Deficient Female Mice Exhibit Lobular-alveolar Budding Defect in the Mammary Gland throughout Development.
(A) Whole mammary mount preparation stain with Carmine Alum shows lobular alveolar budding of p73+/+ and p73-/- female mice at 6, 9 and 12 weeks of age (scale bar = 200 mm). (B) Lobular alveolar budding quantification at indicated ages. Manual quantification was performed on five animals per genotype; values shown represent the average number of side branches per primary branch. p-values represent <0.05 (*), <0.01 (**) and <0.001 (***), and. (C-D) Representative H&E and immunofluorescence (IF) micrographs of the mammary gland from p73+/+ and p73-/- female mice (arrowheads represent myoepithelial layer, asterisks represent luminal layer). IF was performed using antibodies recognizing (C) p73 (red) and myoepithelial marker keratin 14 (green). (D) p73 (red) and p63 (green) co-localization was observed in a subset of the myoepithelial layer in the mammary gland (scale bar = 25 μm).

of p73-/- mammary glands suggesting that decreased lobulo-alveolar budding in p73-/- is not due to impaired p63 expression (Figure 3.15 D).

p73 Regulates a Biological Adhesion Gene Network in Murine Granulosa Cells

To gain mechanistic insight to the defects in follicle development and ovulation in p73-/- ovaries, laser capture microdissection was used to isolate granulosa cells from p73+/+ and p73-/- antral follicles of age-matched nulliparous mice (three mice per genotype). Principal component analysis (PCA) revealed a clear separation between p73+/+ and p73-/- transcriptional changes in antral follicle samples in principal component 1 (PC1) (Figure 3.16 A). Accordingly, we identified 3,209 protein-coding genes differentially expressed between p73+/+ and p73-/- antral follicles, of which 1,603 were enriched in p73+/+ antral follicles and 1,606 were enriched in p73-/- antral follicles. Genome Ontology (GO) enrichment [maximum false discovery rate (FDR <2.22E-16)] identified nine GO categories related to biological adhesion, including extracellular matrix organization, positive regulation of cell adhesion, cell-substrate adhesion, positive regulation of locomotion, extracellular structure organization, positive regulation of cellular component movement and positive regulation of cell motility (Figure 3.16 B). These findings are consistent with previous reports of p73-mediated regulation of cell-cell adhesion and migration through integrin-β4 (Xie et al. 2018), VEGF

A

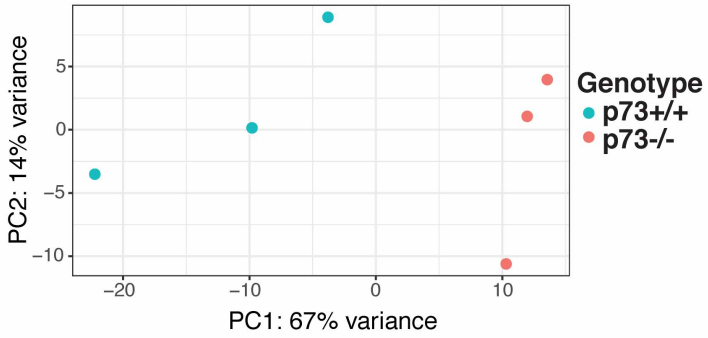

B

#	GO Category
1	Angiogenesis
2	Extracellular matrix organization
3	Positive regulation of cell migration
4	Cell-substrate adhesion
5	Positive regulation of locomotion
6	Extracellular structure organization
7	Blood vessel morphogenesis
8	Positive regulation of cellular component movement
9	Positive regulation of cell motility

Figure 3.16. p73 Regulates a Gene Network Involved in Biological Adhesions in Antral Follicles.
(A) PCA plot of RNA-seq analysis from LCM-isolated p73+/+ and p73-/- antral follicles (n= 3 mice/genotype). (B) Table shows top nine GO categories enriched in p73+/+ vs p73-/- antral follicles (FDR < 2.22E-16).

and TGFβ signaling (Fernandez-Alonso et al. 2015; Martin-Lopez et al. 2017; Bae et al. 2018).

We isolated and cultured primary mouse granulosa cells (MGCs) from p73+/+ mice, and transduced the cells with lentivirus expressing TAp73β for 48 h. Given previous studies showing TAp73β can activate apoptosis through transcriptional regulation of Bcl-2 family members BAD and BIK (Muller et al. 2005), we assessed the effects of ectopic p73 expression in MGCs. We did not observe any difference in cell morphology (Figure 3.17 A) or in the levels of cleaved PARP1 between control MGCs and those expressing ectopic TAp73β during the time course of the experiment (Figure 3.17 B). The rationale for using TAp73β was based on previously published data showing that TAp73β exhibits the highest level of transcriptional activity among p73 isoforms (Lee and La Thangue 1999; Ueda et al. 1999) as well as the fact that the TAp73β isoform is highly expressed in human ovaries (Figure 3.5). We measured global gene expression changes by RNA-seq after ectopic p73 in MGCs isolated from both p73+/+ and p73-/- female mice and identified clear separation of samples after ectopic p73 (Figure 3.17 C). Differential expression of 5,178 genes was identified in p73+/+ MGCs after ectopic expression of TAp73β, including 2,896 upregulated genes. Similarly, we identified 3,391 differentially expressed genes after TAp73β expression in p73-/- MGCs (2,087 upregulated genes). We identified 1,649 genes commonly upregulated in TAp73β expressing MGCs and in p73+/+ antral

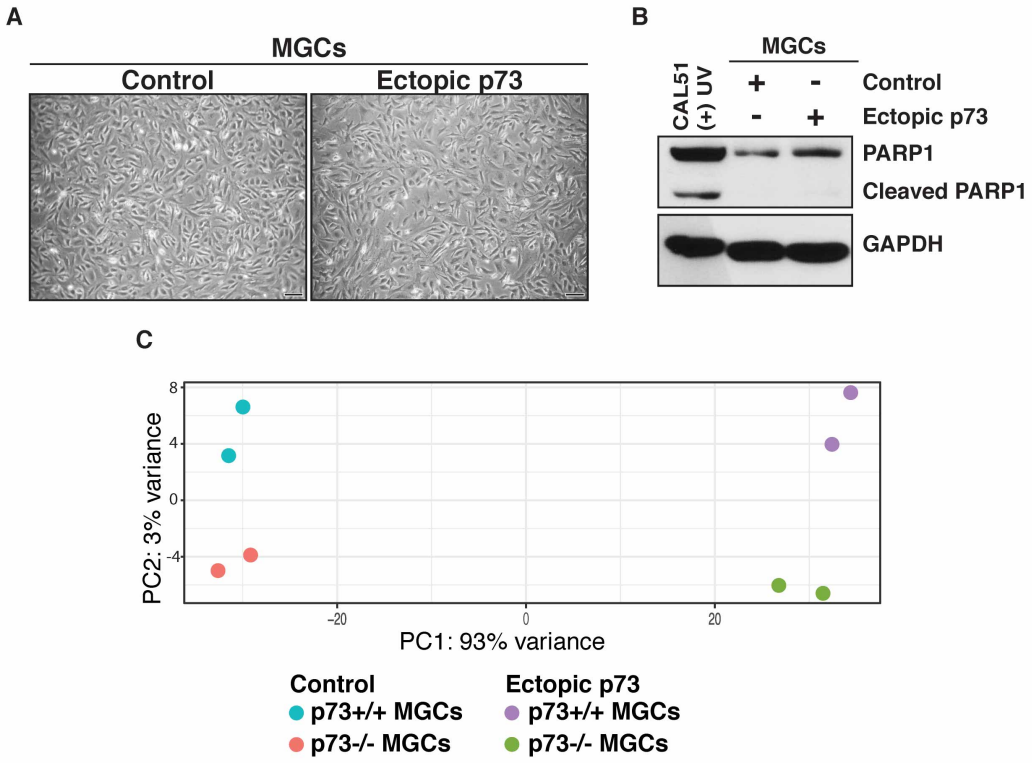

Figure 3.17. Ectopic p73 in Murine Granulosa Cells (MGCs).
(A) Bright field images show normal cell morphology after ectopic p73 or control murine granulosa cells (scale bar = 100 μm). (B) Western blot analysis of the indicated proteins show absence of cleaved PARP1 expression in MGCs after ectopic p73 or control compared to UV treated (50j/m^2) CAL51 cell line. (C) PCA plot of RNA-seq analysis from p73+/+ and p73-/- MGCs after ectopic p73 or control.

follicles [>1 TPM] (Figure 3.18 A). GO pathway enrichment analysis identified nineteen GO categories (FDR <2.22E-16), including biological adhesion and migration (Figure 3.18 B). A core set of 208 genes overlapped in at least 3 of the 19 enriched GO categories (Figure 3.18 C, Figure 3.19), including: Adam10, Adamts12, Icam1, Pxn and Mmp14. Importantly, we identified multiple genes required for the formation of the follicular focimatrix (focal intra-epithelial matrix), which is the extracellular matrix that aggregates between granulosa cells and increases as follicle progress to pre-ovulatory stage (Irving-Rodgers et al. 2004; Irving-Rodgers et al. 2009; Irving-Rodgers et al. 2010). Key focimatrix genes identified include Lama1, Lama, Lama5, Lamb1, Hspg2, Nid1 and Nid2. To determine if p73 regulates the expression of genes required for follicular focimatrix *in vivo*, we performed IF using a laminin antibody in murine ovaries. We observed decreased laminin expression in granulosa cells from p73-/- ovaries compared to p73+/+ (Figure 3.20), further supporting the role of p73 as a key regulator of genes involved in cell-to-cell adhesion and ovarian follicle development.

A

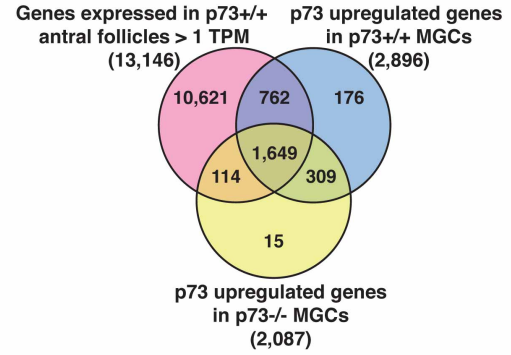

B

#	GO Category
1	Angiogenesis
2	Urogenital system development
3	Kidney development
4	Morphogenesis of an epithelium
5	Transmembrane receptor protein tyrosine kinase signaling pathway
6	Response to wounding
7	Peptidyl-tyrosine phosphorylation
8	Peptidyl-tyrosine modification
9	Extracellular matrix organization
10	Positive regulation of cell migration
11	Cell-substrate adhesion
12	Cell junction organization
13	Positive regulation of locomotion
14	Wound healing
15	Extracellular structure organization
16	Blood vessel morphogenesis
17	Cell morphogenesis involved in neuron differentiation
18	Positive regulation of cellular component movement
19	Positive regulation of cell motility

C

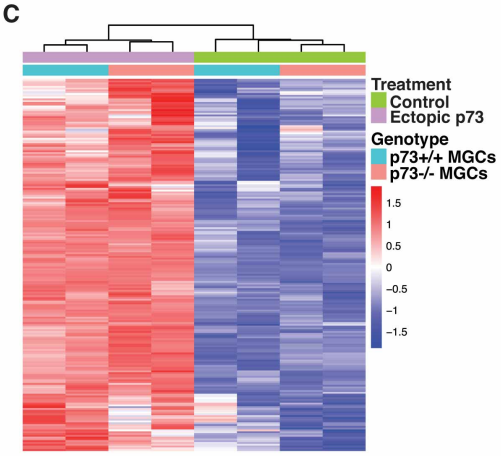

Figure 3.18. Overlap of p73-Regulated Genes in Antral Follicles and MGCs.
(A) Venn diagram showing the overlap between genes expressed in p73+/+ antral follicles (TPM > 1) and upregulated after ectopic p73 expression in p73+/+ and p73-/- MGCs. (B) Table listing the top nineteen GO categories enriched in 1,649 overlapping genes from A. (C) Heatmap of expression for core 208 p73-upregulated granulosa cell genes. These genes were selected by identifying the 1,649 genes in A that were present in three or more of the enriched GO categories from B. (FDR p-value < 0.1).

Core Set of 208 p73-regulated Genes in Granulosa Cells											
MGI Symbol	Nubmer of GO pathways included in	HCC1806 p73 ChIPseq Distance to TSS	MGI_Symbol	Nubmer of GO pathways included in	HCC1806 p73 ChIPseq Distance to TSS	MGI_Symbol	Nubmer of GO pathways included in	HCC1806 p73 ChIPseq Distance to TSS	MGI_Symbol	Nubmer of GO pathways included in	HCC1806 p73 ChIPseq Distance to TSS
Ackr3	6		Efna5	6		Itgb3	15		Ptprm	3	
Actn4	6		**Egflam**	3	18,062	**Jag1**	4	-5,369	**Pxn**	6	797
Acvrl1	7		**Egfr**	10	-24,740	Jak3	3		Pycard	4	
Adam10	5		Emilin1	3		Kif26b	4		**Rap2b**	4	23,322
Adamts12	3		Eng	5		Klf4	4		Rarres2	4	
Adm	4		Enpep	4		Lama1	5		Rdh10	3	
Afap1l2	3	-15,589	Enpp2	8		**Lama2**	3	-16,759	Rgma	3	
Ajuba	5	-1,575	Epha4	8		**Lama5**	6	1,733	Rhoc	4	
Aldh1a2	3	11,527	Ephb2	7		Lamb1	8		Rock2	9	
Amotl1	4	-569 ✔	Ereg	5		Lgals9	4		Ror1	3	
Angpt4	9		Ets1	10		**Lrp4**	5	1,646	**Rxra**	4	-8,075 ✔
Antxr1	3	-5,589	Foxp1	5		Lum	3		Sash1	6	
Anxa1	3	19,195	Fgfr1	12		Map3k7	3		**Sdc1**	4	10,617 ✔
Aplp2	5		**Fgfr2**	9	-543 ✔	Mapk14	5		**Sema3f**	5	
Apoe	4		Flna	7		**Mdm2**	4	*	**Sema4b**	5	694
App	6		Flrt2	4		**Mmp14**	9	-1,952	Sema6a	5	
Ar	3		Flrt3	4		Mvp	3		**Serpinf1**	4	61
Arhgap24	5		Flt1	10		Myadm	5		Sgpl1	4	
Arid5b	3	20,864	Fmod	3		**Myh9**	4	-504	Shc1	3	
Atoh8	4	9,204	Fras1	3		**Myo1e**	6	-12,130	Smoc2	3	
Atp7a	4		**Fscn1**	3	-5,461	Nfatc4	4		Snai2	8	
B4galt1	7		Fzd5	4		**Nid1**	5	-18,785	Socs3	4	
Bag4	4		Fzd7	3		**Nid2**	3	-11,249	**Sorbs1**	3	-2,574
Bmp4	10		**Gas6**	11	-1,212 ✔	Ninj1	3		Sparc	8	
Bmp7	4		Gata2	3		Notch1	16		Sphk1	6	
2410089E03Rik	3		Gcnt2	5		**Notch3**	4	5,270	Spry1	4	
Cav1	7		**Gdnf**	4	-8,281	Npnt	6		**Src**	11	-12,694
Cbl	3		Ghr	3		**Ntn4**	3	18,396	Srf	8	
Cblb	3		Gli2	4		Nptn	3		Stat3	3	
Ccl2	9		Glipr2	4		Pak3	5		Sulf1	8	
Cd34	7		Gpc3	3		Pard3	4		Tcf21	5	
Cd74	6		**Gpx1**	4	*	**Pdgfa**	14	1,308 ✔	Tek	12	
Cdh3	3	9,931 ✔	**Grhl3**	3	2,034 ✔	**Pdgfc**	9	1,997	**Tgfa**	7	-15,941
Cited1	4		**Hbegf**	12	-1,691	Pdgfra	15		Tgfb1	16	
Cmklr1	4		Hdac4	4		Pdgfrb	11		Tgfb2	14	
Col18a1	8		**Hdac7**	7	3,118	Pdpn	4		**Tgfbi**	4	-4,754
Col3a1	6		Hes1	7		Peak1	3		Tgfbr2	9	
Col5a1	5	-2,335	**Hras**	6	-53	Pgf	10		Thbs4	8	
Csf1	7	16,971	Hs2st1	3		Pik3r1	6		Tmsb4x	4	
Cspg4	5		Hspg2	4		Pkd2	4		Thy1	5	
Cst3	3		Hyal1	6		Plcg1	7		**Tnc**	4	-777
Cux1	3		Icam1	6		Plet1	8		**Traf3ip1**	5	6,866
Cx3cl1	4		Igf2	3		Plod3	3		**Trim32**	4	*
Cxcl14	4		Il1r1	4		**Plpp3**	6	-16,740	Trip6	4	
Cxcl16	4		Ilk	13		Plxnd1	4		Tyro3	5	
Dab2ip	7	-990	Inpp5f	3		Ppard	3		Unc5b	3	
Dapk2	4		Irs2	5		Ppm1f	6		**Vav2**	4	-5,511
Ddr2	9		Itga2b	7		Prkcd	5		**Vcl**	5	11,767
Dll1	6		**Itga3**	7	18,322 ✔	**Prkce**	9	16,374 ✔	Vegfc	11	
Dmd	3		**Itga6**	6	-14,968	**Ptk7**	3	-11,966	**Wdpcp**	6	-12,995
Dsp	3	8,632	Itga8	5		**Ptpn1**	3	13,312	Wnt2b	3	
Efemp1	3		Itgb1	4		Ptprj	10		Wnt4	9	

***** Binding at TSS
✔Multiple p73 Binding sites within 25 kb

Figure 3.19. Core Set of 208 p73-Regulated Genes in MGCs.
Table listing the core set of 208 p73-upregulated granulosa cell genes, the number of enriched GO pathways the gene was present in from Figure 3.19 B, and the distance from TSS of each gene (bold) to the nearest p73 peak in HCC1806 cells if present. * represents p73 binding site at TSS. ✔ represents multiple p73 binding sites within 25 kb of TSS.

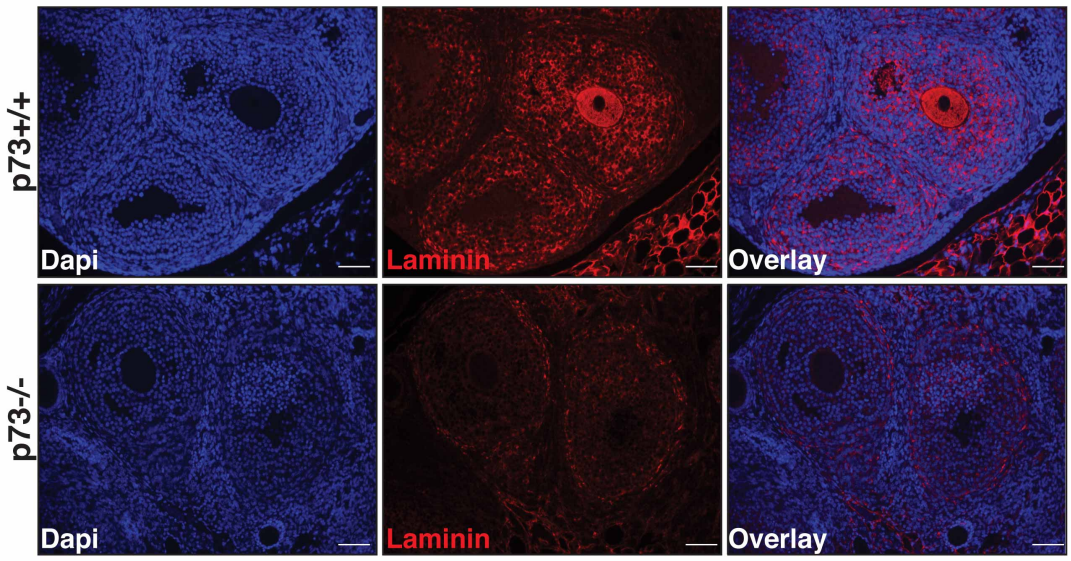

Figure 3.20. Laminin Expression in p73+/+ and p73-/- Ovaries.
Representative IF images show decreased laminin (red) expression in granulosa cells of p73-/- ovaries compared to p73+/+ (scale bar = 50 μm).

Conclusions

In summary, we discovered that p73 is required for proper ovarian follicle development, ovulation and subsequent corpus luteum formation and progesterone production. Similar to prior findings made with TA-specific p73-deficient male mice (Inoue et al. 2014), we observed a significant decrease in levels of circulating progesterone in our p73-/- female mice. Further, we demonstrated that the mammary branching defect observed in p73-/- female mice is secondary to decreased levels of progesterone through a complete rescue of the branching defect after ectopic progesterone administration. Through analysis of gene expression between p73+/+ and p73-/- antral follicles and modulation of p73 expression in primary culture of MGCs, we discovered p73-dependent regulation of genes crucial for biological adhesion and extracellular matrix interactions including focimatrix-associated genes (Lama5, Nid1/2 and Hspg2). We further show decreased laminin staining in p73-/- follicles compared to p73+/+. The results presented in this Chapter led us to hypothesize that p73 acts as critical regulator of cell-to-cell adhesion, extracellular matrix interactions and cell migration to promote proper follicle development, ovulation and fertility. The further testing of this hypothesis was the focus of further research presented in Chapter IV.

CHAPTER IV

P73 REGULATES CELL ADHESION- AND MIGRATION- ASSOCIATED GENE NETWORKS

Introduction

Cell-to-cell adhesion and extracellular matrix interactions directly impact the ability of cells to migrate through their environment (Abercrombie et al. 1971; Heath and Dunn 1978). Cell migration is initiated by actin remodeling of the cytoskeleton that stimulates membrane protrusions at the leading edge of the cell (Condeelis 1993), followed by coordinate assembly of adhesion complexes between cells or extracellular matrix, and disassembly at the trailing of the cell (Parsons et al. 2010). Proper regulation of cell-to-cell adhesion and migration is not only essential in normal tissue development but also during cancer progression and metastasis.

Aside from the role of the p53 family in cell cycle control and DNA damage repair, p53, p63 and p73 regulate cell-to-cell adhesion, extracellular matrix interactions and cell migration. Activation of p53 in mouse embryonic fibroblasts (MEFs) leads to the inhibition of Cdc-42 mediated actin cytoskeleton remodeling and membrane protrusion formation (Gadea et al. 2002). Cdc-42 is part of the Rho family of GTPases, key regulators of actin cytoskeleton modification, cell adhesion and migration (Ridley and Hall 1992;

Nobes and Hall 1995). Loss of p63 expression in keratinocytes and mammary epithelial cells induces cell detachment and downregulation of cell adhesion-associated genes including laminin, fibronectin and several integrins (Carroll et al. 2006).

Similar to its family members, p73 has been shown to regulate cell-to-cell adhesion and migration *in vivo*. For example, loss of p73 leads to defective endothelial cell differentiation and migration during mouse retinal development (Fernandez-Alonso et al. 2015). Retinas isolated from p73-deficeint mice exhibit decreased levels of VEGF and TGF-β, which are essential for angiogenesis and endothelial cell migration (Fernandez-Alonso et al. 2015). Further, p73 regulates the expression of cell-to-cell adhesion- and migration-associated genes required for the proper development of reproductive organs in both male (Holembowski et al. 2014) and female mice (Santos Guasch et al. 2018). Loss of p73 in murine testis leads to defective cell-to-cell adhesion between germ cells and Sertoli nurse cells through the deregulation of tissue inhibitor of metalloproteinase 1 (Timp1) (Holembowski et al. 2014). As described in Chapter 3, we discovered that p73 is required for ovarian follicle development, ovulation and corpus luteum formation (Santos Guasch et al. 2018). Gene expression analysis from p73+/+ and p73-/- antral follicles and ectopic p73 expression in murine granulosa cells led us to identify a p73-dependent gene network involved in granulosa-to-granulosa cell adhesion and migration. Given these results, our next goal

was to study the role of p73 in cell migration using in vitro models and identify genes that were direct transcriptional targets of p73 to gain further mechanistic insights. We report herein that p73 regulates cell migration *in vitro* and loss of p73 expression leads to a decreased rate of migration in primary murine and human cell models as well as multiple transformed cell lines. We identified p73 genomic binding and further validated p73 binding sequences near transcriptional start sites (TSS) of genes necessary for cell adhesion and migration including key components of granulosa cell-associated focimatrix.

Results

p73 Regulates Cell Migration *In Vitro*

To gain further mechanistic insights to the role of p73 on cell migration, we analyzed primary cultures and cell lines with defined p73 status using an established *in vitro* migration assay. In an initial set of experiments, we used mouse embryonic fibroblasts (MEFs) isolated from p73+/+ and p73-/- embryos. To set up the migration assay, magnetically attachable stencils (MAtS) were placed in culture vessels to create “gaps” in monolayer cell cultures (Ashby et al. 2012). The measurement of cell movement into the gaps over time provides a reporter assay for cell adhesion and migration. The MEFs were plated and grown to near confluency

surrounding the MAtS and cultured in serum-free media for 14 h. MAtS were then removed (T = 0 hour) and migration was monitored for 8 h. MEFs isolated from p73-/- embryos had slower cell migration into the gap over time compared to p73+/+, suggesting that lack of p73 significantly decreased cellular migration rate (Figure 4.1 A). Loss of p73 expression was confirmed through qRT-PCR (Figure 4.1 B).

Our findings led us to ask if the decrease in cell migration observed in p73-/- MEFs was cell-type or tissue-specific. We expanded our analysis of p73 in the migration assay to an array of cell line models derived from multiple tissues including primary [human mammary epithelial cells (HMECs)] and transformed cell lines that readily grow in tissue culture [rhabdomyosarcoma (RH30), lung cancer (NCI-H2009 and NCI-H2122) and breast cancer (MDA-MB-231 and HCC1806)]. Lentivirally-delivered shRNA sequences encoding p73 were used to 'knock down' p73 in primary HMECs and all of the indicated transformed cell lines. Cell migration was monitored for 8 h to 11 h, depending on the cell line. We observed that that loss of p73 significantly decreased cellular migration in HMECs, RH30, NCI-H2009, NCI-H2122, MDA-MB-231 and HCC1806 cells compared to the cell

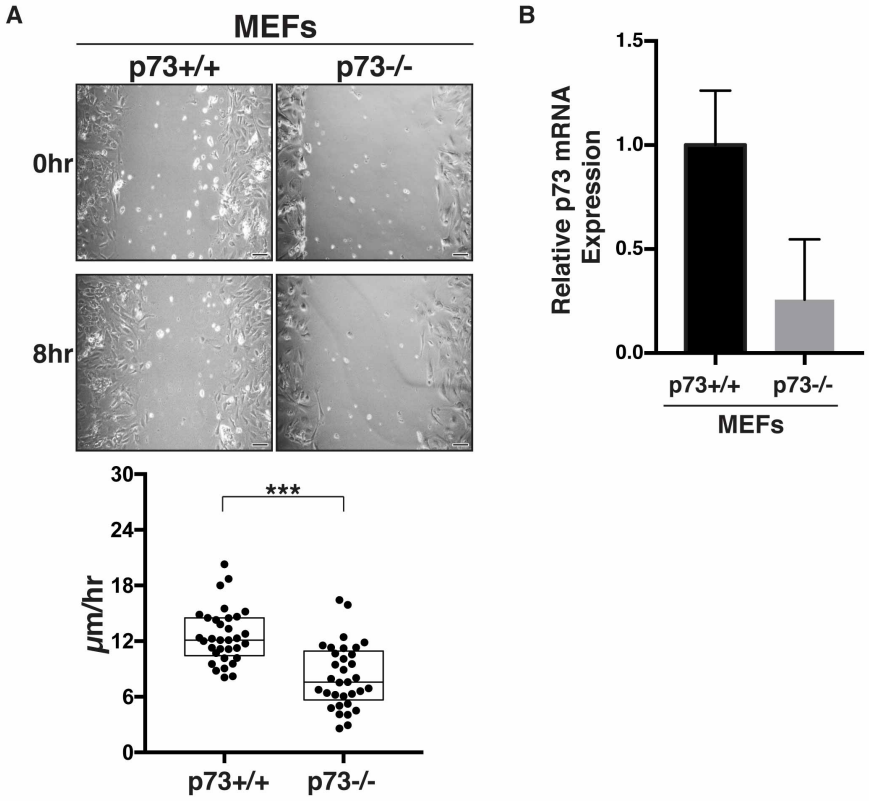

Figure 4.1. Loss of p73 Expression in MEFs Leads to a Decrease in Cell Migration. (A) MEFs isolated from p73+/+ and p73-/- mice, were plated in culture dishes containing magnetic stencils and grown to confluency (scale bar = 100 μm). Each dot represents the percentage gap closure per field of view. Asterisks represent p-values <0.001 (***). (B) qRT-PCR analysis was performed using primers targeting exon6/7 junction of p73 on mRNA isolated from MEFs derived from p73+/+ and p73-/- embryos. Data represent relative mRNA expression normalized to GAPDH per genotype indicated.

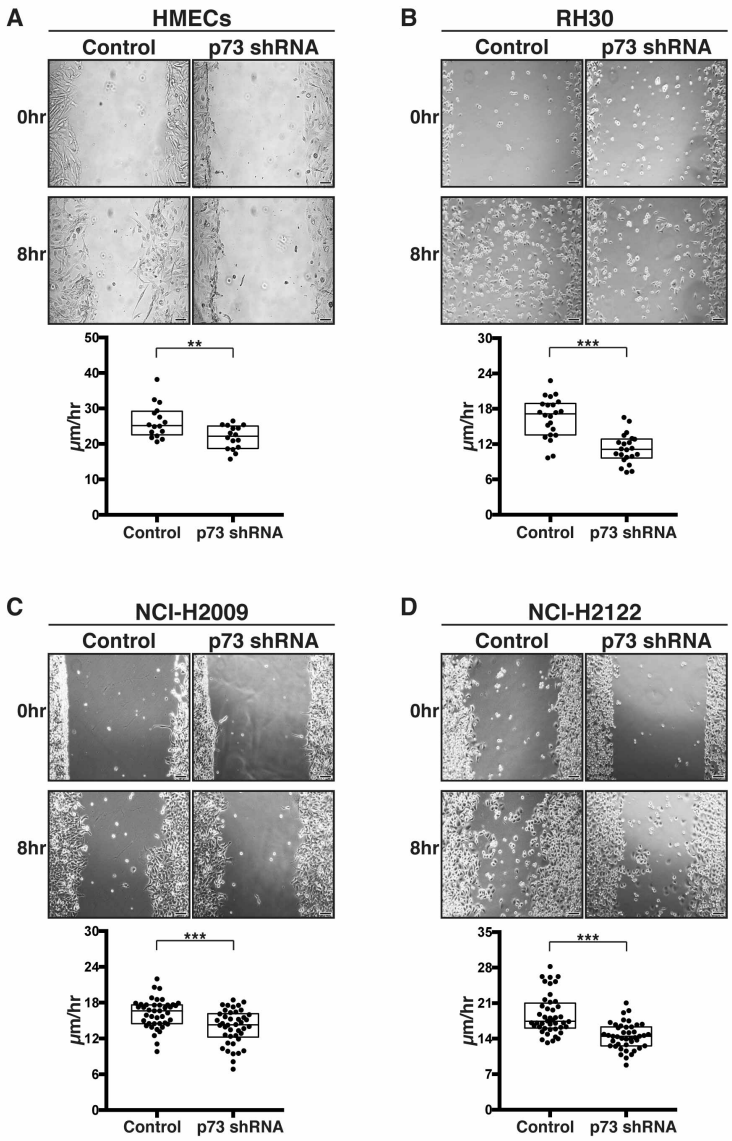

Figure 4.2. p73 Regulates Cell Migration in Human Primary and Transformed Cell Lines.

(A) HMECs, (B) RH30, (C) NCI-H2009 and (D) NCI-H2122 cells stably expressing control shRNA and p73 shRNA were plated in culture dishes containing magnetic stencils and grown to confluency (scale bar = 100 μm). Each dot represents the percentage gap closure per field of view. Asterisks represent p-values <0.01 (**) and <0.001 (***).

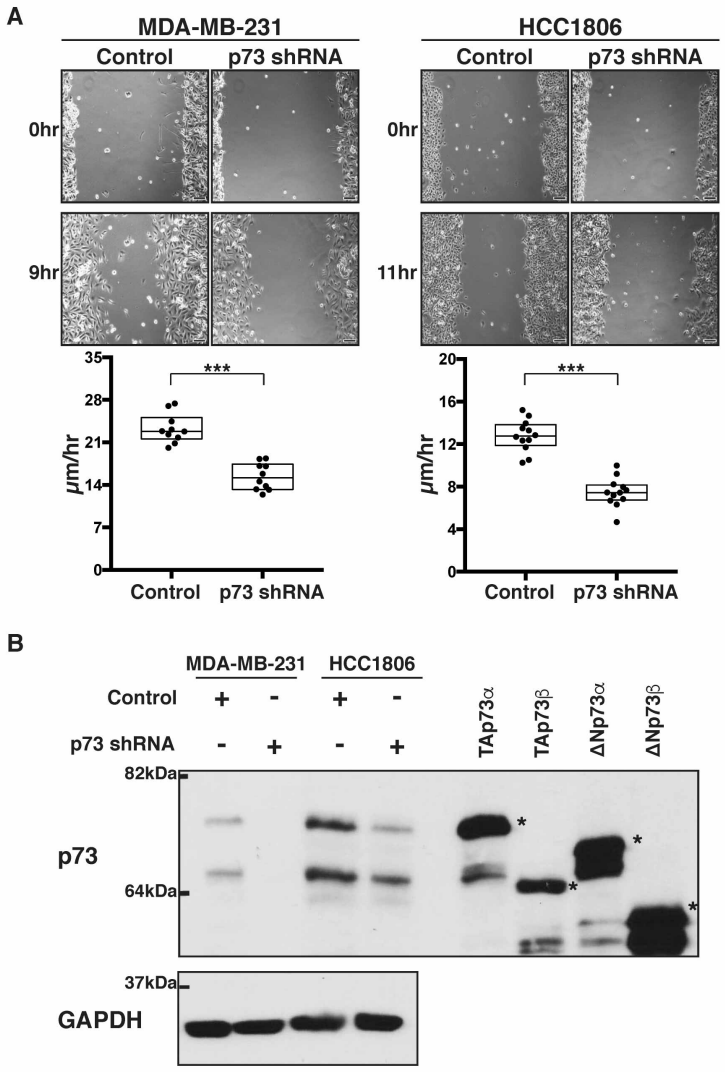

Figure 4.3. p73 Regulates Cell Migration in Breast Cancer Cell Lines.
(A)MDA-MB-231 and HCC1806 cells stably expressing control shRNA and p73 shRNA were plated in culture dishes containing magnetic stencils and grown to confluency (scale bar = 100 μm). Each dot represents the percentage gap closure per field of view. Asterisks represent p-values <0.001 (***). (B) Western analysis of the p73 isoforms in MDA-MB-231 and HCC1806 cells expressing control shRNA and p73shRNA. The indicated ectopically expressed p73 isoforms (*) are included to serve as molecular markers for alignment of the cellularly expressed p73 proteins.

expressing the appropriate vector controls (Figure 4.2 and Figure 4.3 A). Loss of p73 expression was confirmed through Western blot analysis (Figure 4.3 B).

p73 Binds to Adhesion- and Migration-Associated Genes

Given the significant difference in cell migration observed in p73-deficient cells, our next goal was to identify direct transcriptional targets of p73 that are linked to migration processes. We selected a cell line that is amenable to scale up and further genomic analyses. ChIP-seq was performed on the parental HCC1806 cells to determine if p73 directly binds near the transcriptional start site (TSS) of genes involved in cell migration. HCC1806 cells were formaldehyde cross-linked and processed for p73 and RNA polymerase II (Pol II) ChIP-seq. QC analysis of the data demonstrated clear separation between ChIP and input signal for p73 and Pol II (Figure 4.4 A). Because the p73 ChIP replicates were highly correlated (Figure 4.4 B), we pooled the samples for peak calling to increase peak detection sensitivity. We identified 3,555 p73 and 19,696 Pol II genomic binding sites. Motif analysis showed strong enrichment for the p53 family binding motif (Figure 4.4 C) (el-Deiry et al. 1992; Lokshin et al. 2007; Rosenbluth et al. 2008; Smeenk et al. 2008). We identified known binding sites in p73-target genes MDM2 and CDKN1A (Figure 4.4 D and E) (Barak et al. 1993; Juven et al. 1993; Espinosa and Emerson 2001) (Robinson et al. 2011; Thorvaldsdottir

et al. 2013) as well as a binding site in the newly reported p73-target gene ITGB4 (integrin-β4) (Xie et al. 2018).

In order to identify p73-regulated genes that play a role in granulosa-to-granulosa cell adhesion, we focused our analysis on genes that were increased after ectopic p73 expression in MGCs and for which the binding of p73 occurred within 25 kb of the TSS in HCC1806 ChIP-seq. From the 208 p73-regulated core gene set, we found 30 adhesion- and migration-associated genes with a p73-binding site within 25 kb of the TSS of the human gene homologue (Figure 4.5 A). Of immediate interest were p73-binding sites near genes encoding cell-to-cell adhesion and migration including matrix metallopeptisase 14 (MMP14), platelet-derived growth factor A and C (PDGFA and PDGFC), and paxillin (PXN) (Figure 4.5 A and B). Paxillin is a scaffolding protein that regulates cytoskeleton remodeling, cell migration and focal adhesions (Huang et al. 2003; Deramaudt et al. 2014; Hu et al. 2014). Further, we identified p73-binding near the TSS of granulosa cell-associated focimatrix components LAMA5, NID1 and NID2 (Figure 4.5 A and B).

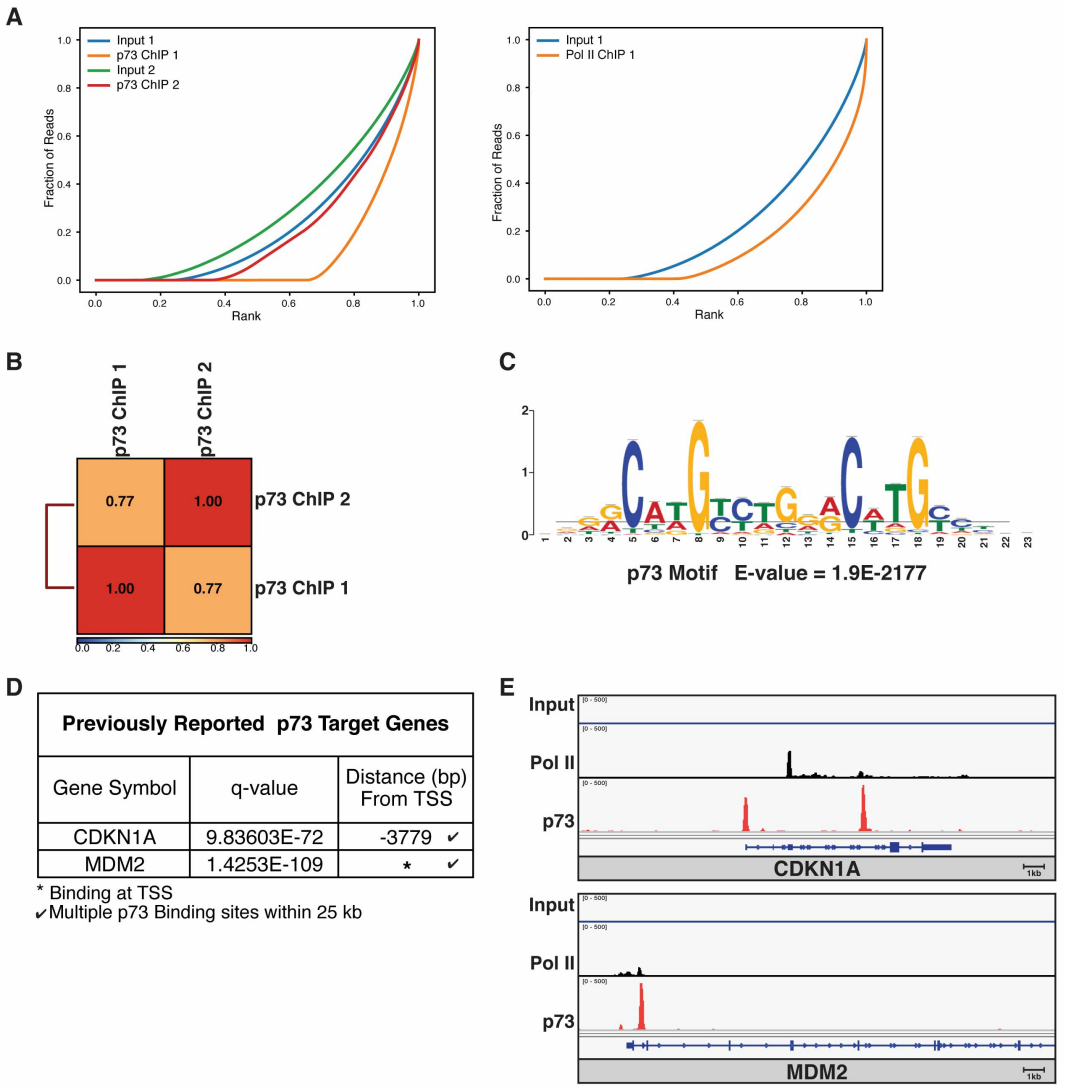

Figure 4.4. ChIP-seq Analysis of p73 Binding in HCC1806.
(A) Finger print plots of p73 and Pol II ChIP-seq with respective input samples (B) Heat map of hierarchically clustered Spearman correlations between p73 ChIP-seq replicates samples. (C) Top motif enriched in p73 ChIP-seq. (D) Table listing known p73 target genes bound by p73 in HCC1806 cells. (E) IGV images of p73 and Pol II binding profiles in CDKN1A and MDM2 genes. Each sample was normalized to 1X depth of coverage. Individual tracks within a gene are scaled equally. RefSeq gene annotations are in blue schematics at the bottom of each panel.

A

p73 Binding Site within 25 kb of the TSS of Adhesion- and Migration-Associated Genes		
Gene Symbol	q-value	Distance (bp) from TSS
AJUBA	6.158E-12	-1575 ✔
AMOTL1	8.79225E-67	-569
ANTXR1	3.14427E-22	-5589
ATOH8	7.88461E-08	9204
COL5A1	1.21966E-10	-2335
CSF1	1.08201E-14	16971
EGFLAM	1.27368E-11	18062
EGFR	3.93432E-12	-24740
FSCN1	1.02783E-23	-5461
HBEGF	8.04896E-08	-1691 ✔
HRAS	1.54227E-54	-53
ITGA3	1.01181E-13	18322
ITGA6	1.84459E-10	-14968
LAMA2	9.83694E-27	-16759
LAMA5	1.06021E-50	1733
MMP14	8.19521E-55	-1952
MYO1E	3.3848E-151	-12130
NID1	3.7301E-17	-18785
NID2	7.5692E-18	-11249
NTN4	1.16888E-21	18396 ✔
PDGFA	4.04464E-36	1308
PDGFC	6.3962E-99	1997
PLPP3	5.54613E-10	-16740 ✔
PRKCE	2.39458E-33	16374
PXN	3.93641E-55	797
SEMA3F	3.04404E-09	953
SRC	1.378E-17	-12694
TRIM32	2.8399E-134	*
VCL	4.73129E-28	11767
WDPCP	1.06569E-14	-12995

* Binding at TSS
✔Multiple p73 Binding sites within 25 kb

B

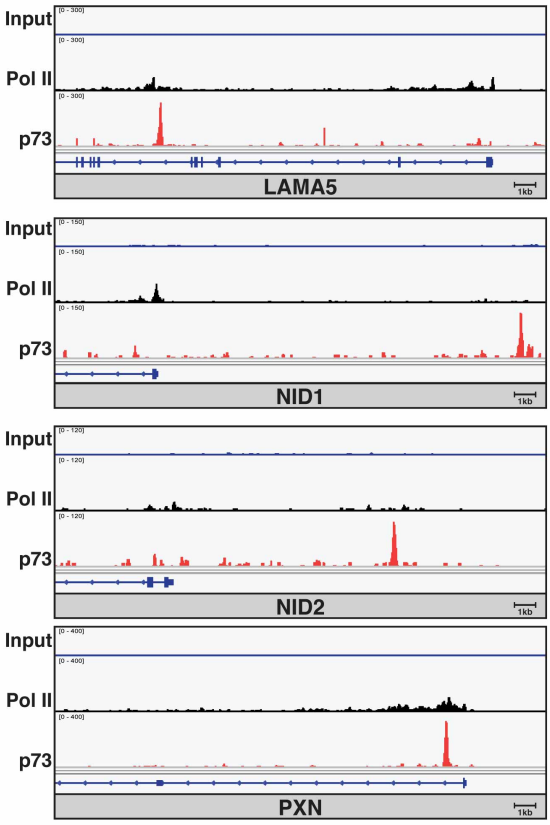

Figure 4.5. p73 Binds to Cell Adhesion- and Migration-Associated Genes.
(A) Table listing adhesion- and migration-associated genes from the core set of 208 genes bound by p73 within 25 kb of their TSS (in HCC1806 cells). For each gene, the q-value of the nearby p73 peak and its distance from the TSS of the gene are included. (B) Integrative Genomics Viewer (IGV) images for selected genes from (A) with tracks for input, p73 and Pol II ChIP-seq in HCC1806 cells. Each sample was normalized to 1X depth of coverage. Individual tracks within a gene are scaled equally. RefSeq gene annotations are in blue schematics at the bottom of each panel on the same scale as the ChIP-seq tracks.

Conclusion

We discovered that loss of p73 expression in MEFs or in human primary cells and transformed cell lines resulted in a significant decrease in the rate of cellular migration. Further, we identified p73 binding sites near the TSS of 30 genes involved in cell adhesion and migration that were regulated in a p73-dependent manner in murine granulosa cells (MGCs). Such genes include focimatrix components (LAMA5, NID1 and NID2) and known regulators of cell adhesion and migration (PXN, MMP14, PDGFA and PDGFC). Consistent with our results, another group demonstrated that loss of endogenous p73 led to decreased cell migration and invasion through transcriptional regulation of an integrin binding protein periostin (POSTN) in glioblastoma (Landre et al. 2016). Other studies have provided conflicting evidence showing overexpression of p73 decreases cell migration in cervical cancer (Rodhe et al. 2013) and colorectal cancer (Bae et al. 2018). However, in these latter studies, it is different to determine if the decreased in cell migration was secondary to the effect of p73 on cell replication.

Cell migration is regulated by the equilibrium between the assembly and disassembly of adhesion complexes at the leading and trailing edge of the cell, respectively. Taking into account our findings (Santos Guasch et al. 2018) and others (Xie et al. 2018) showing that p73 transcriptionally regulates cell adhesion-associated genes, integrin-β4, we posit that p73 transcriptionally regulates genes involved in adhesion complexes necessary

for cell migration, and loss of p73 expression disrupts transcriptional networks that play a regulatory role in cell-to-cell or extracellular adhesion complexes required for proper cell movement.

CHAPTER V

CONCLUSIONS AND FUTURE DIRECTIONS

Introduction

Female reproduction is coordinately regulated by multiple complex signaling pathways across diverse organs including the hypothalamus, the pituitary gland, and the ovaries. The work presented in this dissertation was conducted with the goal of expanding our knowledge of the role of p73 in select tissues, which we discovered were aberrant in our p73-deficient mouse model, including the ovaries that are part of the reproductive system and the mammary glands that are part of the integumentary system. Our findings provide insight to the mechanism by which p73 directly or indirectly regulates ovarian follicle development, ovulation, corpus luteum formation, hormone signaling and mammary gland branching. p73 expression in murine granulosa cells is required for ovarian follicle development and function including corpus luteum formation. Proper formation of the corpus luteum is necessary for maintaining sufficient levels of circulating progesterone required for normal mammary gland development and branching. In fact, we found that ectopic progesterone rescued ovarian follicle development and mammary gland branching in p73-/- female mice. However, p73-/- female mice treated with ectopic progesterone failed to ovulate and form a corpora

lutea normally, suggesting additional roles of p73 ovulation that are not necessarily progesterone-dependent. Through gene expression analysis of p73+/+ and p73-/- antral follicles along with modulation of p73 expression in murine granulosa cells (MGCs), we discovered a p73-dependent gene network involved in biological adhesions, extracellular matrix interactions and cell migration. Collectively, these data support our proposed model that p73 regulates ovarian folliculogenesis and ovulation in part, through regulation of cell adhesion-associated genes and key components of murine focimatrix involved in follicle maturation, ovulation and fertility (Figure 5.1).

We further found that p73 regulates cell migration *in vitro* using an array of cell models and identified p73 genomic binding near the transcriptional start site of multiple genes known to regulate cell adhesion and migration. This final chapter includes new questions that arise from our discoveries and resulting hypotheses that can be tested, to further understand the role of p73 in ovarian follicle development and function as well as fertility.

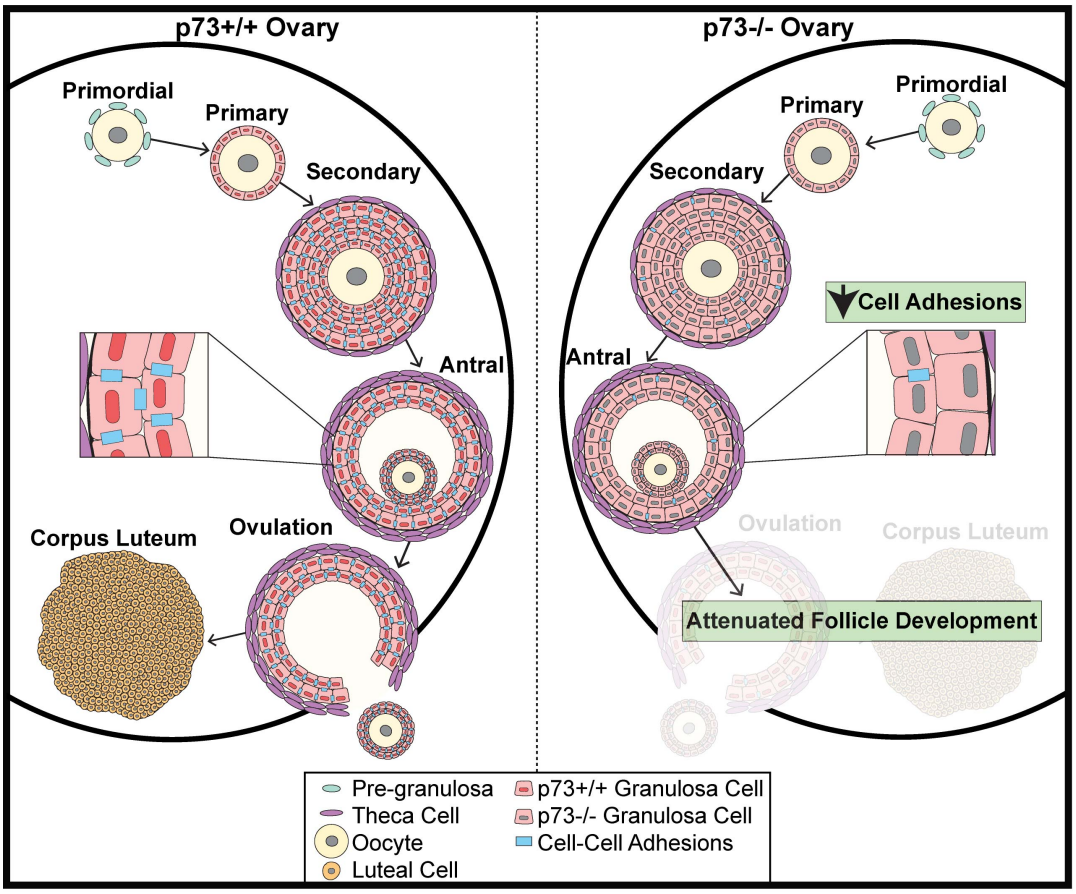

Figure 5.1. Graphical Representation of the Role of p73 in Ovarian Follicle Development.
Diagram demonstrates ovarian follicle development in the presence and absence of p73. On the left, p73 expression in granulosa cells regulates a gene network involved in cell-to-cell adhesions involved in proper follicle development, ovulation and corpus luteum formation. On the right, the absence of p73 leads to attenuated follicle development and impair ovulation.

p73 and Hormone Regulation

In addition to defective follicle development, absence of corpora lutea and a decrease in levels of circulating progesterone in p73-/- mice, we observed a decrease in FSH levels that likely contributed to the reduced number of developing follicles. We used 12 week-old (post-puberty) female mice to determine circulating levels of FSH levels and observed a 50% decrease. Given the cyclic regulation of FSH secretion during the estrous cycle, it would be of interest to define the time point during ovarian development where loss of p73 leads to defective FSH signaling. Future experiments are needed to measure FSH levels in immature p73+/+ and p73-/- female mice (pre-puberty).

FSH, secreted from the pituitary gland, is positively and negatively regulated by activin and inhibin, respectively, which are secreted from granulosa cells (Knight and Glister 2006). However, our analyses of circulating hormones demonstrated that there was not a significant difference in the levels of inhibin A and inhibin B in p73-/- female mice compared to p73+/+; and, we were unable to assay activin due to lack of a suitable assay. Given the positive feedback mechanism between activin and FSH, it will be of interest to determine circulating levels of activin in p73+/+ and p73-/- female mice when an assay is developed that yields reproducible results.

The FSH deregulation observed in p73-/- female mice led us to further investigate if p73 was expressed in the pituitary gland and also if p73 status played a role in overall LH and GH production. We analyzed LH and GH levels and did not observe a difference between p73+/+ and p73-/- female mice. Our data show that p73 is expressed in the pars intermedia and not in pars distalis where FSH, LH and GH are produced. Thus, we speculate that there are other factors at play in p73-deficient mice that lead to a decrease in FSH levels. It is known that FSH and LH production in the pituitary gland is stimulated by hypothalamus-secreted GnRH (Amoss et al. 1971). Of note, previous studies have demonstrated that p73-deficient mice exhibit hippocampal dysgenesis and hydrocephalus (Yang et al. 2000; Talos et al. 2010; Marshall et al. 2016). We also observed hippocampal dysgenesis and hydrocephalus to varying degrees on a mouse-to-mouse basis across our cohort of p73-deficient mice. Thus, it is possible that structural changes in the p73-/- murine brains, caused by hippocampal dysgenesis and hydrocephalus, impact the hypothalamus or pituitary gland function. Future studies focused on determining the impact that the varying degrees of the hippocampal dysgenesis and hydrocephalus have on the hypothalamus-pituitary gland signaling and GnRH secretion may be of value. In addition, it would be of interest to identify and quantify the various populations of gonadotropin-secreting cells using FSH- and LH-specific markers as well as single cell gene expression analysis in the pars distalis and pars intermedia

from p73+/+ and p73-/- pituitary glands. These types of experiment would allow us to identify p73 expression in specific cell populations.

p73 and Ovarian Steroidogenesis

Our gene expression analysis from p73+/+ and p73-/- antral follicles shows p73-dependent regulation of genes that encode key components of granulosa cell-associated focimatrix. Focimatrix levels have been previously linked with steroidogenesis and CYP11A1 (Irving-Rodgers et al. 2009; Matti et al. 2010) during ovarian follicle development. Consistent with defective focimatrix formation in our p73-deficient ovarian follicles, we observed a significant decrease in expression of Cyp11a1, the rate-limiting enzyme in cholesterol biosynthesis (Boyd et al. 1975), as well as other hormonally regulated genes including prolactin receptor (Prlr), luteinizing hormone/choriogonadotropin receptor (Lhcgr), oxytocin receptor (Oxtr), steroidogenic factor 1 (Nr5a1) and activin B receptor (Acvr1c) in p73-/- antral follicles. Nr5a1 is a transcriptional activator required for the formation of steroidogenic tissues and cell-specific knockout experiments have shown Nr5a1 is necessary for male and female fertility (Jeyasuria et al. 2004; Ferraz-de-Souza et al. 2011). Mice that lack Acvr1c expression in granulosa cells exhibit striking similarities to our p73-/- mice including defective follicle development, absence of corpora lutea and decreased levels of circulating FSH (Sandoval-Guzman et al. 2012) providing a possible mechanism for the

decreased FSH levels in our p73-/- females. Future studies are needed to determine the direct or indirect mechanism by which p73 regulates the expression of genes required for proper steroidogenesis and hormone signaling in antral follicles. For example, it would be of interest to determine if ectopic FSH rescues the ovarian follicle development defect observed in p73-/- female mice as well as changes the modulation of genes involved in granulosa cell steroidogenesis.

p73 and the Ciliated Cells of the Murine Oviduct

p73 is required for multiciliated cell development (Marshall et al. 2016; Nemajerova et al. 2016) and we observed expression of p73 in ciliated cells that line the oviductal epithelium in mice (Marshall et al. 2016); and, an absence of these cells in p73-deficient mice. A major role of ciliated cells in the oviduct is to transport the oocyte to the uterus for implantation (Halbert et al. 1976; Critoph and Dennis 1977). Mouse models that lack ciliated cells such as Foxj1 (Gomperts et al. 2004) and Gemc1 (Terre et al. 2016) gene knockouts, have similar phenotypes to our p73-deficient mice (Marshall et al. 2016), including female and male infertility. Gemc1-/- ovaries exhibit a follicle development defect similar to our p73-/- female mice (Terre et al. 2016). Given these finding with other mouse models, we are not able to rule out a possible paracrine mechanism between the ciliated cells in the oviduct and the granulosa cells or other follicle components in the ovaries. It would

be of interest to determine if ciliated cells have additional roles in fertility besides transport of the oocyte, in terms of a direct effect on ovarian follicle development and ovulation through cell-to-cell signaling mechanisms. We hypothesize that p73 is required in both granulosa cells within the follicle and ciliated cells in the oviduct to promote proper follicle development, ovulation, oocyte implantation and fertility. Analysis of tissue-specific (Foxl2- and Foxj1-specific) p73-knockout mouse models could provide mechanistic insight to the individual roles of p73 in granulosa and ciliated cells. Foxl2 is a granulosa cell-specific marker that colocalizes with p73 expression in murine ovarian follicles (Santos Guasch et al. 2018). Our laboratory recently published that p73 acts as a transcriptional regulator of Foxj1 (Marshall et al. 2016). Given the infertility defects observed in mouse models that lack ciliated cells, it would be important to determine if mice that lack p73 in Foxj1-positive cells in the oviduct have normal follicle development, ovulation and corpus luteum formation.

p73 and Human Female Fertility

Our discovery that p73 is required for ovarian follicle development, ovulation, corpora lutea formation, progesterone production and fertility (Santos Guasch et al. 2018) provides insight to the complex signaling mechanisms necessary for female reproduction. Since multiple human conditions have been linked to ovarian dysfunction, including primary ovarian

insufficiency (POI) and polycystic ovarian syndrome (PCOS), a future direction from our findings is to determine if p73 plays a role in these conditions. One approach is to perform a phenome-wide association study (PheWAS). PheWAS allows for the identification of medical diagnoses (ICD billing codes) with genetic variants by using de-identified electronic health records linked to genomic data from a large patient cohort (e.g. BioVU at Vanderbilt). The reproductive phenotypes in p73-/- female mice could be queried to determine if associations can be identified between p73 genetic variants and ovarian dysfunction-related medical diagnoses. The analyses could also be extended to various p73-target genes identified as part of this dissertation research (Chapter 4). In addition, we might be able to identify genetic variants in steroidogenesis genes associated with ovarian dysfunction as previous studies have identified single nucleotide polymorphisms (SNPs) in multiple steroidogenesis genes associated with increased susceptibility to PCOS (Crespo et al. 2018).

p73/p63 and Mammary Gland Branching

Analysis of our p73-deficient mouse model led us to discover a mammary gland branching phenotype that had not yet been reported. Our experiments showed that loss of p73 leads to decrease mammary gland branching at different stages throughout development. We provided evidence showing that the mammary gland branching defect observed in

p73-/- female mice is secondary to decreased levels of progesterone (absent corpora lutea) through a complete rescue of the branching defect after ectopic progesterone administration. However, it is of interest that decreased mammary gland branching is observed in 6-week old p73-/- female mice compared to p73+/+ given that these mice have not entered puberty. This observation suggests a possible cell-autonomous role for p73 initiating branching and priming the mammary gland for puberty, perhaps through regulation of epithelial cell differentiation as we reported in the airway (Marshall et al. 2016). Further studies are needed to identify if p73 serves as a transcriptional enhancer in progenitor cells that are involved in mammary gland branching in pre-pubertal female mice. Given our *in vitro* cell migration data, we hypothesize that p73 regulates myoepithelial cell migration to promote mammary gland branching.

Further, we demonstrated nuclear p73 positivity in cells expressing keratin 14, a myoepithelial cell layer marker. Similar to our observations in the tracheal epithelium (Marshall et al. 2016), we showed that p63 colocalizes with a subset of p73-expressing cells myoepithelial cells. Given the potential for hetero-oligomerization between p73 and p63 (Harms and Chen 2006), we analyzed p63 expression in mammary glands of p73-deficient mice. We observed an increase in p63-positive cells in the myoepithelial layer suggesting an increase in a progenitor cell population and likely a decrease in epithelial cells “marked” for differentiation along a

specific lineage. To determine if there is interplay of p63 in respect to its interacting partner p73, future transcriptional profiling experiments are needed to identify p63-target genes in the presence or absence of p73. For example, it will be crucial to identify if the transcriptional profile of p63 changes in a p73-deficient mammary gland. Further, single cell RNA-seq analyses on dissociated epithelial cells from p73+/+ and p73-/- mammary glands, in relation to lineage-specific markers would provide a better understanding of the unique and overlapping roles of p63 and p73 in mammary gland development.

p73 and Cell Migration

As described in Chapter 4, we provided evidence that p73 regulates cell migration in primary mouse and human cell models as well as in several human cancer cell lines. The loss of endogenous p73 expression resulted in a significant decrease in the rate of cell migration across all the cell models studied. We further identified 30 adhesion- and migration-associated genes with a p73-binding site within 25 kb of the TSS that were regulated by p73 in murine granulosa cells. Of immediate interest were p73-binding near genes encoding crucial regulators of cell adhesion, migration and cancer metastasis (PXN and MMP-14) in addition to focimatrix components LAMA5, NID1 and NID2.

Paxillin (PXN) is a focal adhesion adapter protein that regulates extracellular signal transduction, cytoskeleton remodeling and cell migration (Huang et al. 2003; Deramaudt et al. 2014; Hu et al. 2014). Previous studies have shown that paxillin acquires gain-of-function mutations associated with poor patient prognosis in aggressive breast (Madan et al. 2006; Short et al. 2007), lung (Jagadeeswaran et al. 2008; Mackinnon et al. 2011), prostate (Sen et al. 2012), melanoma (Velasco-Velazquez et al. 2008) and colorectal cancers (Yang et al. 2010). Future studies are needed to determine if p73 regulates cell migration and metastasis in a paxillin-dependent manner in the several epithelial cell types listed above.

Matrix metalloproteinase 14 (MMP-14) plays a role in the breakdown of extracellular matrix and tissue remodeling during mammary gland branching (Mori et al. 2013; Feinberg et al. 2016). Mmp-14 expression has been shown to localize to the luminal and myoepithelial layer of murine mammary gland and loss of Mmp-14 results in impaired mammary epithelial branching in 3D organoid cultures (Mori et al. 2013; Feinberg et al. 2016). Previous studies have shown that MMP-14 regulates cell migration and invasion as well as promoting epithelial-to-mesenchymal transition in nasopharyngeal carcinoma (Yan et al. 2015). It would be of interest to identify MMP-14 localization with respect to p73 in the mammary gland epithelium as well as MMP-14 expression in p73-overexpressing cancers.

Conclusions

In conclusion, the dissertation research presented herein has advanced our understanding of the role of p73 in murine ovarian follicle development, ovulation, corpora lutea formation and progesterone production. The results obtained from the experiments described in Chapters 3 and 4 provide evidence that p73 regulates cell-to-cell adhesions and promotes cell migration, and that these transcriptional networks are defective in p73-deficient mice leading to granulosa cell dysfunction and attenuation of corpora lutea development. As part of our studies, we also discovered a mammary gland branching defect in p73-/- female mice, secondary to the diminished corpora lutea, which could be rescued through ectopic progesterone administration. Overall, our findings support a model in which p73 is required for proper ovarian follicle development, in part, through the regulation of genes involved in granulosa-to-granulosa cell adhesion (Figure 5.1). Hopefully, these fundamental aspects of our discoveries can be translated to human application in women with ovarian dysfunction with resultant infertility.

REFERENCES

Abercrombie M, Heaysman JE, Pegrum SM. 1971. The locomotion of fibroblasts in culture. IV. Electron microscopy of the leading lamella. *Exp Cell Res* **67**: 359-367.

Allen WM. 1941. The Chemical and Physiological Properties, and Clinical Uses of the Corpus Luteum Hormone, Progesterone. *Bull N Y Acad Med* **17**: 508-518.

Amoss M, Burgus R, Blackwell R, Vale W, Fellows R, Guillemin R. 1971. Purification, amino acid composition and N-terminus of the hypothalamic luteinizing hormone releasing factor (LRF) of ovine origin. *Biochem Biophys Res Commun* **44**: 205-210.

Amso NN, Crow J, Shaw RW. 1994. Comparative immunohistochemical study of oestrogen and progesterone receptors in the fallopian tube and uterus at different stages of the menstrual cycle and the menopause. *Hum Reprod* **9**: 1027-1037.

Andrews S. 2018. FastQC v0.11.5.

Ashby WJ, Wikswo JP, Zijlstra A. 2012. Magnetically attachable stencils and the non-destructive analysis of the contribution made by the underlying matrix to cell migration. *Biomaterials* **33**: 8189-8203.

Aten RF, Kolodecik TR, Behrman HR. 1995. A cell adhesion receptor antiserum abolishes, whereas laminin and fibronectin glycoprotein components of extracellular matrix promote, luteinization of cultured rat granulosa cells. *Endocrinology* **136**: 1753-1758.

Auchus RJ, Lee TC, Miller WL. 1998. Cytochrome b5 augments the 17,20-lyase activity of human P450c17 without direct electron transfer. *J Biol Chem* **273**: 3158-3165.

Bae WK, Hong CS, Park MR, Sun EG, Lee JH, Kang K, Ryu KH, Shim HJ, Hwang JE, Cho SH et al. 2018. TAp73 inhibits cell invasion and migration by directly activating KAI1 expression in colorectal carcinoma. *Cancer letters* **415**: 106-116.

Baker SJ, Fearon ER, Nigro JM, Hamilton SR, Preisinger AC, Jessup JM, vanTuinen P, Ledbetter DH, Barker DF, Nakamura Y et al. 1989.

Chromosome 17 deletions and p53 gene mutations in colorectal carcinomas. *Science* **244**: 217-221.

Barak Y, Juven T, Haffner R, Oren M. 1993. mdm2 expression is induced by wild type p53 activity. *The EMBO journal* **12**: 461-468.

Barbareschi M, Pecciarini L, Cangi MG, Macri E, Rizzo A, Viale G, Doglioni C. 2001. p63, a p53 homologue, is a selective nuclear marker of myoepithelial cells of the human breast. *The American journal of surgical pathology* **25**: 1054-1060.

Barbieri CE, Pietenpol JA. 2005. p53 family members: similar biochemistry, different biology. *Cancer Biol Ther* **4**: 419-420.

Bergeron L, Perez GI, Macdonald G, Shi L, Sun Y, Jurisicova A, Varmuza S, Latham KE, Flaws JA, Salter JC et al. 1998. Defects in regulation of apoptosis in caspase-2-deficient mice. *Genes & development* **12**: 1304-1314.

Beumer TL, Roepers-Gajadien HL, Gademan IS, van Buul PP, Gil-Gomez G, Rutgers DH, de Rooij DG. 1998. The role of the tumor suppressor p53 in spermatogenesis. *Cell Death Differ* **5**: 669-677.

Blandino G, Dobbelstein M. 2004. p73 and p63: why do we still need them? *Cell Cycle* **3**: 886-894.

Bocchinfuso WP, Korach KS. 1997. Mammary gland development and tumorigenesis in estrogen receptor knockout mice. *J Mammary Gland Biol Neoplasia* **2**: 323-334.

Bocchinfuso WP, Lindzey JK, Hewitt SC, Clark JA, Myers PH, Cooper R, Korach KS. 2000. Induction of mammary gland development in estrogen receptor-alpha knockout mice. *Endocrinology* **141**: 2982-2994.

Borum K. 1961. Oogenesis in the mouse. A study of the meiotic prophase. *Exp Cell Res* **24**: 495-507.

Bourdon JC, Fernandes K, Murray-Zmijewski F, Liu G, Diot A, Xirodimas DP, Saville MK, Lane DP. 2005. p53 isoforms can regulate p53 transcriptional activity. *Genes & development* **19**: 2122-2137.

Boyd GS, Arthur JR, Beckett GJ, Mason JI, Trzeciak WH. 1975. The role of cholesterol and cytochrome P-450 in the cholesterol side chain

cleavage reaction in adrenal cortex and corpora lutea. *J Steroid Biochem* **6**: 427-436.

Brannian JD, Shiigi SM, Stouffer RL. 1992. Gonadotropin surge increases fluorescent-tagged low-density lipoprotein uptake by macaque granulosa cells from preovulatory follicles. *Biology of reproduction* **47**: 355-360.

Brown HM, Dunning KR, Robker RL, Boerboom D, Pritchard M, Lane M, Russell DL. 2010. ADAMTS1 cleavage of versican mediates essential structural remodeling of the ovarian follicle and cumulus-oocyte matrix during ovulation in mice. *Biology of reproduction* **83**: 549-557.

Byers M, Kuiper GG, Gustafsson JA, Park-Sarge OK. 1997. Estrogen receptor-beta mRNA expression in rat ovary: down-regulation by gonadotropins. *Mol Endocrinol* **11**: 172-182.

Byers SL, Wiles MV, Dunn SL, Taft RA. 2012. Mouse estrous cycle identification tool and images. *PLoS ONE* **7**: e35538.

Caligioni CS. 2009. Assessing reproductive status/stages in mice. *Curr Protoc Neurosci* **Appendix 4**: Appendix 4I.

Candi E, Rufini A, Terrinoni A, Dinsdale D, Ranalli M, Paradisi A, De Laurenzi V, Spagnoli LG, Catani MV, Ramadan S et al. 2006. Differential roles of p63 isoforms in epidermal development: selective genetic complementation in p63 null mice. *Cell Death Differ* **13**: 1037-1047.

Carabatsos MJ, Elvin J, Matzuk MM, Albertini DF. 1998. Characterization of oocyte and follicle development in growth differentiation factor-9-deficient mice. *Dev Biol* **204**: 373-384.

Carletti MZ, Christenson LK. 2009. Rapid effects of LH on gene expression in the mural granulosa cells of mouse periovulatory follicles. *Reproduction* **137**: 843-855.

Carroll DK, Carroll JS, Leong CO, Cheng F, Brown M, Mills AA, Brugge JS, Ellisen LW. 2006. p63 regulates an adhesion programme and cell survival in epithelial cells. *Nature cell biology* **8**: 551-561.

Chan WM, Siu WY, Lau A, Poon RY. 2004. How many mutant p53 molecules are needed to inactivate a tetramer? *Mol Cell Biol* **24**: 3536-3551.

Chandra A, Copen CE, Stephen EH. 2013. Infertility and impaired fecundity in the United States, 1982-2010: data from the National Survey of Family Growth. *Natl Health Stat Report*: 1-18, 11 p following 19.

Chen L, Russell PT, Larsen WJ. 1993. Functional significance of cumulus expansion in the mouse: roles for the preovulatory synthesis of hyaluronic acid within the cumulus mass. *Mol Reprod Dev* **34**: 87-93.

Chene P. 2001. The role of tetramerization in p53 function. *Oncogene* **20**: 2611-2617.

Chung BC, Matteson KJ, Voutilainen R, Mohandas TK, Miller WL. 1986. Human cholesterol side-chain cleavage enzyme, P450scc: cDNA cloning, assignment of the gene to chromosome 15, and expression in the placenta. *Proc Natl Acad Sci U S A* **83**: 8962-8966.

Clark BJ, Wells J, King SR, Stocco DM. 1994. The purification, cloning, and expression of a novel luteinizing hormone-induced mitochondrial protein in MA-10 mouse Leydig tumor cells. Characterization of the steroidogenic acute regulatory protein (StAR). *J Biol Chem* **269**: 28314-28322.

Condeelis J. 1993. Life at the leading edge: the formation of cell protrusions. *Annu Rev Cell Biol* **9**: 411-444.

Conneely OM, Mulac-Jericevic B, Lydon JP. 2003. Progesterone-dependent regulation of female reproductive activity by two distinct progesterone receptor isoforms. *Steroids* **68**: 771-778.

Couse JF, Yates MM, Walker VR, Korach KS. 2003. Characterization of the hypothalamic-pituitary-gonadal axis in estrogen receptor (ER) Null mice reveals hypergonadism and endocrine sex reversal in females lacking ERalpha but not ERbeta. *Mol Endocrinol* **17**: 1039-1053.

Crespo RP, Bachega T, Mendonca BB, Gomes LG. 2018. An update of genetic basis of PCOS pathogenesis. *Arch Endocrinol Metab* **62**: 352-361.

Critoph FN, Dennis KJ. 1977. Ciliary activity in the human oviduct. *Obstet Gynecol Surv* **32**: 602-603.

Crow J, Amso NN, Lewin J, Shaw RW. 1994. Morphology and ultrastructure of fallopian tube epithelium at different stages of the menstrual cycle and menopause. *Hum Reprod* **9**: 2224-2233.

Croxatto HB, Ortiz ME. 1975. Egg transport in the fallopian tube. *Gynecol Invest* **6**: 215-225.

Croxatto HB, Ortiz ME, Diaz S, Hess R, Balmaceda J, Croxatto HD. 1978. Studies on the duration of egg transport by the human oviduct. II. Ovum location at various intervals following luteinizing hormone peak. *Am J Obstet Gynecol* **132**: 629-634.

Curry TE, Jr., Mann JS, Huang MH, Keeble SC. 1992. Gelatinase and proteoglycanase activity during the periovulatory period in the rat. *Biology of reproduction* **46**: 256-264.

Curry TE, Jr., Osteen KG. 2003. The matrix metalloproteinase system: changes, regulation, and impact throughout the ovarian and uterine reproductive cycle. *Endocr Rev* **24**: 428-465.

De Laurenzi V, Costanzo A, Barcaroli D, Terrinoni A, Falco M, Annicchiarico-Petruzzelli M, Levrero M, Melino G. 1998. Two new p73 splice variants, gamma and delta, with different transcriptional activity. *J Exp Med* **188**: 1763-1768.

De Laurenzi V, Rossi A, Terrinoni A, Barcaroli D, Levrero M, Costanzo A, Knight RA, Guerrieri P, Melino G. 2000. p63 and p73 transactivate differentiation gene promoters in human keratinocytes. *Biochem Biophys Res Commun* **273**: 342-346.

DeLeo AB, Jay G, Appella E, Dubois GC, Law LW, Old LJ. 1979. Detection of a transformation-related antigen in chemically induced sarcomas and other transformed cells of the mouse. *Proc Natl Acad Sci U S A* **76**: 2420-2424.

Deramaudt TB, Dujardin D, Noulet F, Martin S, Vauchelles R, Takeda K, Ronde P. 2014. Altering FAK-paxillin interactions reduces adhesion, migration and invasion processes. *PLoS ONE* **9**: e92059.

Deutsch GB, Zielonka EM, Coutandin D, Weber TA, Schafer B, Hannewald J, Luh LM, Durst FG, Ibrahim M, Hoffmann J et al. 2011. DNA damage in oocytes induces a switch of the quality control factor TAp63alpha from dimer to tetramer. *Cell* **144**: 566-576.

Deyoung MP, Johannessen CM, Leong CO, Faquin W, Rocco JW, Ellisen LW. 2006. Tumor-Specific p73 Up-regulation Mediates p63 Dependence in Squamous Cell Carcinoma. *Cancer Res* **66**: 9362-9368.

Diller L, Kassel J, Nelson CE, Gryka MA, Litwak G, Gebhardt M, Bressac B, Ozturk M, Baker SJ, Vogelstein B et al. 1990. p53 functions as a cell cycle control protein in osteosarcomas. *Mol Cell Biol* **10**: 5772-5781.

Dobin A, Davis CA, Schlesinger F, Drenkow J, Zaleski C, Jha S, Batut P, Chaisson M, Gingeras TR. 2013. STAR: ultrafast universal RNA-seq aligner. *Bioinformatics* **29**: 15-21.

Dodt M, Roehr JT, Ahmed R, Dieterich C. 2012. FLEXBAR-Flexible Barcode and Adapter Processing for Next-Generation Sequencing Platforms. *Biology* **1**: 895-905.

Donehower LA, Harvey M, Slagle BL, McArthur MJ, Montgomery CA, Jr., Butel JS, Bradley A. 1992. Mice deficient for p53 are developmentally normal but susceptible to spontaneous tumours. *Nature* **356**: 215-221.

Dotsch V, Bernassola F, Coutandin D, Candi E, Melino G. 2010. p63 and p73, the ancestors of p53. *Cold Spring Harbor perspectives in biology* **2**: a004887.

Dufort I, Rheault P, Huang XF, Soucy P, Luu-The V. 1999. Characteristics of a highly labile human type 5 17beta-hydroxysteroid dehydrogenase. *Endocrinology* **140**: 568-574.

Dupont S, Krust A, Gansmuller A, Dierich A, Chambon P, Mark M. 2000. Effect of single and compound knockouts of estrogen receptors alpha (ERalpha) and beta (ERbeta) on mouse reproductive phenotypes. *Development* **127**: 4277-4291.

Durkin ME, Qian X, Popescu NC, Lowy DR. 2013. Isolation of Mouse Embryo Fibroblasts. *Bio Protoc* **3**.

el-Deiry WS, Kern SE, Pietenpol JA, Kinzler KW, Vogelstein B. 1992. Definition of a consensus binding site for p53. *Nat Genet* **1**: 45-49.

el-Deiry WS, Tokino T, Velculescu VE, Levy DB, Parsons R, Trent JM, Lin D, Mercer WE, Kinzler KW, Vogelstein B. 1993. WAF1, a potential mediator of p53 tumor suppression. *Cell* **75**: 817-825.

Eliyahu D, Goldfinger N, Pinhasi-Kimhi O, Shaulsky G, Skurnik Y, Arai N, Rotter V, Oren M. 1988. Meth A fibrosarcoma cells express two transforming mutant p53 species. *Oncogene* **3**: 313-321.

Eliyahu D, Michalovitz D, Eliyahu S, Pinhasi-Kimhi O, Oren M. 1989. Wild-type p53 can inhibit oncogene-mediated focus formation. *Proc Natl Acad Sci U S A* **86**: 8763-8767.

Eppig JJ, Wigglesworth K. 2000. Development of mouse and rat oocytes in chimeric reaggregated ovaries after interspecific exchange of somatic and germ cell components. *Biology of reproduction* **63**: 1014-1023.

Eppig JJ, Wigglesworth K, Hirao Y. 2000. Metaphase I arrest and spontaneous parthenogenetic activation of strain LTXBO oocytes: chimeric reaggregated ovaries establish primary lesion in oocytes. *Dev Biol* **224**: 60-68.

Espinosa JM, Emerson BM. 2001. Transcriptional regulation by p53 through intrinsic DNA/chromatin binding and site-directed cofactor recruitment. *Mol Cell* **8**: 57-69.

Familiari G, Verlengia C, Nottola SA, Renda T, Micara G, Aragona C, Zardi L, Motta PM. 1996. Heterogeneous distribution of fibronectin, tenascin-C, and laminin immunoreactive material in the cumulus-corona cells surrounding mature human oocytes from IVF-ET protocols--evidence that they are composed of different subpopulations: an immunohistochemical study using scanning confocal laser and fluorescence microscopy. *Mol Reprod Dev* **43**: 392-402.

Feinberg TY, Rowe RG, Saunders TL, Weiss SJ. 2016. Functional roles of MMP14 and MMP15 in early postnatal mammary gland development. *Development* **143**: 3956-3968.

Fernandez-Alonso R, Martin-Lopez M, Gonzalez-Cano L, Garcia S, Castrillo F, Diez-Prieto I, Fernandez-Corona A, Lorenzo-Marcos ME, Li X, Claesson-Welsh L et al. 2015. p73 is required for endothelial cell differentiation, migration and the formation of vascular networks regulating VEGF and TGFbeta signaling. *Cell Death Differ* **22**: 1287-1299.

Ferraz-de-Souza B, Lin L, Achermann JC. 2011. Steroidogenic factor-1 (SF-1, NR5A1) and human disease. *Mol Cell Endocrinol* **336**: 198-205.

Finlay CA, Hinds PW, Levine AJ. 1989. The p53 proto-oncogene can act as a suppressor of transformation. *Cell* **57**: 1083-1093.

Finlay CA, Hinds PW, Tan TH, Eliyahu D, Oren M, Levine AJ. 1988. Activating mutations for transformation by p53 produce a gene product

that forms an hsc70-p53 complex with an altered half-life. *Mol Cell Biol* **8**: 531-539.

Forsyth IA, Neville MC. 2009. Introduction: the myoepithelial cell and milk letdown; entrance to the multifunctional role of oxytocin. *J Mammary Gland Biol Neoplasia* **14**: 221-222.

Foster DL, Ryan KD. 1979. Endocrine mechanisms governing transition into adulthood: a marked decrease in inhibitory feedback action of estradiol on tonic secretion of luteinizing hormone in the lamb during puberty. *Endocrinology* **105**: 896-904.

Fowler RE, Fox NL, Edwards RG, Steptoe PC. 1978. Steroid production from 17alpha-hydroxypregnenolone and dehydroepiandrosterone by human granulosa cells in vitro. *J Reprod Fertil* **54**: 109-117.

Fraser HM, Dickson SE, Lunn SF, Wulff C, Morris KD, Carroll VA, Bicknell R. 2000. Suppression of luteal angiogenesis in the primate after neutralization of vascular endothelial growth factor. *Endocrinology* **141**: 995-1000.

Fulop C, Szanto S, Mukhopadhyay D, Bardos T, Kamath RV, Rugg MS, Day AJ, Salustri A, Hascall VC, Glant TT et al. 2003. Impaired cumulus mucification and female sterility in tumor necrosis factor-induced protein-6 deficient mice. *Development* **130**: 2253-2261.

Gadea G, Lapasset L, Gauthier-Rouviere C, Roux P. 2002. Regulation of Cdc42-mediated morphological effects: a novel function for p53. *The EMBO journal* **21**: 2373-2382.

Geback T, Schulz MM, Koumoutsakos P, Detmar M. 2009. TScratch: a novel and simple software tool for automated analysis of monolayer wound healing assays. *Biotechniques* **46**: 265-274.

Goldman JM, Murr AS, Cooper RL. 2007. The rodent estrous cycle: characterization of vaginal cytology and its utility in toxicological studies. *Birth Defects Res B Dev Reprod Toxicol* **80**: 84-97.

Gomperts BN, Gong-Cooper X, Hackett BP. 2004. Foxj1 regulates basal body anchoring to the cytoskeleton of ciliated pulmonary epithelial cells. *Journal of cell science* **117**: 1329-1337.

Gonfloni S, Di Tella L, Caldarola S, Cannata SM, Klinger FG, Di Bartolomeo C, Mattei M, Candi E, De Felici M, Melino G et al. 2009.

Inhibition of the c-Abl-TAp63 pathway protects mouse oocytes from chemotherapy-induced death. *Nature medicine* **15**: 1179-1185.

Gonzalez-Cano L, Fuertes-Alvarez S, Robledinos-Anton N, Bizy A, Villena-Cortes A, Farinas I, Marques MM, Marin MC. 2015. p73 is required for ependymal cell maturation and neurogenic SVZ cytoarchitecture. *Dev Neurobiol* **76**: 730-747.

Gosden RG, Hunter RH, Telfer E, Torrance C, Brown N. 1988. Physiological factors underlying the formation of ovarian follicular fluid. *J Reprod Fertil* **82**: 813-825.

Grespi F, Amelio I, Tucci P, Annicchiarico-Petruzzelli M, Melino G. 2012. Tissue-specific expression of p73 C-terminal isoforms in mice. *Cell Cycle* **11**: 4474-4483.

Grive KJ, Freiman RN. 2015. The developmental origins of the mammalian ovarian reserve. *Development* **142**: 2554-2563.

Grob TJ, Novak U, Maisse C, Barcaroli D, Luthi AU, Pirnia F, Hugli B, Graber HU, De Laurenzi V, Fey MF et al. 2001. Human delta Np73 regulates a dominant negative feedback loop for TAp73 and p53. *Cell Death Differ* **8**: 1213-1223.

Groome NP, Illingworth PJ, O'Brien M, Pai R, Rodger FE, Mather JP, McNeilly AS. 1996. Measurement of dimeric inhibin B throughout the human menstrual cycle. *J Clin Endocrinol Metab* **81**: 1401-1405.

Hagglund AC, Ny A, Leonardsson G, Ny T. 1999. Regulation and localization of matrix metalloproteinases and tissue inhibitors of metalloproteinases in the mouse ovary during gonadotropin-induced ovulation. *Endocrinology* **140**: 4351-4358.

Halbert SA, Tam PY, Blandau RJ. 1976. Egg transport in the rabbit oviduct: the roles of cilia and muscle. *Science* **191**: 1052-1053.

Halevy O, Rodel J, Peled A, Oren M. 1991. Frequent p53 mutations in chemically induced murine fibrosarcoma. *Oncogene* **6**: 1593-1600.

Hall PA, McKee PH, Menage HD, Dover R, Lane DP. 1993. High levels of p53 protein in UV-irradiated normal human skin. *Oncogene* **8**: 203-207.

Hanukoglu I. 1992. Steroidogenic enzymes: structure, function, and role in regulation of steroid hormone biosynthesis. *J Steroid Biochem Mol Biol* **43**: 779-804.

Harms K, Nozell S, Chen X. 2004. The common and distinct target genes of the p53 family transcription factors. *Cell Mol Life Sci* **61**: 822-842.

Harms KL, Chen X. 2006. The functional domains in p53 family proteins exhibit both common and distinct properties. *Cell Death Differ* **13**: 890-897.

Hasegawa M, Zhang Y, Niibe H, Terry NH, Meistrich ML. 1998. Resistance of differentiating spermatogonia to radiation-induced apoptosis and loss in p53-deficient mice. *Radiat Res* **149**: 263-270.

Hazzard TM, Christenson LK, Stouffer RL. 2000. Changes in expression of vascular endothelial growth factor and angiopoietin-1 and -2 in the macaque corpus luteum during the menstrual cycle. *Mol Hum Reprod* **6**: 993-998.

Hazzard TM, Molskness TA, Chaffin CL, Stouffer RL. 1999. Vascular endothelial growth factor (VEGF) and angiopoietin regulation by gonadotrophin and steroids in macaque granulosa cells during the peri-ovulatory interval. *Mol Hum Reprod* **5**: 1115-1121.

Heath JP, Dunn GA. 1978. Cell to substratum contacts of chick fibroblasts and their relation to the microfilament system. A correlated interference-reflexion and high-voltage electron-microscope study. *Journal of cell science* **29**: 197-212.

Hennighausen L, Robinson GW. 2005. Information networks in the mammary gland. *Nat Rev Mol Cell Biol* **6**: 715-725.

Hillier SG. 1994. Current concepts of the roles of follicle stimulating hormone and luteinizing hormone in folliculogenesis. *Hum Reprod* **9**: 188-191.

Hirai M, Hirata S, Osada T, Hagihara K, Kato J. 1994. Androgen receptor mRNA in the rat ovary and uterus. *J Steroid Biochem Mol Biol* **49**: 1-7.

Hirshfield AN. 1991. Development of follicles in the mammalian ovary. *Int Rev Cytol* **124**: 43-101.

Holembowski L, Kramer D, Riedel D, Sordella R, Nemajerova A, Dobbelstein M, Moll UM. 2014. TAp73 is essential for germ cell

adhesion and maturation in testis. *The Journal of cell biology* **204**: 1173-1190.

Hsueh AJ, Adashi EY, Jones PB, Welsh TH, Jr. 1984. Hormonal regulation of the differentiation of cultured ovarian granulosa cells. *Endocr Rev* **5**: 76-127.

Hu W, Feng Z, Teresky AK, Levine AJ. 2007. p53 regulates maternal reproduction through LIF. *Nature* **450**: 721-724.

Hu YL, Lu S, Szeto KW, Sun J, Wang Y, Lasheras JC, Chien S. 2014. FAK and paxillin dynamics at focal adhesions in the protrusions of migrating cells. *Sci Rep* **4**: 6024.

Huang C, Rajfur Z, Borchers C, Schaller MD, Jacobson K. 2003. JNK phosphorylates paxillin and regulates cell migration. *Nature* **424**: 219-223.

Huet C, Pisselet C, Mandon-Pepin B, Monget P, Monniaux D. 2001. Extracellular matrix regulates ovine granulosa cell survival, proliferation and steroidogenesis: relationships between cell shape and function. *J Endocrinol* **169**: 347-360.

Inoue S, Tomasini R, Rufini A, Elia AJ, Agostini M, Amelio I, Cescon D, Dinsdale D, Zhou L, Harris IS et al. 2014. TAp73 is required for spermatogenesis and the maintenance of male fertility. *Proc Natl Acad Sci U S A* **111**: 1843-1848.

Institute B. 2018. Picard Toolkit. *Broad Institute, GitHub repository*.

Irving-Rodgers HF, Catanzariti KD, Aspden WJ, D'Occhio MJ, Rodgers RJ. 2006. Remodeling of extracellular matrix at ovulation of the bovine ovarian follicle. *Mol Reprod Dev* **73**: 1292-1302.

Irving-Rodgers HF, Harland ML, Rodgers RJ. 2004. A novel basal lamina matrix of the stratified epithelium of the ovarian follicle. *Matrix Biol* **23**: 207-217.

Irving-Rodgers HF, Harland ML, Sullivan TR, Rodgers RJ. 2009. Studies of granulosa cell maturation in dominant and subordinate bovine follicles: novel extracellular matrix focimatrix is co-ordinately regulated with cholesterol side-chain cleavage CYP11A1. *Reproduction* **137**: 825-834.

Irving-Rodgers HF, Hummitzsch K, Murdiyarso LS, Bonner WM, Sado Y, Ninomiya Y, Couchman JR, Sorokin LM, Rodgers RJ. 2010. Dynamics of extracellular matrix in ovarian follicles and corpora lutea of mice. *Cell and tissue research* **339**: 613-624.

Irwin MS, Kondo K, Marin MC, Cheng LS, Hahn WC, Kaelin WG, Jr. 2003. Chemosensitivity linked to p73 function. *Cancer Cell* **3**: 403-410.

Iwamasa J, Shibata S, Tanaka N, Matsuura K, Okamura H. 1992. The relationship between ovarian progesterone and proteolytic enzyme activity during ovulation in the gonadotropin-treated immature rat. *Biology of reproduction* **46**: 309-313.

Jagadeeswaran R, Surawska H, Krishnaswamy S, Janamanchi V, Mackinnon AC, Seiwert TY, Loganathan S, Kanteti R, Reichman T, Nallasura V et al. 2008. Paxillin is a target for somatic mutations in lung cancer: implications for cell growth and invasion. *Cancer Res* **68**: 132-142.

Jeyasuria P, Ikeda Y, Jamin SP, Zhao L, De Rooij DG, Themmen AP, Behringer RR, Parker KL. 2004. Cell-specific knockout of steroidogenic factor 1 reveals its essential roles in gonadal function. *Mol Endocrinol* **18**: 1610-1619.

Jordan JJ, Menendez D, Inga A, Nourredine M, Bell D, Resnick MA. 2008. Noncanonical DNA motifs as transactivation targets by wild type and mutant p53. *PLoS genetics* **4**: e1000104.

Jost CA, Marin MC, Kaelin WG, Jr. 1997. p73 is a simian [correction of human] p53-related protein that can induce apoptosis. *Nature* **389**: 191-194.

Juven T, Barak Y, Zauberman A, George DL, Oren M. 1993. Wild type p53 can mediate sequence-specific transactivation of an internal promoter within the mdm2 gene. *Oncogene* **8**: 3411-3416.

Kaghad M, Bonnet H, Yang A, Creancier L, Biscan JC, Valent A, Minty A, Chalon P, Lelias JM, Dumont X et al. 1997. Monoallelically expressed gene related to p53 at 1p36, a region frequently deleted in neuroblastoma and other human cancers. *Cell* **90**: 809-819.

Kandoth C, McLellan MD, Vandin F, Ye K, Niu B, Lu C, Xie M, Zhang Q, McMichael JF, Wyczalkowski MA et al. 2013. Mutational landscape and significance across 12 major cancer types. *Nature* **502**: 333-339.

Kastan MB, Zhan Q, el-Deiry WS, Carrier F, Jacks T, Walsh WV, Plunkett BS, Vogelstein B, Fornace AJ, Jr. 1992. A mammalian cell cycle checkpoint pathway utilizing p53 and GADD45 is defective in ataxia-telangiectasia. *Cell* **71**: 587-597.

Kastner P, Krust A, Turcotte B, Stropp U, Tora L, Gronemeyer H, Chambon P. 1990. Two distinct estrogen-regulated promoters generate transcripts encoding the two functionally different human progesterone receptor forms A and B. *The EMBO journal* **9**: 1603-1614.

Katayama T, Shiota K, Takahashi M. 1990. Activin A increases the number of follicle-stimulating hormone cells in anterior pituitary cultures. *Mol Cell Endocrinol* **69**: 179-185.

Khan-Dawood FS, Goldsmith LT, Weiss G, Dawood MY. 1989. Human corpus luteum secretion of relaxin, oxytocin, and progesterone. *J Clin Endocrinol Metab* **68**: 627-631.

Kidder GM, Mhawi AA. 2002. Gap junctions and ovarian folliculogenesis. *Reproduction* **123**: 613-620.

Kim SY, Ebbert K, Cordeiro MH, Romero M, Zhu J, Serna VA, Whelan KA, Woodruff TK, Kurita T. 2015. Cell autonomous phosphoinositide 3-kinase activation in oocytes disrupts normal ovarian function through promoting survival and overgrowth of ovarian follicles. *Endocrinology* **156**: 1464-1476.

Knight PG, Glister C. 2006. TGF-beta superfamily members and ovarian follicle development. *Reproduction* **132**: 191-206.

Kolde R. 2015. pheatmap: Pretty Heatmaps. R package version 1.0.8., https://CRAN.R-project.org/package=pheatmap.

Krege JH, Hodgin JB, Couse JF, Enmark E, Warner M, Mahler JF, Sar M, Korach KS, Gustafsson JA, Smithies O. 1998. Generation and reproductive phenotypes of mice lacking estrogen receptor beta. *Proc Natl Acad Sci U S A* **95**: 15677-15682.

Kurita T, Cunha GR, Robboy SJ, Mills AA, Medina RT. 2005. Differential expression of p63 isoforms in female reproductive organs. *Mechanisms of development* **122**: 1043-1055.

Landre V, Antonov A, Knight R, Melino G. 2016. p73 promotes glioblastoma cell invasion by directly activating POSTN (periostin) expression. *Oncotarget* **7**: 11785-11802.

Lane DP, Crawford LV. 1979. T antigen is bound to a host protein in SV40-transformed cells. *Nature* **278**: 261-263.

Lee CW, La Thangue NB. 1999. Promoter specificity and stability control of the p53-related protein p73. *Oncogene* **18**: 4171-4181.

Leong CO, Vidnovic N, DeYoung MP, Sgroi D, Ellisen LW. 2007. The p63/p73 network mediates chemosensitivity to cisplatin in a biologically defined subset of primary breast cancers. *J Clin Invest* **117**: 1370-1380.

Li H, Durbin R. 2009. Fast and accurate short read alignment with Burrows-Wheeler transform. *Bioinformatics* **25**: 1754-1760.

Li H, Handsaker B, Wysoker A, Fennell T, Ruan J, Homer N, Marth G, Abecasis G, Durbin R, Genome Project Data Processing S. 2009. The Sequence Alignment/Map format and SAMtools. *Bioinformatics* **25**: 2078-2079.

Liao Y, Smyth GK, Shi W. 2014. featureCounts: an efficient general purpose program for assigning sequence reads to genomic features. *Bioinformatics* **30**: 923-930.

Lie BL, Leung E, Leung PC, Auersperg N. 1996. Long-term growth and steroidogenic potential of human granulosa-lutein cells immortalized with SV40 large T antigen. *Mol Cell Endocrinol* **120**: 169-176.

Lim H, Paria BC, Das SK, Dinchuk JE, Langenbach R, Trzaskos JM, Dey SK. 1997. Multiple female reproductive failures in cyclooxygenase 2-deficient mice. *Cell* **91**: 197-208.

Linzer DI, Levine AJ. 1979. Characterization of a 54K dalton cellular SV40 tumor antigen present in SV40-transformed cells and uninfected embryonal carcinoma cells. *Cell* **17**: 43-52.

Liu G, Nozell S, Xiao H, Chen X. 2004. DeltaNp73beta is active in transactivation and growth suppression. *Mol Cell Biol* **24**: 487-501.

Livera G, Petre-Lazar B, Guerquin MJ, Trautmann E, Coffigny H, Habert R. 2008. p63 null mutation protects mouse oocytes from radio-induced apoptosis. *Reproduction* **135**: 3-12.

Lokshin M, Li Y, Gaiddon C, Prives C. 2007. p53 and p73 display common and distinct requirements for sequence specific binding to DNA. *Nucleic acids research* **35**: 340-352.

Love MI, Huber W, Anders S. 2014. Moderated estimation of fold change and dispersion for RNA-seq data with DESeq2. *Genome biology* **15**: 550.

Lubahn DB, Moyer JS, Golding TS, Couse JF, Korach KS, Smithies O. 1993. Alteration of reproductive function but not prenatal sexual development after insertional disruption of the mouse estrogen receptor gene. *Proc Natl Acad Sci U S A* **90**: 11162-11166.

Lydon JP, DeMayo FJ, Conneely OM, O'Malley BW. 1996. Reproductive phenotpes of the progesterone receptor null mutant mouse. *J Steroid Biochem Mol Biol* **56**: 67-77.

Lydon JP, DeMayo FJ, Funk CR, Mani SK, Hughes AR, Montgomery CA, Jr., Shyamala G, Conneely OM, O'Malley BW. 1995. Mice lacking progesterone receptor exhibit pleiotropic reproductive abnormalities. *Genes & development* **9**: 2266-2278.

Machanick P, Bailey TL. 2011. MEME-ChIP: motif analysis of large DNA datasets. *Bioinformatics* **27**: 1696-1697.

Mackinnon AC, Tretiakova M, Henderson L, Mehta RG, Yan BC, Joseph L, Krausz T, Husain AN, Reid ME, Salgia R. 2011. Paxillin expression and amplification in early lung lesions of high-risk patients, lung adenocarcinoma and metastatic disease. *Journal of clinical pathology* **64**: 16-24.

Madan R, Smolkin MB, Cocker R, Fayyad R, Oktay MH. 2006. Focal adhesion proteins as markers of malignant transformation and prognostic indicators in breast carcinoma. *Hum Pathol* **37**: 9-15.

Mahmood T, Saridogan E, Smutna S, Habib AM, Djahanbakhch O. 1998. The effect of ovarian steroids on epithelial ciliary beat frequency in the human Fallopian tube. *Hum Reprod* **13**: 2991-2994.

Malkin D, Li FP, Strong LC, Fraumeni JF, Jr., Nelson CE, Kim DH, Kassel J, Gryka MA, Bischoff FZ, Tainsky MA et al. 1990. Germ line p53 mutations in a familial syndrome of breast cancer, sarcomas, and other neoplasms. *Science* **250**: 1233-1238.

Marshall CB, Mays DJ, Beeler JS, Rosenbluth JM, Boyd KL, Santos Guasch GL, Shaver TM, Tang LJ, Liu Q, Shyr Y et al. 2016. p73 Is Required for Multiciliogenesis and Regulates the Foxj1-Associated Gene Network. *Cell Rep* **14**: 2289-2300.

Martin M. 2011. Cutadapt removes adapter sequences from high-throughput sequencing reads. *EMBnet* **17**: 10-12.

Martin-Lopez M, Maeso-Alonso L, Fuertes-Alvarez S, Balboa D, Rodriguez-Cortez V, Weltner J, Diez-Prieto I, Davis A, Wu Y, Otonkoski T et al. 2017. p73 is required for appropriate BMP-induced mesenchymal-to-epithelial transition during somatic cell reprogramming. *Cell death & disease* **8**: e3034.

Matti N, Irving-Rodgers HF, Hatzirodos N, Sullivan TR, Rodgers RJ. 2010. Differential expression of focimatrix and steroidogenic enzymes before size deviation during waves of follicular development in bovine ovarian follicles. *Mol Cell Endocrinol* **321**: 207-214.

McGee EA, Hsueh AJ. 2000. Initial and cyclic recruitment of ovarian follicles. *Endocr Rev* **21**: 200-214.

McNatty KP, Makris A, De Grazia C, Osathanondh R, Ryan KJ. 1979. The production of progesterone, androgens and oestrogens by human granulosa cells in vitro and in vivo. *J Steroid Biochem* **11**: 775-779.

Medina-Bolivar C, Gonzalez-Arnay E, Talos F, Gonzalez-Gomez M, Moll UM, Meyer G. 2014. Cortical hypoplasia and ventriculomegaly of p73-deficient mice: Developmental and adult analysis. *The Journal of comparative neurology* **522**: 2663-2679.

Melino G, De Laurenzi V, Vousden KH. 2002. p73: Friend or foe in tumorigenesis. *Nature reviews* **2**: 605-615.

Mills AA, Zheng B, Wang XJ, Vogel H, Roop DR, Bradley A. 1999. p63 is a p53 homologue required for limb and epidermal morphogenesis. *Nature* **398**: 708-713.

Mittaz L, Russell DL, Wilson T, Brasted M, Tkalcevic J, Salamonsen LA, Hertzog PJ, Pritchard MA. 2004. Adamts-1 is essential for the development and function of the urogenital system. *Biology of reproduction* **70**: 1096-1105.

Moll UM, Slade N. 2004. p63 and p73: roles in development and tumor formation. *Mol Cancer Res* **2**: 371-386.

Monk M, McLaren A. 1981. X-chromosome activity in foetal germ cells of the mouse. *J Embryol Exp Morphol* **63**: 75-84.

Moon YS, Tsang BK, Simpson C, Armstrong DT. 1978. 17 beta-Estradiol biosynthesis in cultured granulosa and thecal cells of human ovarian follicles: stimulation by follicle-stimulating hormone. *J Clin Endocrinol Metab* **47**: 263-267.

Mori H, Lo AT, Inman JL, Alcaraz J, Ghajar CM, Mott JD, Nelson CM, Chen CS, Zhang H, Bascom JL et al. 2013. Transmembrane/cytoplasmic, rather than catalytic, domains of Mmp14 signal to MAPK activation and mammary branching morphogenesis via binding to integrin beta1. *Development* **140**: 343-352.

Mori T, Suzuki A, Nishimura T, Kambegawa A. 1977. Evidence for androgen participation in induced ovulation in immature rats. *Endocrinology* **101**: 623-626.

Mork L, Tang H, Batchvarov I, Capel B. 2012. Mouse germ cell clusters form by aggregation as well as clonal divisions. *Mechanisms of development* **128**: 591-596.

Morrison MM, Hutchinson K, Williams MM, Stanford JC, Balko JM, Young C, Kuba MG, Sanchez V, Williams AJ, Hicks DJ et al. 2013. ErbB3 downregulation enhances luminal breast tumor response to antiestrogens. *J Clin Invest* **123**: 4329-4343.

Morrison MM, Young CD, Wang S, Sobolik T, Sanchez VM, Hicks DJ, Cook RS, Brantley-Sieders DM. 2015. mTOR Directs Breast Morphogenesis through the PKC-alpha-Rac1 Signaling Axis. *PLoS genetics* **11**: e1005291.

Motta PM, Nottola SA, Makabe S. 1997. Natural history of the female germ cell from its origin to full maturation through prenatal ovarian development. *Eur J Obstet Gynecol Reprod Biol* **75**: 5-10.

Mulac-Jericevic B, Mullinax RA, DeMayo FJ, Lydon JP, Conneely OM. 2000. Subgroup of reproductive functions of progesterone mediated by progesterone receptor-B isoform. *Science* **289**: 1751-1754.

Muller M, Schilling T, Sayan AE, Kairat A, Lorenz K, Schulze-Bergkamen H, Oren M, Koch A, Tannapfel A, Stremmel W et al. 2005. TAp73/Delta Np73 influences apoptotic response, chemosensitivity and prognosis in hepatocellular carcinoma. *Cell Death Differ* **12**: 1564-1577.

Murray-Zmijewski F, Lane DP, Bourdon JC. 2006. p53/p63/p73 isoforms: an orchestra of isoforms to harmonise cell differentiation and response to stress. *Cell Death Differ* **13**: 962-972.

Nakahari T, Nishimura A, Shimamoto C, Sakai A, Kuwabara H, Nakano T, Tanaka S, Kohda Y, Matsumura H, Mori H. 2011. The regulation of ciliary beat frequency by ovarian steroids in the guinea pig Fallopian tube: interactions between oestradiol and progesterone. *Biomed Res* **32**: 321-328.

Nakhuda GS, Zimmermann RC, Bohlen P, Liao F, Sauer MV, Kitajewski J. 2005. Inhibition of the vascular endothelial cell (VE)-specific adhesion molecule VE-cadherin blocks gonadotropin-dependent folliculogenesis and corpus luteum formation and angiogenesis. *Endocrinology* **146**: 1053-1059.

Natraj U, Richards JS. 1993. Hormonal regulation, localization, and functional activity of the progesterone receptor in granulosa cells of rat preovulatory follicles. *Endocrinology* **133**: 761-769.

Nelson JF, Felicio LS, Randall PK, Sims C, Finch CE. 1982. A longitudinal study of estrous cyclicity in aging C57BL/6J mice: I. Cycle frequency, length and vaginal cytology. *Biology of reproduction* **27**: 327-339.

Nemajerova A, Kramer D, Siller SS, Herr C, Shomroni O, Pena T, Gallinas Suazo C, Glaser K, Wildung M, Steffen H et al. 2016. TAp73 is a central transcriptional regulator of airway multiciliogenesis. *Genes & development* **30**: 1300-1312.

Niemantsverdriet M, Vermeij WP, Backendorf C. 2005. RT-PCR analysis of p73 splice variants, ease or tease? *Leukemia* **19**: 1685-1686.

Nobes CD, Hall A. 1995. Rho, rac and cdc42 GTPases: regulators of actin structures, cell adhesion and motility. *Biochemical Society transactions* **23**: 456-459.

Oktay K, Karlikaya G, Akman O, Ojakian GK, Oktay M. 2000. Interaction of extracellular matrix and activin-A in the initiation of follicle growth in the mouse ovary. *Biology of reproduction* **63**: 457-461.

Orisaka M, Tajima K, Tsang BK, Kotsuji F. 2009. Oocyte-granulosa-theca cell interactions during preantral follicular development. *J Ovarian Res* **2**: 9.

Osada M, Ohba M, Kawahara C, Ishioka C, Kanamaru R, Katoh I, Ikawa Y, Nimura Y, Nakagawara A, Obinata M et al. 1998. Cloning and functional analysis of human p51, which structurally and functionally resembles p53. *Nature medicine* **4**: 839-843.

Paik DY, Janzen DM, Schafenacker AM, Velasco VS, Shung MS, Cheng D, Huang J, Witte ON, Memarzadeh S. 2012. Stem-like epithelial cells are concentrated in the distal end of the fallopian tube: a site for injury and serous cancer initiation. *Stem cells (Dayton, Ohio)* **30**: 2487-2497.

Palermo R. 2007. Differential actions of FSH and LH during folliculogenesis. *Reprod Biomed Online* **15**: 326-337.

Park M, Shin E, Won M, Kim JH, Go H, Kim HL, Ko JJ, Lee K, Bae J. 2010. FOXL2 interacts with steroidogenic factor-1 (SF-1) and represses SF-1-induced CYP17 transcription in granulosa cells. *Mol Endocrinol* **24**: 1024-1036.

Park OK, Mayo KE. 1991. Transient expression of progesterone receptor messenger RNA in ovarian granulosa cells after the preovulatory luteinizing hormone surge. *Mol Endocrinol* **5**: 967-978.

Parkening TA, Collins TJ, Smith ER. 1982. Plasma and pituitary concentrations of LH, FSH, and prolactin in aging C57BL/6 mice at various times of the estrous cycle. *Neurobiol Aging* **3**: 31-35.

Parsons JT, Horwitz AR, Schwartz MA. 2010. Cell adhesion: integrating cytoskeletal dynamics and cellular tension. *Nat Rev Mol Cell Biol* **11**: 633-643.

Patek E. 1974. The epithelium of the human Fallopian tube. A surface ultrastructural and cytochemical study. *Acta Obstet Gynecol Scand Suppl* **31**: 1-28.

Patek E, Nilsson L, Johannisson E. 1972. Scanning electron microscopic study of the human fallopian tube. Report II. Fetal life, reproductive life, and postmenopause. *Fertil Steril* **23**: 719-733.

Patton DL, Moore DE, Spadoni LR, Soules MR, Halbert SA, Wang SP. 1989. A comparison of the fallopian tube's response to overt and silent salpingitis. *Obstet Gynecol* **73**: 622-630.

Peng XR, Hsueh AJ, LaPolt PS, Bjersing L, Ny T. 1991. Localization of luteinizing hormone receptor messenger ribonucleic acid expression in

ovarian cell types during follicle development and ovulation. *Endocrinology* **129**: 3200-3207.

Pepling ME, de Cuevas M, Spradling AC. 1999. Germline cysts: a conserved phase of germ cell development? *Trends Cell Biol* **9**: 257-262.

Pepling ME, Spradling AC. 2001. Mouse ovarian germ cell cysts undergo programmed breakdown to form primordial follicles. *Dev Biol* **234**: 339-351.

Perez CA, Ott J, Mays DJ, Pietenpol JA. 2007. p63 consensus DNA-binding site: identification, analysis and application into a p63MH algorithm. *Oncogene*.

Petrik JJ, Gentry PA, Feige JJ, LaMarre J. 2002. Expression and localization of thrombospondin-1 and -2 and their cell-surface receptor, CD36, during rat follicular development and formation of the corpus luteum. *Biology of reproduction* **67**: 1522-1531.

Pozniak CD, Barnabe-Heider F, Rymar VV, Lee AF, Sadikot AF, Miller FD. 2002. p73 is required for survival and maintenance of CNS neurons. *J Neurosci* **22**: 9800-9809.

Purdie CA, Harrison DJ, Peter A, Dobbie L, White S, Howie SE, Salter DM, Bird CC, Wyllie AH, Hooper ML et al. 1994. Tumour incidence, spectrum and ploidy in mice with a large deletion in the p53 gene. *Oncogene* **9**: 603-609.

Quinlan AR, Hall IM. 2010. BEDTools: a flexible suite of utilities for comparing genomic features. *Bioinformatics* **26**: 841-842.

Rabinovici J, Spencer SJ, Doldi N, Goldsmith PC, Schwall R, Jaffe RB. 1992. Activin-A as an intraovarian modulator: actions, localization, and regulation of the intact dimer in human ovarian cells. *J Clin Invest* **89**: 1528-1536.

Ramirez F, Ryan DP, Gruning B, Bhardwaj V, Kilpert F, Richter AS, Heyne S, Dundar F, Manke T. 2016. deepTools2: a next generation web server for deep-sequencing data analysis. *Nucleic acids research* **44**: W160-165.

Reynolds LP, Grazul-Bilska AT, Redmer DA. 2000. Angiogenesis in the corpus luteum. *Endocrine* **12**: 1-9.

Reynolds LP, Killilea SD, Redmer DA. 1992. Angiogenesis in the female reproductive system. *FASEB J* **6**: 886-892.

Richards JS. 1980. Maturation of ovarian follicles: actions and interactions of pituitary and ovarian hormones on follicular cell differentiation. *Physiol Rev* **60**: 51-89.

Richards JS, Hedin L, Caston L. 1986. Differentiation of rat ovarian thecal cells: evidence for functional luteinization. *Endocrinology* **118**: 1660-1668.

Richards JS, Midgley AR, Jr. 1976. Protein hormone action: a key to understanding ovarian follicular and luteal cell development. *Biology of reproduction* **14**: 82-94.

Ridley AJ, Hall A. 1992. The small GTP-binding protein rho regulates the assembly of focal adhesions and actin stress fibers in response to growth factors. *Cell* **70**: 389-399.

Robinson JT, Thorvaldsdottir H, Winckler W, Guttman M, Lander ES, Getz G, Mesirov JP. 2011. Integrative genomics viewer. *Nature biotechnology* **29**: 24-26.

Robker RL, Russell DL, Espey LL, Lydon JP, O'Malley BW, Richards JS. 2000. Progesterone-regulated genes in the ovulation process: ADAMTS-1 and cathepsin L proteases. *Proc Natl Acad Sci U S A* **97**: 4689-4694.

Rocco JW, Leong CO, Kuperwasser N, DeYoung MP, Ellisen LW. 2006. p63 mediates survival in squamous cell carcinoma by suppression of p73-dependent apoptosis. *Cancer Cell* **9**: 45-56.

Rodgers RJ, Irving-Rodgers HF, Russell DL. 2003. Extracellular matrix of the developing ovarian follicle. *Reproduction* **126**: 415-424.

Rodhe J, Kavanagh E, Joseph B. 2013. TAp73beta-mediated suppression of cell migration requires p57Kip2 control of actin cytoskeleton dynamics. *Oncotarget* **4**: 289-297.

Romano RA, Ortt K, Birkaya B, Smalley K, Sinha S. 2009. An active role of the DeltaN isoform of p63 in regulating basal keratin genes K5 and K14 and directing epidermal cell fate. *PLoS ONE* **4**: e5623.

Romano RA, Smalley K, Magraw C, Serna VA, Kurita T, Raghavan S, Sinha S. 2012. DeltaNp63 knockout mice reveal its indispensable role

as a master regulator of epithelial development and differentiation. *Development* **139**: 772-782.

Rosenbluth JM, Mays DJ, Jiang A, Shyr Y, Pietenpol JA. 2011. Differential regulation of the p73 cistrome by mammalian target of rapamycin reveals transcriptional programs of mesenchymal differentiation and tumorigenesis. *Proc Natl Acad Sci U S A* **108**: 2076-2081.

Rosenbluth JM, Mays DJ, Pino MF, Tang LJ, Pietenpol JA. 2008. A gene signature-based approach identifies mTOR as a regulator of p73. *Mol Cell Biol* **28**: 5951-5964.

Rothchild I. 1981. The regulation of the mammalian corpus luteum. *Recent Prog Horm Res* **37**: 183-298.

Rotter V, Schwartz D, Almon E, Goldfinger N, Kapon A, Meshorer A, Donehower LA, Levine AJ. 1993. Mice with reduced levels of p53 protein exhibit the testicular giant-cell degenerative syndrome. *Proc Natl Acad Sci U S A* **90**: 9075-9079.

Rotter V, Witte ON, Coffman R, Baltimore D. 1980. Abelson murine leukemia virus-induced tumors elicit antibodies against a host cell protein, P50. *J Virol* **36**: 547-555.

Rubinson DA, Dillon CP, Kwiatkowski AV, Sievers C, Yang L, Kopinja J, Rooney DL, Zhang M, Ihrig MM, McManus MT et al. 2003. A lentivirus-based system to functionally silence genes in primary mammalian cells, stem cells and transgenic mice by RNA interference. *Nat Genet* **33**: 401-406.

Rufini A, Niklison-Chirou MV, Inoue S, Tomasini R, Harris IS, Marino A, Federici M, Dinsdale D, Knight RA, Melino G et al. 2012. TAp73 depletion accelerates aging through metabolic dysregulation. *Genes & development* **26**: 2009-2014.

Russell DL, Doyle KM, Ochsner SA, Sandy JD, Richards JS. 2003a. Processing and localization of ADAMTS-1 and proteolytic cleavage of versican during cumulus matrix expansion and ovulation. *J Biol Chem* **278**: 42330-42339.

Russell DL, Ochsner SA, Hsieh M, Mulders S, Richards JS. 2003b. Hormone-regulated expression and localization of versican in the rodent ovary. *Endocrinology* **144**: 1020-1031.

Salathe M, Bookman RJ. 1999. Mode of Ca2+ action on ciliary beat frequency in single ovine airway epithelial cells. *J Physiol* **520 Pt 3**: 851-865.

Salustri A, Yanagishita M, Underhill CB, Laurent TC, Hascall VC. 1992. Localization and synthesis of hyaluronic acid in the cumulus cells and mural granulosa cells of the preovulatory follicle. *Dev Biol* **151**: 541-551.

Sandoval-Guzman T, Gongrich C, Moliner A, Guo T, Wu H, Broberger C, Ibanez CF. 2012. Neuroendocrine control of female reproductive function by the activin receptor ALK7. *FASEB J* **26**: 4966-4976.

Santos Guasch GL, Beeler JS, Marshall CB, Shaver TM, Sheng Q, Johnson KN, Boyd KL, Venters BJ, Cook RS, Pietenpol JA. 2018. p73 Is Required for Ovarian Follicle Development and Regulates a Gene Network Involved in Cell-to-Cell Adhesion. *iScience* **8**: 236-249.

Sarraj MA, Drummond AE. 2012. Mammalian foetal ovarian development: consequences for health and disease. *Reproduction* **143**: 151-163.

Sasaki Y, Naishiro Y, Oshima Y, Imai K, Nakamura Y, Tokino T. 2005. Identification of pigment epithelium-derived factor as a direct target of the p53 family member genes. *Oncogene* **24**: 5131-5136.

Schmale H, Bamberger C. 1997. A novel protein with strong homology to the tumor suppressor p53. *Oncogene* **15**: 1363-1367.

Schmidt D, Ovitt CE, Anlag K, Fehsenfeld S, Gredsted L, Treier AC, Treier M. 2004. The murine winged-helix transcription factor Foxl2 is required for granulosa cell differentiation and ovary maintenance. *Development* **131**: 933-942.

Schomberg DW, Couse JF, Mukherjee A, Lubahn DB, Sar M, Mayo KE, Korach KS. 1999. Targeted disruption of the estrogen receptor-alpha gene in female mice: characterization of ovarian responses and phenotype in the adult. *Endocrinology* **140**: 2733-2744.

Sen A, De Castro I, Defranco DB, Deng FM, Melamed J, Kapur P, Raj GV, Rossi R, Hammes SR. 2012. Paxillin mediates extranuclear and intranuclear signaling in prostate cancer proliferation. *J Clin Invest* **122**: 2469-2481.

Sen A, Hammes SR. 2010. Granulosa cell-specific androgen receptors are critical regulators of ovarian development and function. *Mol Endocrinol* **24**: 1393-1403.

Sen A, Prizant H, Light A, Biswas A, Hayes E, Lee HJ, Barad D, Gleicher N, Hammes SR. 2014. Androgens regulate ovarian follicular development by increasing follicle stimulating hormone receptor and microRNA-125b expression. *Proc Natl Acad Sci U S A* **111**: 3008-3013.

Short SM, Yoder BJ, Tarr SM, Prescott NL, Laniauskas S, Coleman KA, Downs-Kelly E, Pettay JD, Choueiri TK, Crowe JP et al. 2007. The expression of the cytoskeletal focal adhesion protein paxillin in breast cancer correlates with HER2 overexpression and may help predict response to chemotherapy: a retrospective immunohistochemical study. *Breast J* **13**: 130-139.

Smeenk L, van Heeringen SJ, Koeppel M, van Driel MA, Bartels SJ, Akkers RC, Denissov S, Stunnenberg HG, Lohrum M. 2008. Characterization of genome-wide p53-binding sites upon stress response. *Nucleic acids research* **36**: 3639-3654.

Smyth CD, Miro F, Whitelaw PF, Howles CM, Hillier SG. 1993. Ovarian thecal/interstitial androgen synthesis is enhanced by a follicle-stimulating hormone-stimulated paracrine mechanism. *Endocrinology* **133**: 1532-1538.

Srivastava S, Zou ZQ, Pirollo K, Blattner W, Chang EH. 1990. Germ-line transmission of a mutated p53 gene in a cancer-prone family with Li-Fraumeni syndrome. *Nature* **348**: 747-749.

Steele RE, Weisz J. 1974. Changes in sensitivity of the estradiol-LH feedback system with puberty in the female rat. *Endocrinology* **95**: 513-520.

Stiewe T, Theseling CC, Putzer BM. 2002. Transactivation-deficient Delta TA-p73 inhibits p53 by direct competition for DNA binding: implications for tumorigenesis. *J Biol Chem* **277**: 14177-14185.

Su X, Paris M, Gi YJ, Tsai KY, Cho MS, Lin YL, Biernaskie JA, Sinha S, Prives C, Pevny LH et al. 2009. TAp63 prevents premature aging by promoting adult stem cell maintenance. *Cell Stem Cell* **5**: 64-75.

Suh EK, Yang A, Kettenbach A, Bamberger C, Michaelis AH, Zhu Z, Elvin JA, Bronson RT, Crum CP, McKeon F. 2006. p63 protects the female germ line during meiotic arrest. *Nature* **444**: 624-628.

Szoltys M, Slomczynska M. 2000. Changes in distribution of androgen receptor during maturation of rat ovarian follicles. *Exp Clin Endocrinol Diabetes* **108**: 228-234.

Talos F, Abraham A, Vaseva AV, Holembowski L, Tsirka SE, Scheel A, Bode D, Dobbelstein M, Bruck W, Moll UM. 2010. p73 is an essential regulator of neural stem cell maintenance in embryonal and adult CNS neurogenesis. *Cell Death Differ* **17**: 1816-1829.

Teilmann SC, Clement CA, Thorup J, Byskov AG, Christensen ST. 2006. Expression and localization of the progesterone receptor in mouse and human reproductive organs. *J Endocrinol* **191**: 525-535.

Terre B, Piergiovanni G, Segura-Bayona S, Gil-Gomez G, Youssef SA, Attolini CS, Wilsch-Brauninger M, Jung C, Rojas AM, Marjanovic M et al. 2016. GEMC1 is a critical regulator of multiciliated cell differentiation. *The EMBO journal* **35**: 942-960.

Tetsuka M, Hillier SG. 1996. Androgen receptor gene expression in rat granulosa cells: the role of follicle-stimulating hormone and steroid hormones. *Endocrinology* **137**: 4392-4397.

Thorvaldsdottir H, Robinson JT, Mesirov JP. 2013. Integrative Genomics Viewer (IGV): high-performance genomics data visualization and exploration. *Briefings in bioinformatics* **14**: 178-192.

Tian XC, Berndtson AK, Fortune JE. 1995. Differentiation of bovine preovulatory follicles during the follicular phase is associated with increases in messenger ribonucleic acid for cytochrome P450 side-chain cleavage, 3 beta-hydroxysteroid dehydrogenase, and P450 17 alpha-hydroxylase, but not P450 aromatase. *Endocrinology* **136**: 5102-5110.

Tingen C, Kim A, Woodruff TK. 2009. The primordial pool of follicles and nest breakdown in mammalian ovaries. *Mol Hum Reprod* **15**: 795-803.

Tomasini R, Tsuchihara K, Tsuda C, Lau SK, Wilhelm M, Ruffini A, Tsao MS, Iovanna JL, Jurisicova A, Melino G et al. 2009. TAp73 regulates the spindle assembly checkpoint by modulating BubR1 activity. *Proc Natl Acad Sci U S A* **106**: 797-802.

Tomasini R, Tsuchihara K, Wilhelm M, Fujitani M, Rufini A, Cheung CC, Khan F, Itie-Youten A, Wakeham A, Tsao MS et al. 2008. TAp73 knockout shows genomic instability with infertility and tumor suppressor functions. *Genes & development* **22**: 2677-2691.

Trink B, Okami K, Wu L, Sriuranpong V, Jen J, Sidransky D. 1998. A new human p53 homologue. *Nature medicine* **4**: 747-748.

Tschan MP, Grob TJ, Peters UR, Laurenzi VD, Huegli B, Kreuzer KA, Schmidt CA, Melino G, Fey MF, Tobler A et al. 2000. Enhanced p73 expression during differentiation and complex p73 isoforms in myeloid leukemia. *Biochem Biophys Res Commun* **277**: 62-65.

Ueda Y, Hijikata M, Takagi S, Chiba T, Shimotohno K. 1999. New p73 variants with altered C-terminal structures have varied transcriptional activities. *Oncogene* **18**: 4993-4998.

Uramoto H, Sugio K, Oyama T, Nakata S, Ono K, Morita M, Funa K, Yasumoto K. 2004. Expression of deltaNp73 predicts poor prognosis in lung cancer. *Clin Cancer Res* **10**: 6905-6911.

Velasco-Velazquez MA, Salinas-Jazmin N, Mendoza-Patino N, Mandoki JJ. 2008. Reduced paxillin expression contributes to the antimetastatic effect of 4-hydroxycoumarin on B16-F10 melanoma cells. *Cancer Cell Int* **8**: 8.

Ventura A, Meissner A, Dillon CP, McManus M, Sharp PA, Van Parijs L, Jaenisch R, Jacks T. 2004. Cre-lox-regulated conditional RNA interference from transgenes. *Proc Natl Acad Sci U S A* **101**: 10380-10385.

Verdugo P. 1980. Ca2+-dependent hormonal stimulation of ciliary activity. *Nature* **283**: 764-765.

Vilgelm A, El-Rifai W, Zaika A. 2008. Therapeutic prospects for p73 and p63: rising from the shadow of p53. *Drug Resist Updat* **11**: 152-163.

Wang J, Vasaikar S, Shi Z, Greer M, Zhang B. 2017. WebGestalt 2017: a more comprehensive, powerful, flexible and interactive gene set enrichment analysis toolkit. *Nucleic acids research*.

Ware VC. 1982. The role of androgens in follicular development in the ovary. I. A quantitative analysis of oocyte ovulation. *J Exp Zool* **222**: 155-167.

Welt CK, Martin KA, Taylor AE, Lambert-Messerlian GM, Crowley WF, Jr., Smith JA, Schoenfeld DA, Hall JE. 1997. Frequency modulation of follicle-stimulating hormone (FSH) during the luteal-follicular transition: evidence for FSH control of inhibin B in normal women. *J Clin Endocrinol Metab* **82**: 2645-2652.

Wilhelm MT, Rufini A, Wetzel MK, Tsuchihara K, Inoue S, Tomasini R, Itie-Youten A, Wakeham A, Arsenian-Henriksson M, Melino G et al. 2010. Isoform-specific p73 knockout mice reveal a novel role for delta Np73 in the DNA damage response pathway. *Genes & development* **24**: 549-560.

Woodruff TK, Shea LD. 2007. The role of the extracellular matrix in ovarian follicle development. *Reprod Sci* **14**: 6-10.

Xie N, Vikhreva P, Annicchiarico-Petruzzelli M, Amelio I, Barlev N, Knight RA, Melino G. 2018. Integrin-beta4 is a novel transcriptional target of TAp73. *Cell Cycle*: 1-6.

Yan T, Lin Z, Jiang J, Lu S, Chen M, Que H, He X, Que G, Mao J, Xiao J et al. 2015. MMP14 regulates cell migration and invasion through epithelial-mesenchymal transition in nasopharyngeal carcinoma. *Am J Transl Res* **7**: 950-958.

Yang A, Kaghad M, Caput D, McKeon F. 2002. On the shoulders of giants: p63, p73 and the rise of p53. *Trends Genet* **18**: 90-95.

Yang A, Kaghad M, Wang Y, Gillett E, Fleming MD, Dotsch V, Andrews NC, Caput D, McKeon F. 1998. p63, a p53 homolog at 3q27-29, encodes multiple products with transactivating, death-inducing, and dominant-negative activities. *Mol Cell* **2**: 305-316.

Yang A, McKeon F. 2000. P63 and P73: P53 mimics, menaces and more. *Nat Rev Mol Cell Biol* **1**: 199-207.

Yang A, Schweitzer R, Sun D, Kaghad M, Walker N, Bronson RT, Tabin C, Sharpe A, Caput D, Crum C et al. 1999. p63 is essential for regenerative proliferation in limb, craniofacial and epithelial development. *Nature* **398**: 714-718.

Yang A, Walker N, Bronson R, Kaghad M, Oosterwegel M, Bonnin J, Vagner C, Bonnet H, Dikkes P, Sharpe A et al. 2000. p73-deficient mice have neurological, pheromonal and inflammatory defects but lack spontaneous tumours. *Nature* **404**: 99-103.

Yang HJ, Chen JZ, Zhang WL, Ding YQ. 2010. Focal adhesion plaque associated cytoskeletons are involved in the invasion and metastasis of human colorectal carcinoma. *Cancer Invest* **28**: 127-134.

Zhang Y, Liu T, Meyer CA, Eeckhoute J, Johnson DS, Bernstein BE, Nusbaum C, Myers RM, Brown M, Li W et al. 2008. Model-based analysis of ChIP-Seq (MACS). *Genome biology* **9**: R137.

Zhu J, Jiang J, Zhou W, Chen X. 1998. The potential tumor suppressor p73 differentially regulates cellular p53 target genes. *Cancer Res* **58**: 5061-5065.